

An Annotated Compilation and Appraisal of Electron Swarm Data in Electronegative Gases

J. W. Gallagher, E. C. Beaty, J. Dutton,* and L. C. Pitchford†

Joint Institute for Laboratory Astrophysics, National Bureau of Standards and University of Colorado, Boulder, Colorado 80309

Available data on the electron transport properties and electron swarm coefficients are discussed for the following electronegative gases: SF₆, CF₄, C₂F₆, C₃F₈, C₄F₁₀, CCl₂F₂, O₂, air, H₂O, CO₂, F₂, NF₃, Cl₂, Br₂, I₂, N₂O, NO, HCl, NH₃. Graphical presentations comparing measured and calculated data are given for the electron drift velocity, the ratio of diffusion to mobility, the electron attachment and ionization coefficients, and the electron growth constant as functions of E/N , the reduced field strength, for each gas. Graphs of the detachment and excitation coefficients are presented where these data are available. Data originally reported in terms of rate coefficients as functions of mean electron energy are graphically presented in that form. Recommendations concerning reliability are made.

Key words: air; carbon dioxide; electron diffusion; electron drift velocity; electron swarm coefficients; electron transport; electronegative gases; halogenated hydrocarbons; nitrogen oxides; nitrogen trifluoride; oxygen; sulphur hexafluoride; water.

Contents

	Page		Page
1. Introduction	109	5.2. Halogenated Hydrocarbons.....	118
2. Definitions and Methods of Data Handling.....	110	5.3. Oxygen.....	126
3. Experimental Techniques.....	112	5.4. Air	130
3.1. Drift Velocities and Longitudinal Diffusion	112	5.5. Water	133
3.2. Transverse Diffusion Measurements	113	5.6. Carbon Dioxide	135
3.3. Steady State Spatial Variation of Current ..	113	5.7. Halogens and NF ₃	139
3.4. Pulsed Avalanches.....	113	5.8. Nitrogen Oxides	144
3.5. Errors.....	113	5.9. Miscellaneous Gases.....	147
4. Computations Using the Boltzmann Equation ..	114	6. Summary	149
5. Data Review	114	7. Acknowledgments.....	150
5.1. Sulfur Hexafluoride	114	8. References	150

1. Introduction

Electronegative gases, those which have the ability to attach free electrons and form stable negative ions, have numerous applications. These range from their use as insulation for the components of high voltage distribution systems, to their use as donors in excimer lasers and scavengers in physical-chemical systems. Applications such as these require a knowledge of the coefficients that represent the average behavior of electron swarms in these gases in the presence of an electric field. Such swarm data are useful both in

the direct prediction of the electric characteristics of these gases and as a source of cross sections for electron-molecule collision processes. This article is an annotated compilation of data collected from the literature on spatial transport coefficients and swarm parameters of the electronegative gases: SF₆, the halogenated hydrocarbons, air, O₂, H₂O, CO₂, NH₃, the halogens and NF₃, the nitrogen oxides (N₂O, NO, and NO₂), the hydrogen halides, and SO₂. Methods by which the data were acquired are described and discussed. Graphical presentations of the data are given for all cases. Recommendations concerning the reliability of the data are made. Although some of the swarm data for individual electronegative molecules have been collected previously, this is the first general compilation of swarm data for the whole group of gases.

In 1974, Dutton¹ wrote a review of electron swarm data in gases of general interest which included data available at the time on four weakly electronegative gases O₂, NO, CO₂, air. For these four gases the presentation given below primarily represents an update of the discussions by Dutton,

*Present address: Department of Physics, University College of Swansea, Swansea, Wales, U. K.

†Present address: Sandia National Laboratory, Albuquerque, NM 87185

© 1983 by the U.S. Secretary of Commerce on behalf of the United States. This copyright is assigned to the American Institute of Physics and the American Chemical Society.
Reprints available from ACS; see Reprint List at back of issue.

but some earlier data are included for comparison and to give a complete picture. For the gases that were not covered by Dutton, we give as complete as possible a compilation of published swarm data. Also in 1974, Huxley and Crompton published their book, *The Diffusion and Drift of Electrons in Gases*,² in which they gave a comprehensive description of the theory of electron drift and diffusion and its application to swarm experiments as well as a compilation of data for electron transport coefficients in gases of general interest including some of the electronegative gases: O₂, CO₂, air, H₂O. These two publications extend and update several earlier books and articles on the subject.³⁻¹⁰ Christophorou's book³ contains a graphical compilation of data available prior to 1971 on drift velocities and diffusion-to-mobility ratios in most of the electronegative gases (with the exception SF₆) but contains no tabular listings of data. An extensive discussion of attachment rates and cross sections is also provided (Ref. 3, Chap. 6).

Recently there has been an increasing demand for very accurate transport data for use in many technologies. Increased interest in electron swarm data in general is evidenced by the introduction of the International Seminar on Swarm Experiments^{11,12} as a satellite meeting to the International Conference on the Physics of Electronic and Atomic Collisions. Several reports at the 1981 Seminar on Swarm Experiments emphasized the general advances in the theory and analysis of swarm data and the impact these advances have made on experimental design. The accuracy of the two-term method of solution of the Boltzmann equation, which is typically used in the analysis of swarm measurements, has been scrutinized and conditions where it is invalid have been identified.¹³ In this connection two more general multiterm solution techniques have been developed.^{13,14} Improvements in experimental methods include the application of signal averaging techniques to pulsed Townsend measurements¹⁵ and of optical scanning to steady state Townsend measurements, as well as general advances in electronics.

One impetus for the present compilation of swarm parameters in electronegative gases stems from recent efforts to develop gaseous insulators and gaseous dielectrics with specific properties. From a practical point of view, electronegative gases have tremendous potential as insulators in high-voltage transmission lines and can operate as high-voltage switches with the proper choice of component gases. Swarm parameters describe the electrical properties of these gases by quantifying the transport of electrons through the gases under equilibrium conditions. Swarm data are also needed to calculate sparking potentials and predict electrical breakdown in gases. Interest in swarm data for insulating gases is apparent from papers given at several recent conferences^{12,16-20} as well as the book, *Electrical Breakdown in Gases*, edited by J. M. Meek and J. D. Craggs.^{21,22} Swarm data on the gases with highest dielectric strengths (SF₆, the perfluorocarbons, and CCl₂F₂) are included in this review, as are the more commonly used insulators and their electronegative constituents (air, O₂, CO₂ and H₂O).

Swarm parameters in CO₂ are also of interest because of the need for such data in modeling CO₂ laser systems. Similarly, the role of halogens and NF₃ in rare gas-halide lasers has stimulated interest in swarm data on these highly reac-

tive and experimentally difficult gases. Nygaard and co-workers²³ and Chantry²⁴ have recently reviewed these data.

Nitrogen oxides play an important role in the ion chemistry of the upper atmosphere, and consequently interest is high in electron swarm data for these molecules. Nitrous oxide is also used in laser systems and as an electron scavenger. Parkes²⁵ reviewed some of the data relating to detachment from NO⁻ and N₂O⁻ as well as from oxygen ions.

Most of the data we discuss below were measured in, or calculated for, pure gases (with the exception of air). Swarm data for pure gases cannot always be used reliably to predict swarm parameters for gas mixtures.²⁶ Occasionally data reported were taken in mixtures in which the nonelectronegative component was used to inhibit reactions masking the interactions of the swarm electrons with the electronegative gas. Swarm parameters as a function of mixture ratio have not been included, however, because of the overwhelming quantity of associated data.

Section 2 gives definitions of the quantities measured and calculated and of the symbols used in the subsequent discussion, as well as a brief discussion of the data handling procedures. Section 3 describes standard experimental techniques, Sec. 4 discusses swarm computations, and Sec. 5 discusses and presents the data separately for each gas or logical group of gases (such as the halogens) in the following order: drift velocity, diffusion coefficient, and ratio of diffusion coefficient to mobility, and electron density gain and loss processes. The absence from this report of data for a particular parameter and gas indicates either that no data or only data of highly questionable value have been published for that gas or that the only available data were compiled by Dutton.¹

Dutton¹ included an annotated bibliographic index to electron swarm data which was revised and updated in 1980 and is available as Report #20 of the JILA Information Center.²⁷

2. Definitions and Method of Data Handling

An electron swarm is a cloud of electrons of density n in a gas of much higher number density, N , in a system the properties of which are dependent on the interactions of the individual electrons with the gas molecules (or atoms) rather than with each other or with the container walls. Electron swarms are typically studied in the presence of an electric field. The electric field increases the mean energy of the electrons while affecting the neutrals only through collisions with the higher energy electrons. The electron energy can therefore be substantially higher than that of the neutral gas, and electron collisions with the heavier gas molecules lead to a large random component of electron motion. The electron motion is fully described by the "electron energy distribution function" which is a function of the neutral gas composition and the energy gain per mean free path from the electric field (see Huxley and Crompton, Ref. 2, Chapter 4). For an electric field of strength E , the latter quantity is proportional to E/N , the "reduced field strength." For the data considered here, the gas temperature T is relatively low (near 300 K unless otherwise stated) and has little influence on the distribution function except when the electron mean energy approaches that of the surrounding gas, which occurs at very

low values of E/N . By definition, the electrons in the swarm are in equilibrium with the field.

Much experimental effort has been devoted to obtaining equilibrium in the spatial or temporal range where the measurements are made. The swarm is then described by "hydrodynamic" transport parameters which are independent of position and time. Extension of these equilibrium concepts to nonuniform field and nonequilibrium situations is a topic of current research, but will not be treated in this article, and the application of the data reported here to such situations is not recommended. For example, in cases where swarm coefficients depend on N as well as E/N , caution must be exercised in applying these data to situations where N deviates significantly from the conditions under which the measurements reported were performed.

The steady-state properties of swarm studies are those relating to spatial transport, the rates of creation and destruction of electrons, and the rates of energy transfer to the neutral gas. The parameters specifically included in this data review are discussed briefly below.

In an electric field the center of mass of the electron swarm acquires a velocity, termed the drift velocity W , in the direction opposite to the field (see Huxley and Crompton, Ref. 2, p. 70). The electron mobility μ is defined as the ratio of the drift velocity to the electric field strength and, for present purposes, mobility is considered to be an alternate way of specifying drift velocity.

Diffusion is the tendency of the swarm to spread as a result of its random motion in such a way as to make the density uniform and is characterized by a diffusion coefficient D . When an electric field is present, the diffusion is not, in general, isotropic (see Huxley and Crompton, Ref. 2, Chap. 11). Two parameters, the transverse or lateral diffusion coefficient D_T (perpendicular to the field) and the longitudinal diffusion coefficient D_L (parallel to the field) then characterize the diffusive motion. The ratio of diffusion coefficient to mobility D/μ has a rather special role, as measurements of D_T/μ can be made independent of D_T or μ . In the limit of small electric fields this ratio tends toward the mean energy of the electrons, and as such it is a measure of the electron temperature. At higher fields, the electron swarm is not in thermal equilibrium and no temperature is defined, but D_T/μ is a convenient measure of the energy content of the swarm. In this context D_T/μ is termed as the "characteristic energy" (see Huxley and Crompton, Ref. 2, p. 82). This terminology does not refer to D_T/μ . In some cases, the quantity reported is k_T , the Townsend energy factor, which is related to the characteristic energy by

$$eD_T/\mu = F(3/2 kT)k_T,$$

where k is the Boltzmann constant, and F is a factor dependent on the electron energy distribution, which is 2/3 for a Maxwellian distribution (see Dutton, Ref. 1, Sec. 3.2, and Huxley and Crompton, Ref. 2, Sec. 1.10, for discussion of k_T).

The change in the number of the electrons in a swarm may result from electron attachment (coefficient η) to neutral particles, electron detachment (coefficient δ) from negative ions in collision with other gas molecules, and ionization (coefficient α) of neutrals. The coefficients η , δ , and α repre-

sent the average change in n , the electron density, per unit drift distance x , as a result of the indicated reaction. Sections 3.4 and 3.7 of Dutton's review¹ give extended discussions of the definitions and interpretation of η , the attachment coefficient and α , the Townsend primary ionization coefficient, respectively. Chapter 5 of Huxley and Crompton's book² also discusses the definitions of these quantities. For some range of values of E/N the electron density will be simultaneously influenced by all three processes, but the spatial current growth in a Townsend discharge (see Sec. 3.3 below) may be exponential over a large range of distance. It is convenient in these circumstances to define the parameter λ , as the electron growth constant (or effective ionization coefficient) per unit distance, i.e., $n(x) = n(0)e^{\lambda x}$, where $n(0)$ is the number of electrons released simultaneously into the gas at $x = 0$. Where only ionization and attachment occur, $\lambda = \alpha - \eta$ and is the average net gain of free electrons per unit drift distance. The region of E/N where λ approaches zero is significant in predicting discharge inception or electrical breakdown in gases. Inelastic collisions other than those giving rise to ionization are quantified by the excitation coefficient denoted by ϵ . Another process that can cause a change in the number of electrons is recombination, but because of the low electron and positive ion densities in the swarms considered here, it is not included in the present review.

The swarm coefficients referred to in the previous paragraph are defined as the average number of events occurring when one electron drifts a unit distance in the direction opposite to the electric field. In general they are related to the corresponding two-body rate coefficients, k_2 , by $Nk_2 = SW$,

TABLE I. Swarm parameters. Symbolic notation and common scale factors and units.

Symbol	Definition or quantity	Common scale factors and units
N	Gas number density	10^{22} m^{-3}
N'	Gas number density for a specific component in a mixture	10^{22} m^{-3}
p	Gas pressure	Pa
T	Gas temperature	K
W	Electron drift velocity	10^3 m s^{-1}
E/N	Reduced field strength	10^{-21} V m^2
$D_T N$	Transverse diffusion coefficient $\cdot N$	$10^{24} \text{ m}^{-1} \text{ s}^{-1}$
$D_L N$	Longitudinal diffusion coefficient $\cdot N$	$10^{24} \text{ m}^{-1} \text{ s}^{-1}$
D_T/μ	Ratio of transverse diffusion coefficient to mobility	V
D_L/μ	Ratio of longitudinal diffusion coefficient to mobility	V
D_{TH}/μ	Ratio of diffusion coefficient for $E/N = 0$ to mobility	V
η/N	Attachment coefficient/ N	10^{-22} m^2
η^*/N	(Effective attachment coefficient, including effects of both attachment and detachment)/ N	
α/N	Ionization coefficient/ N	10^{-22} m^2
δ/N	Detachment coefficient/ N	10^{-22} m^2
λ/N	Electron growth constant/ N	10^{-22} m^2
ϵ/N	Excitation coefficient/ N	10^{-22} m^2
k_2	Two body rate constant	$10^{-16} \text{ m}^3 \text{ s}^{-1}$
k_3	Three body rate constant	$10^{-42} \text{ m}^6 \text{ s}^{-1}$
k_T	Townsend energy factor	dimensionless

TABLE 2. Common conversions for swarm data units.^a

Quantity	Symbols and SI units (A)	Some commonly used symbols and units (B)	Factor, A/B, to apply to commonly used units to obtain SI units used in this paper
Particle density	$N(\text{m}^{-3})$	$N(\text{cm}^{-3})$	10^6
Particle density	$N(\text{m}^{-3})$	$p(\text{Torr})$	$3.54 \times 10^{22} \frac{273 \text{ K}}{T(\text{K})}$
Temperature	$T(\text{K})$	$T(\text{K})$	1
Pressure	$p(\text{Pa})$	$p(\text{Torr})$	133
Reduced field	$E/N(\text{V m}^{-2})$	$E/p(\text{V/cm Torr})$	$2.83 \times 10^{-21} \frac{T(\text{K})}{273 \text{ K}}$
Reduced field	$E/N(\text{V m}^{-2})$	$E/N(\text{Td})$	10^{-21}
Drift velocity	$W(\text{m s}^{-1})$	$W(\text{cm s}^{-1})$	10^{-2}
Diffusion coefficient	$DN(10^{22} \text{ m}^{-1} \text{ s}^{-1})$	$Dp\left(\frac{\text{cm}^2 \text{ Torr}}{\text{s}}\right)$	$3.54 \times 10^{18} \frac{273 \text{ K}}{T(\text{K})}$
Diffusion/mobility	$D/\mu(\text{V})$	$D/\mu(\text{V})$	1
Swarm coefficients	$S/N(\text{m}^2)$	$S/p\left(\frac{1}{\text{cm Torr}}\right)$	$2.83 \times 10^{-21} \frac{T(\text{K})}{273}$

^a Pressure is incorporated in many of the units commonly used. The related conversions to the units used in this paper are not a simple numerical factor but require incorporation of the ratio $T(\text{K})/273 \text{ K}$ or its inverse in the conversion factor, where $T(\text{K})$ is the temperature at which the measurements were made or to which the data have been normalized.

where S is a coefficient per unit drift distance. For three-body processes, the relationship is $N^2 k_3 = SW$, where k_3 is the three-body rate coefficient.

The swarm coefficients per unit distance depend on N as well as on E/N , and are conveniently represented as S/N for two-body reactions and as S/N^2 for three-body reactions. Similarly, since D depends on N as well as E/N , it is convenient to consider instead the parameter DN . The swarm is then specified by $W, D/\mu, DN, S/N$, and/or S/N^2 , which are functions only of E/N and the gas composition. The data presented in this article are given primarily in terms of these parameters. In some cases, particularly for the halogens, NF_3 and some of the halogenated hydrocarbons, some of the data on attachment are reported in terms of a two-body rate coefficient as a function of the mean electron energy. Conversion of these data to S/N as a function of E/N would require values of W and mean energy as functions of E/N , and these are not accurately known for these gases. Thus, the data are presented below as a function of mean electron energy as originally reported.

The specific parameters and corresponding multiples of SI units in which they are expressed throughout this article are summarized in Table 1. Data are frequently published in units other than these SI units. In these cases conversions to the SI units were made using the relationships listed in Table 2.

As a rule, experimental data are reported in the literature as specific points, while calculated data are reported as continuous curves. These conventions are adhered to in this article. Experimental data are represented in the figures by separate symbols identified in the figure legend or caption with the reference from which they were taken. Calculated data are represented by smooth lines beginning and ending with symbols identified with the appropriate reference.

If the original data were published in tabular form, our figures were prepared directly from those tables. However, in most cases, the data were published in the form of graphs, and the graphs were enlarged and the coordinates of the data

points obtained using standard digitization procedures. These procedures are estimated to introduce an error of no more than $\pm 3\%$. Tables of the data presented in the figures in this article have been compiled and are deposited with PAPS.^a

3. Experimental Techniques

Most of the experimental data reported here were obtained using variations on a small number of general methods which are briefly described below. Although these methods are conceptually straightforward the analysis of the measured data to obtain accurate transport and swarm coefficients is complex. Simplifying assumptions concerning the effects of boundaries, diffusion, secondary ionization, and, especially in the case of electronegative gases, ion-molecule reactions and detachment, have frequently been made in analyzing data obtained by these methods. Huxley and Crompton² give a comprehensive discussion of the approximations based on these assumptions and the variations on experimental methods and related analyses that have been devised to minimize the experimental uncertainties resulting from these approximations.

3.1. Drift Velocities and Longitudinal Diffusion

Drift velocities and longitudinal diffusion are most often determined by time-of-flight techniques. At low values of E/N where there is negligible ionization, the time-of-flight is frequently determined by means of a drift tube containing two electrical shutters, the first to function as a gate to admit

^a See AIP document no. PAPS JPCRD-12-0109-108 for 108 pages of tables of electron swarm data for electronegative gases. Order by PAPS number and journal references from American Institute of Physics, Physics Auxiliary Publication Service, 335 East 45th Street, New York, N. Y. 10017. The price is \$1.50 for each microfiche (98 pages), or \$5.00 for photocopies of up to 30 pages with \$0.15 for each additional page over 30 pages. Air-mail additional. Make checks payable to the American Institute of Physics.

electrons into a uniform field drift space at a known time and the second to sample the density of electrons traveling the measured distance between the shutters as a function of time. From these measurements, electron drift velocities and, with more extensive analysis, longitudinal diffusion coefficients are obtained. Alternatively, a pulse of electrons produced photoelectrically at the cathode of a uniform field electrode system may be sampled through a small hole in the anode (see, for example, Nelson and Davis³⁴). Many variations on details such as the construction and separation of the shutters and on the analysis of the resulting data exist. A comprehensive discussion of drift velocity measurements is given in Huxley and Crompton's book, Ref. 2, Chap. 10.

3.2. Transverse Diffusion Measurements

Transverse diffusion is usually determined using a drift tube in which the electrons enter a uniform-field region through a small orifice or slit and are collected at a segmented anode, so that the spatial distribution of the steady-state swarm perpendicular to the electric field is measured. D_T/μ is determined from the ratios of the currents arriving at different segments of the anode. Townsend's original analysis³⁰ was refined by Huxley and Bennett,³¹ as described by Huxley and Crompton,² Chap. 11.

3.3. Steady-State Spatial Variation of Current

When an initial current I_0 is released by an external source of radiation from the cathode of a uniform-field electrode system and the only inelastic process occurring is electron attachment, the change of electron current with d , the distance from the cathode, at a constant value of E/N is given by $I = I_0 e^{-\eta d}$. The measurement of the steady-state electron current as a function of d can be used to determine the attachment coefficient. Similarly, if the conditions are such that only primary ionization occurs, the spatial growth at constant E/N is given by $I = I_0 e^{ad}$, and the ionization coefficient can be determined. Of course, these special conditions are often not satisfied, especially for high E/N , and extensive analysis incorporating ionization, attachment, detachment, and ion-molecule reactions is required to determine swarm coefficients from these measurements [see Dutton,¹ Eq. (16)]. The values of coefficients of the processes involved which fit the experimental data are often subject to uncertainties as large as $\pm 50\%$. Recently, Davies²⁹ developed more sophisticated fitting procedures for the analysis of spatial current growth measurements in attaching gases in which the electron growth constant can be determined with little ambiguity.

3.4. Pulsed Avalanches

At values of E/N sufficiently high to give rise to ionization, a pulse of electrons photoelectrically released from the cathode of a uniform field gap will give rise to an electron avalanche. The resulting transient current, in which the electron and ion components are easily distinguishable because

of the much higher drift velocities of the electrons, may be studied by high-speed pulse techniques.

Measurement of the electron density as a function of time, either electronically or by observation of the light emitted from the discharge, provides values of the ionization coefficient and electron drift velocity.³³ This type of measurement is often referred to as a pulsed Townsend discharge.³² Concerns involving interpretation and analysis of results to give swarm coefficients are similar to those for steady-state Townsend measurements.

3.5. Errors

Several specific sources of error are common in swarm measurements. One is the presence of impurities in the gas which may have a significant influence on the quantities observed, as evidenced by measurements in intentional mixtures. A second is the effect of surfaces both in the distortion of the electric fields and the spatial distribution of electrons and as a source of secondary electrons. A third is the measurement of partial gas density in mixtures.

Other sources of error are related to the interpretation of measured quantities to obtain swarm coefficients, especially in electronegative gases where the electron number density varies due to attachment and, at higher E/N , ionization. Various aspects of the complete reaction scheme such as detachment from negative ions and charge transfer, as well as more complex reactions such as formation and attachment to clusters, may be unidentified by the investigator or ignored in the interest of reducing the analysis to manageable proportions. The use of mass spectrometric techniques is essential to identify a complete reaction scheme, as well as to monitor impurity concentrations.

Additional sources of error in the analysis of experimental data include the assumption of idealized geometry, and the neglect of diffusion effects (see e.g., Huxley and Crompton's book,² Chap. 5). As discussed in Sec. 3.3, the reported transport and swarm coefficients are often derived from curve-fitting procedures in which the parameters describing the reaction scheme are incorporated into an analytic expression that describes the observations. Often a range of parameters gives a satisfactory fit, resulting in uncertainties as large as $\pm 50\%$. Using advances in computer techniques, Edelson and McAfee³⁵ developed improved fitting procedures with which analyses can be made with reliable estimates of confidence limits and applied these methods to SF_6 (see Sec. 5.1.c). Edelson and McAfee discuss the criteria for application of this technique.

Quantitative statements concerning uncertainties inherent in general techniques have not been made because characteristics of the specific gas systems to which the techniques are applied superimpose limiting sources of uncertainty. Thus, uncertainties are discussed separately for each case. Wherever possible, the sources of error which were considered or neglected by the original authors and their estimated uncertainties are given. However, because different researchers use different standards for their uncertainty statements, the data with the smallest specified uncertainty are not necessarily the most reliable.

4. Computations Using the Boltzmann Equation

The swarm parameters discussed so far are measures of the macroscopic properties of an electron cloud moving through a neutral gas under the influence of an electric field. The Boltzmann equation provides a connection between these microscopic cross sections and these measurable macroscopic parameters (see e.g., Huxley and Crompton, Ref. 2, Chap. 6).

The Boltzmann equation is the equation of continuity for electrons in a six-dimensional phase space and describes the time evolution of the electron energy distribution function $f(r, v, t)$.³⁶ Electron transport and excitation coefficients are calculated as averages or integrals involving f . The electron energy distribution function contains all the information about the electron swarm and the calculated swarm parameters are averages in the same sense that the experiments measure average quantities. The key to a model or theoretical calculation is then the electron energy distribution function.

The Boltzmann equation may be written as³⁶

$$\frac{df}{dt} + v \cdot \nabla_r f + a \cdot \nabla_v f = C(f), \quad (1)$$

where a is the acceleration due to the applied field and C is the collision operator. In order of the terms in Eq. (1), the time evolution of f arises from a spatial flux, a flux in velocity space, and a redistribution of electron energy resulting from collisions with neutral particles. Electrons may lose recoil energy in elastic collisions with neutrals, gain recoil energy if the electron energy is less than the neutral energy, and gain or lose discrete amounts of energy in exciting or deexciting the neutrals to or from the various rotational, vibrational, or electronic levels. Space charge fields and Coulomb collisions are negligible due to the small charge densities involved in swarm experiments.

Solutions of the Boltzmann equation are complicated because f depends on the six phase space variables and time. An additional complication is that the collision operator C is a combination of multiplicative and integral operators. However, in the hydrodynamic regime, i.e., the regime of interest in typical swarm situations where the measured parameters are free of boundary effects and any change in current is exponential in both time and distance, we can make several simplifying assumptions that cast the Boltzmann equation into a form amenable to numerical solution.³⁷ Even in the hydrodynamic limit, however, much effort has been devoted to techniques for solving the Boltzmann equation and studying the various approximations that make numerical solutions of the equation practical (see Refs. 13 and 14 and references therein).

By far the most common solution technique is the "two-term" approximation.^{36,38} Here the spatial dependence of f is assumed small and is treated in second order.^{39,40} Thus, since the current growth is exponential in time, $\partial f / \partial t = \text{constant} \times f$ and $f(r, v, t) \approx f(v) e^{\alpha t}$. The two-term approximation is then invoked, i.e., the angular dependence of f (the angle being that between the electron velocity vector and the field direction) can be approximated by the first two terms of a

spherical harmonic (or because of the cylindrical symmetry, Legendre) expansion. The approximation leads to calculated values of electron transport and rate coefficients that agree reasonably well with the more rigorous calculations in most cases.^{13,14,38,41-43}

An alternate technique for the calculation of swarm parameters is the use of Monte Carlo methods which avoid entirely the use of the Boltzmann equation. In these numerical simulations of the swarm motion the trajectories of individual electrons are followed through a large number of collisions with the exact outcome of each collision being modeled on the basis of a random number. This technique offers the advantage that boundary effects may be included and no assumptions are made about either the r or v dependence of the distribution. This advantage is offset by the comparatively long computational times involved. Also, for calculations of equilibrium or steady-state swarm phenomena, the boundary effects may be safely neglected.

There are two general categories of applications for the solution of the Boltzmann equation:

- 1) iterative extraction of low-energy electron-neutral scattering cross sections from measured swarm data (e.g., Huxley and Crompton's book,² Chapter 13); and
- 2) calculations of swarm parameters from a given set of cross sections (see for example Ref. 44).

These two categories differ in purpose but are the same computationally. In the first category the cross sections may be extracted from swarm data in a trial and error sense by comparing calculated values of swarm parameters with measurements using an estimate for the cross sections. Cross sections are then adjusted using the comparison as a guide, until the calculated and measured values agree. For example, the cross sections in He determined in this way are considered to be among the most accurate available.⁴⁵

The second category listed above is of more interest here. The electron energy distribution function in a gas mixture can be very different from those of the individual mixture components under the same experimental conditions. The mixture distribution cannot be determined directly from the distribution of the pure gas components. It is necessary to go through the Boltzmann equation using as input the component gas cross sections. Thus swarm parameters in mixtures may be calculated from the constituent gas cross sections.

The accuracy of the calculations of swarm parameters depends on the method used to solve the Boltzmann equation. For many applications, the accuracy of the "two-term" approximation is sufficient. With few exceptions, the theoretical values of swarm parameters reported here were calculated using that approximation.

5. Data Review

5.1. Sulfur Hexafluoride

Sulfur hexafluoride is widely used as a gaseous insulator and an arc interrupting medium in electrical power systems, and most of the research on electron swarms in the gas appears to have been motivated toward understanding the phenomena associated with electrical breakdown. A dominant characteristic of electron swarms in SF_6 is that low energy

electrons are very rapidly attached to form negative ions, and the rapid disappearance of free electrons greatly complicates the measurement of other swarm parameters. At high E/N ionization helps balance the loss by attachment. Small shifts in the energy distribution function can substantially change the balance between electron gain and loss. As SF_6 was not reviewed by Dutton,¹ we have attempted to be as complete as possible in reporting all available data in the present review.

In two papers published in 1979, Kline, Davies, Chen, and Chantry⁴⁴ and Yoshizawa, Sakai, Tagashira, and Sakamoto⁴⁶ reviewed the available cross section data for collisions of electrons in SF_6 . In each of these papers the electron energy distribution function was calculated by solving the Boltzmann equation, and the swarm parameters were computed using the distribution function and the relevant cross sections. The paper by Kline and co-workers also reported some new, presumably more reliable, cross section data which are rather different from those assumed by Yoshizawa and co-workers. On the other hand Yoshizawa and co-workers used a more accurate method of solving the Boltzmann equation. These papers support the conclusion that the dominant phenomena of electron swarms in SF_6 are well understood, but there are considerable uncertainties in the magnitudes of some of the transport coefficients.

a. Drift Velocity, SF_6

Naidu and Prasad⁴⁷ used sampling techniques to measure the electron drift velocity of a group of electrons for the E/N between 340 and $640 \times 10^{-21} \text{ V m}^2$, and the results are displayed in Fig. 1.1. These data are the only measured values available from a direct and recognized method and are, therefore, recommended as the most reliable. The authors estimate the uncertainties at 5%.

Teich and Sangi⁴⁸ reported data for approximately the same E/N range in a conference proceeding which is not widely available. They provide no description of experimental method and give their results in the form of a simple equation. These data are also displayed in Fig. 1.1.

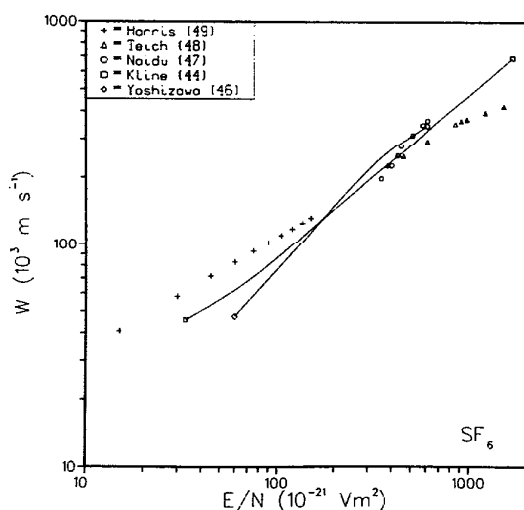


FIGURE 1.1. W for electrons in SF_6 as a function of E/N .

Harris and Jones⁴⁹ reported data on the drift velocity of electrons in SF_6 for E/N between 15 and $150 \times 10^{-21} \text{ V m}^2$. (The same results, with less explanation, were also given by Dutton, Harris, and Jones.⁵⁰) Their method involved a detailed accounting for electrons removed by diffusion back to the cathode. While this method is indirect, in other gases it yields data in error by only 15%. The results of these measurements, which are given as an equation, are also represented in Fig. 1.1.

Kline and co-workers and Yoshizawa and co-workers both calculated drift velocities which are displayed in Fig. 1.1. Yoshizawa considered the consequences of spatial growth of the electron density on the distribution function and found surprisingly large effects. Kline and co-workers did not consider these higher order effects since they used the conventional two-term approximation and did not include the increase in the number of electrons due to ionization.

b. (Diffusion Coefficient)/Mobility, SF_6

Naidu and Prasad⁴⁷ also reported values for D_T/μ . These data were derived from measurements of the ratios of currents to concentric ring electrodes. Taken as a whole the data set displays inconsistencies which the authors discuss. They note that most of the discordant data involved use of the outermost rings, and they suggest these data are the result of "anomalous" diffusion. Anomalous diffusion is defined as a significant physical effect and not the result of measurement error; however, no explanation is given for the causes. The authors suggest that the data derived from the inner rings is reliable, and these data are shown in Fig. 1.2.

Maller and Naidu⁵¹ later reported similar measurements which are quite close to the results of Naidu and Prasad. These are also shown in Fig. 1.2.

Kline and co-workers⁴⁴ calculated values of D_T/μ along with other swarm parameters, and their results are included in Fig. 1.2. There is a discrepancy between theory and experiment which on present evidence cannot be resolved and more work is necessary.

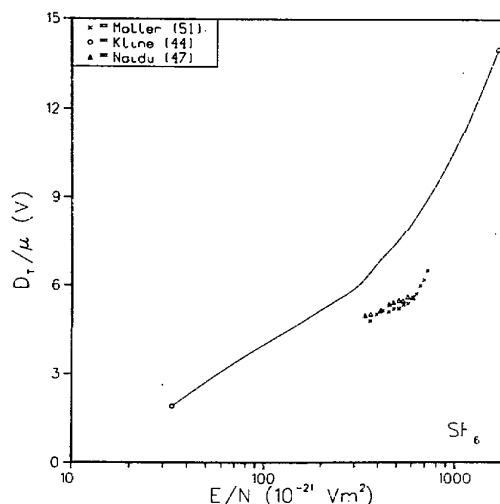


FIGURE 1.2. D_T/μ in SF_6 as a function of E/N .

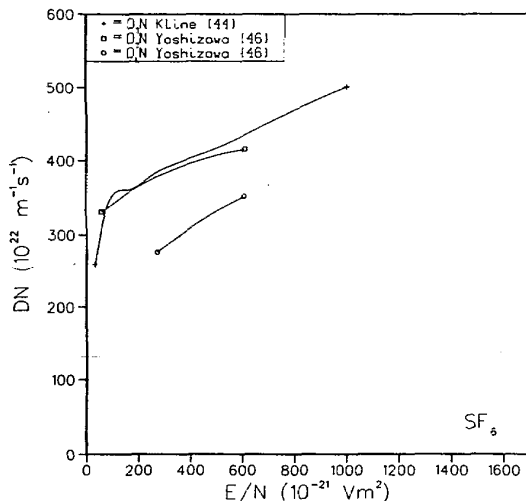


FIGURE 1.3. DN in SF_6 as a function of E/N .

No direct experimental data are available on the diffusion coefficient for electrons in SF_6 . Yoshizawa and co-workers⁴⁶ included diffusion coefficient calculations as part of their Boltzmann equation analysis. As with drift velocity, data were calculated using several definitions, but in this case the different definitions yield data that vary only slightly (for the relatively low values of E/N investigated). Figure 1.3 includes the results they have labeled as D_L and D_T values appropriate to a steady-state Townsend discharge.

Also included in Fig. 1.3 are values of $D_T N$ which the present authors calculated from the W and D_T/μ values reported by Kline and co-workers. At low E/N these results do not disagree significantly with those of Yoshizawa and co-workers. At high E/N the Kline data must be considered uncertain because the increase in the number of electrons due to ionization was neglected.

c. Electron Gain and Loss Processes, SF_6

As discussed above, the cross sections for attachment to sulphur hexafluoride at low energies is extremely large. A continuing question has been: "What effect does this large cross section have on the measurement of the attachment coefficient at the nonthermal E/N and mean energies of interest in this review?" For this reason, some discussion of the low energy attachment cross sections and thermal attachment rates has been included here. Similar discussions have not been presented for other gases for which the impact of attachment on measured swarm parameters is less dramatic at low E/N .

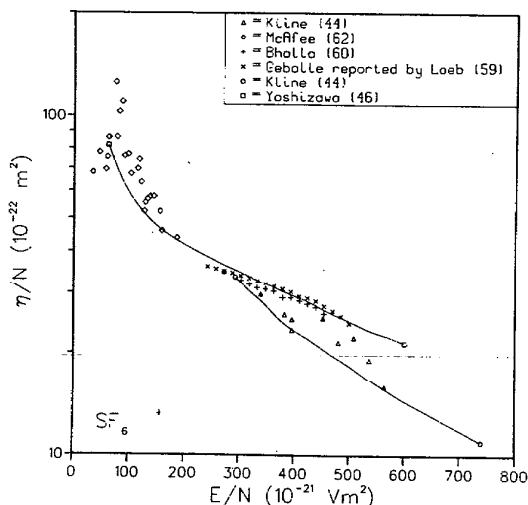
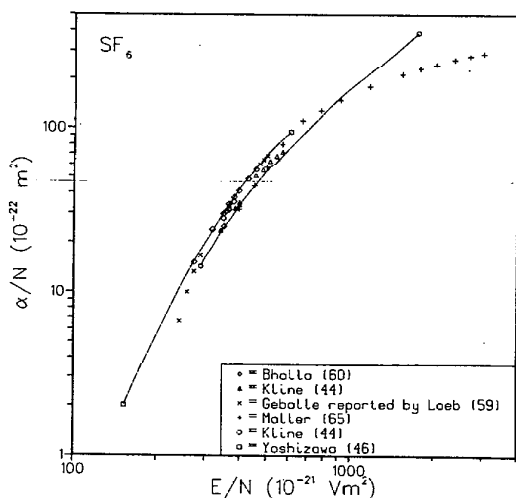
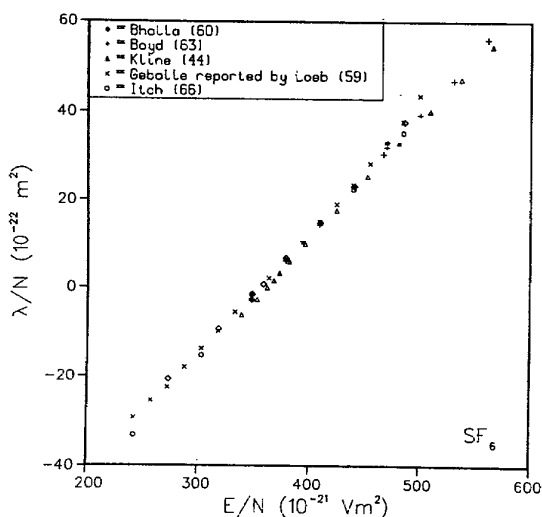
Kline and co-workers⁴⁴ discuss the relative contributions made by various energy regions to the attachment coefficient. These authors report that the attachment cross section is $5.5 \times 10^{-10} \text{ m}^2$ at 0.01 eV, and falls rapidly at higher energies, decreasing to $3 \times 10^{-12} \text{ m}^2$ at 0.3 eV. Chutjian⁵² has reported further measurements at very low energy, which offer the possibility of better energy resolution. Above

about 0.3 eV, dissociative attachment is the dominant attachment process. Fehsenfeld⁵³ reported that the zero field attachment rate constant is $2220 \times 10^{-16} \text{ m}^3 \text{ s}^{-1}$ at temperatures between 290 and 500 K. Crompton and co-workers⁵⁴ recently gave a preliminary report of a more precise experimental method which yields a similar conclusion. In view of the weak temperature dependence, k_2 can be expected to be weakly dependent on E/N for small E/N . Fehsenfeld found the reaction rate to be proportional to gas density indicating a two-body reaction. Actually a two-step process is involved with the initial attachment collision producing an excited negative ion with a lifetime of $> 50 \mu\text{s}$.⁵⁵ For the gas densities normally used in electron swarm and gas discharge work, there is a high probability that the excited state will be collisionally stabilized. Foster and Beauchamp⁵⁶ reported that at low densities radiative decay is also important in stabilizing excited SF_6^- negative ions.

Several dissociative attachment processes are known to occur in SF_6 , producing a variety of negative ions. Kline and co-workers report that for the energy range 0.3–2.5 eV, the dominant negative ion is SF_5^- and above about 2.5 eV, it is F^- . Other ions formed are SF_4^- , F_2^- , and SF_2^- , none of which are dominant at any energy. The principal reason for concern with the identity of the ions is the impact on interpreting data relating to detachment.

Most of the available data on electron reactions in SF_6 have come from analysis of spatial current growth in Townsend discharges. The first electron swarm data on SF_6 were reported by Hochberg and Sandberg^{57,58} who gave values of the ionization coefficient inferred from observations of a Townsend discharge. Their analysis did not recognize the possibility of electron attachment. As these have been superseded by more recent data, they are excluded from further consideration here. Data on SF_6 including attachment were also obtained by Geballe and Harrison (as reported by Loeb⁵⁹). Bhalla and Craggs⁶⁰ also reported measured values of η/W and α/N obtained using pulsed Townsend techniques for gas densities between 16.5 and $600 \times 10^{22} \text{ m}^{-3}$. The cathode current, I_0 , needed for the data analysis is assumed constant as the electrode separation is varied, and was inferred from current-voltage measurements at fixed separation at the lowest gas densities. However, for $N \geq 80 \times 10^{22} \text{ m}^{-3}$ this technique of obtaining I_0 was inapplicable, and led to a 20% uncertainty in the derived swarm coefficients. Therefore, only the low density data are included here.

Kline and co-workers⁴⁴ also measured α/N , η^*/N , and λ/N using a Townsend discharge and Davies'²⁹ method of analysis. These authors define η^*/N as the "effective attachment coefficient" which includes the effect of detachment and subsequent ion-molecule reactions. The results of O'Neill and Craggs,⁷² discussed below, indicate that detachment is negligible for E/N at (and presumably below) $430 \times 10^{-21} \text{ V m}^2$, in which case η^*/N is equivalent to η/N . Special consideration was given to determining the E/N value for which $\lambda = 0$, which is $362 \times 10^{-21} \text{ V m}^2$. These data for η^*/N , α/N , and λ/N which are displayed as functions of E/N in Figs. 1.4, 1.5, and 1.6, respectively, along with swarm coefficients measured by Geballe and Harrison and by Bhalla and Craggs, are probably the most reliable available for E/N between 350 and $600 \times 10^{-21} \text{ V m}^2$.

FIGURE 1.4. η/N in SF_6 as a function of E/N .FIGURE 1.5. α/N in SF_6 as a function of E/N .FIGURE 1.6. λ/N in SF_6 as a function of E/N .

In 1955 McAfee⁶¹ reported results on electron attachment in SF_6 which involved examining the transient currents following a pulse of light in a Townsend discharge. These data were described as preliminary, and as later results from the same experimental group are significantly different, we assume that the 1955 data have been superceded. In 1963 McAfee and Edelson⁶² reported attachment coefficient data in SF_6 derived from a pulsed Townsend discharge, but gave no description of experimental or data analysis techniques. In 1964 Edelson and McAfee⁶³ reported a detailed description of their data analysis and used the 1963 SF_6 attachment data as an illustration. The transient currents provide detailed information about a variety of processes, and by doing an extensive statistical analysis of their data, Edelson and McAfee provide direct evidence that their derived coefficients are statistically significant. These attachment data, displayed in Fig. 1.4, are the only data available at low E/N . Although from the point-of-view of the data analysis it is statistically significant, the maximum in η/N should be treated with caution, because both calculations and the known energy dependence of the electron attachment cross section in SF_6 suggest that there is no maximum.

Other data available from steady-state Townsend discharge measurements are also displayed in the figures. Boyd and Crichton⁶³ repeated the steady-state Townsend measurements with careful attention to detail and report data for α/N and λ/N . Their measurements covered a wide range of gas densities (between 16.5 and $1320 \times 10^{22} \text{ m}^{-3}$) and lead to the conclusion, which is no longer contested, that the swarm coefficients are proportional to gas density. Their data are not significantly different from those of Harrison and Geballe. Their values for λ/N are included in Fig. 1.6.

Maller and Naidu^{64,65} also used the steady-state Townsend method. In 1975, they reported values of α/N and η/N for mixtures of SF_6 with other gases, and the following year they extended measurements to pure SF_6 and to higher values of E/N . Their α/N data are included in Fig. 1.5. Recently, Itoh and co-workers⁶⁶ determined λ/N in mixtures of SF_6 and N_2 using a pulsed Townsend discharge and extended these measurements to pure SF_6 . Their data for λ/N are given in Fig. 1.6.

Figures 1.4 and 1.5 also show data calculated by Kline and co-workers⁴⁴ and by Yoshizawa and co-workers.⁴⁶ Those of Kline and co-workers are recommended because they used more accurate cross sections.

Some other data have been reported but are not included in Figs. 1.4–1.6. Bortnik and Panoff⁶⁷ reported Townsend discharge measurements with results similar to those displayed. Dutton, Harris, and Jones⁶⁸ and Dutton and Harris⁶⁹ also reported studies of current growth in a Townsend discharge but with a tentative conclusion that the swarm coefficients were not linearly dependent on the gas density in the samples originally used, a conclusion which was not confirmed in samples from a different supplier and not evident in any other data. Many investigations have been carried out on steady-state Townsend discharges in SF_6 and, in general, the data are remarkably consistent.

Application of the pulsed Townsend technique at high E/N requires a very rapid light pulse. Teich and Branston⁷⁰ used this technique in SF_6 with a laser light source, but were

unable to identify all the phenomena contributing to their transient currents. They reached a general conclusion that detachment is an important process in SF_6 at gas densities above about $16 \times 10^{22} \text{ m}^{-3}$ but did not report detachment data. In some special circumstances the observations could be interpreted adequately to yield values of λ in the E/N range between 108 and $130 \times 10^{-21} \text{ V m}^2$. The results of this measurement are not significantly different from those obtained from the steady-state Townsend method.

Eccles and co-workers⁷¹ reported detachment data, but with no identification of the detaching ion species. The relative ion concentrations change with N and E/N . Their principal conclusion is that for low E/N the detachment coefficient is so small that it is negligible in the analysis of steady-state Townsend currents.

To obtain detachment data, O'Neill and Craggs⁷² used a double-gas drift tube arrangement in which negative ions were formed by attachment in the first chamber and detached in the second. Negative ions reaching the anode were identified by mass analysis. The density dependence of the anode current implied that either the detachment was not a two-body process or that the detaching species were involved in some other competing process, the rate of which was dependent on N . The detachment coefficient for SF_6^- was determined from the analysis of the negative-ion current and the current growth curves utilizing a reaction scheme including attachment, ionization, detachment and charge transfer, and ion-conversion reactions involving SF_5^- and F^- as well as SF_6^- . It was estimated to be $0.8 \times 10^{-22} \text{ m}^2$ for $E/N = 433 \times 10^{-21} \text{ V m}^2$ and $N = 16 \times 10^{22} \text{ m}^{-3}$. This supports Eccles' conclusion that detachment from SF_6^- is negligible in the analysis of steady state Townsend measurements.

Except for the work of Kline and co-workers, analyses of steady-state Townsend data have included the assumption that electron detachment is negligible. In SF_6 gas it is likely that more than one negative ion species is present, and some of these may be in excited states. Following attachment any excitation can be expected to decay and ion-molecule reactions will produce other ion species. Meaningful data on the detachment coefficients, including specification of the ion species and the state of excitation, are needed in SF_6 .

5.2. Halogenated Hydrocarbons

These electronegative compounds which are chemically inert and thermally stable are among the best gaseous insulators. Data on transport properties and swarm coefficients have been obtained primarily for two groups of these gases: (1) the perfluoroalkanes, $\text{C}_n\text{F}_{2n+2}$, i.e., CF_4 , C_2F_6 , C_3F_8 , and C_4F_{10} , and (2) dichlorofluoromethane (CCl_2F_2) and similar compounds, but data on properties of other halocarbon compounds are also available.

a. Drift Velocity, Halogenated Hydrocarbons

Using standard drift tube techniques, Naidu and Prasad⁷³ measured the drift velocity for all of the first four perfluoroalkanes: for E/N between 120 and $270 \times 10^{-21} \text{ V m}^2$ for CF_4 , and for E/N between 270 and $600 \times 10^{-21} \text{ V m}^2$ for C_2F_6 , C_3F_8 , and C_4F_{10} , and for N between 2 and $10 \times 10^{22} \text{ m}^{-3}$. In an earlier conference proceedings,⁷⁴ Prasad and

Naidu reported drift velocities and swarm coefficients for electrons in C_3F_8 , but it is assumed that this publication is superceded by Ref. 73 which covers the same range of E/N . Christophorou and co-workers⁷⁵ measured the drift velocity in CF_4 for much lower average electron energies, i.e., for $0.1 < E/N < 12 \times 10^{-21} \text{ V m}^2$.

The two sets of data for CF_4 are shown in Fig. 2.1 which suggest that, as with N_2 , there is a broad range of E/N over which W does not monotonically increase with E/N . The data of Naidu and Prasad for C_2F_6 , C_3F_8 , and C_4F_{10} are given in Fig. 2.2. The electron drift velocity at a given E/N decreases as the size of the molecule increases and is independent of gas density. These, the only data available, are recommended to the user.

Using the same techniques, Naidu and Prasad⁷⁶ measured the only reported values of the electron drift velocity in CCl_2F_2 , and these data are plotted in Fig. 2.3.

b. (Diffusion Coefficient)/Mobility, Halogenated Hydrocarbons

Naidu and Prasad⁷³ observed the radial diffusion of electrons and negative ions using a multiple-ring collector to obtain values of D_T/μ for the first four perfluoroalkanes (CF_4 , C_2F_6 , C_3F_8 , C_4F_{10}). Their data were derived from measurements of the ratio of currents to adjacent rings for two separate gap lengths.

Lakshminarasimha, Lucas, and Price,⁷⁷ with a more sophisticated analysis technique employing the full radial current-distribution profile and current amplification to obtain D_T/μ in CF_4 , extended measurements to much lower values of E/N . The results of these two measurements in CF_4 are compared in Fig. 2.4. The data of Naidu and Prasad are somewhat lower than those of Lakshminarasimha and co-workers. The slight gas density dependence of D_T/μ observed in other perfluoroalkanes was not observed in CF_4 .

For C_2F_6 , C_3F_8 , and C_4F_{10} , the values of D_T/μ measured by Naidu and Prasad,⁷³ shown in Fig. 2.5, are the only data that have been reported. For C_3F_8 and C_4F_{10} these authors observed an increase in D_T/μ with gas density for N between 2 and $10 \times 10^{22} \text{ m}^{-3}$. Again, earlier measurements on C_3F_8 by Prasad and Naidu⁷⁴ are assumed superceded by the values reported in Ref. 73.

Naidu and Prasad⁷⁶ also reported data on D_T/μ in CCl_2F_2 for E/N between 300 and $650 \times 10^{-21} \text{ V m}^2$, measured using the same technique at gas densities of 2 and $6.7 \times 10^{22} \text{ m}^{-3}$. These data display a large scatter for $E/N < 390 \times 10^{-21} \text{ V m}^2$. Naidu and Prasad attribute this to uncertainties of $\pm 3\%$ in E/N which, in turn, lead to uncertainties of up to 10% in the values of α and η used in determining D_T/μ . Naidu and Prasad estimate an uncertainty in D_T/μ of $\pm 2\%$ for E/N above $390 \times 10^{-21} \text{ V m}^2$. Maller and Naidu⁵¹ measured the transport coefficients in mixtures of CCl_2F_2 with nitrogen and, as part of this work, reported values of D_T/μ for pure CCl_2F_2 with an uncertainty of $\pm 15\%$ for $E/N = 390 \times 10^{-21} \text{ V m}^2$ and 6% for E/N above $450 \times 10^{-21} \text{ V m}^2$. The two sets of experimental data are compared in Fig. 2.6, which shows that the data of Naidu and Prasad are consistently lower than those of Maller and Naidu, although the two sets agree to within the errors estimated by the authors. The data of Maller and Naidu, which extend over a broader range of E/N , are recommended.

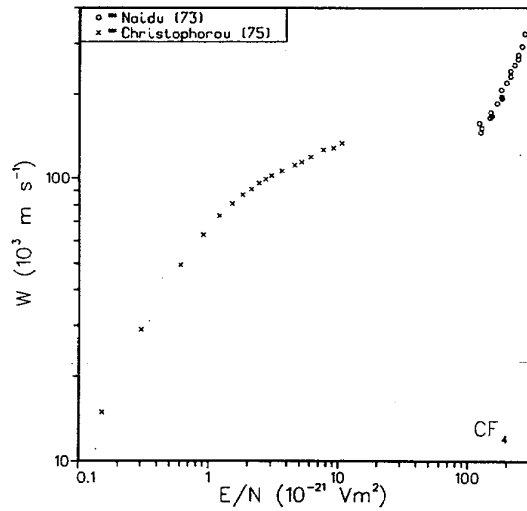


FIGURE 2.1. W for electrons in CF_4 as a function of E/N .

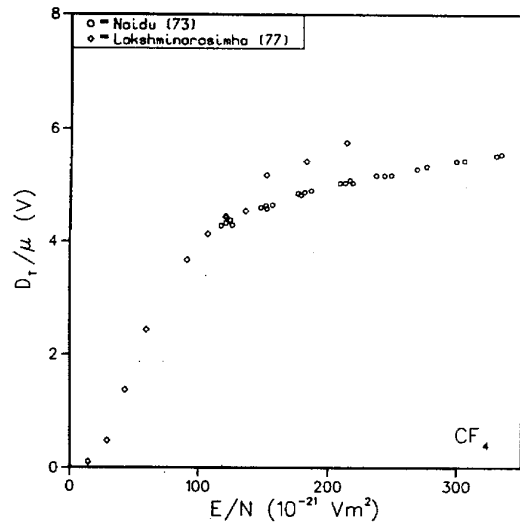


FIGURE 2.4. D_T/μ in CF_4 as a function of E/N .

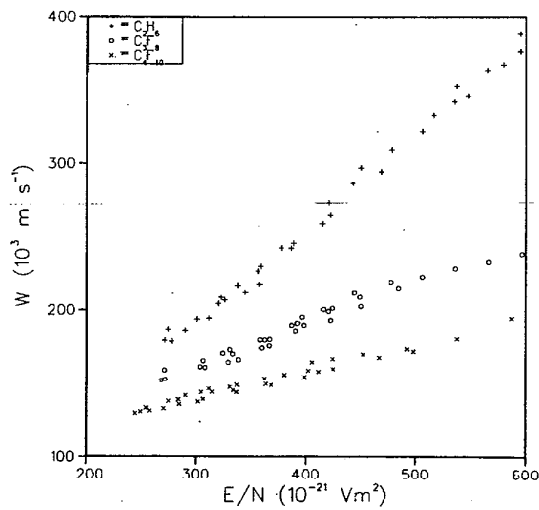


FIGURE 2.2. W for electrons in C_2F_6 , C_3F_8 , and C_4F_{10} as functions of E/N . All data were taken from Naidu and Prasad (Ref. 73).

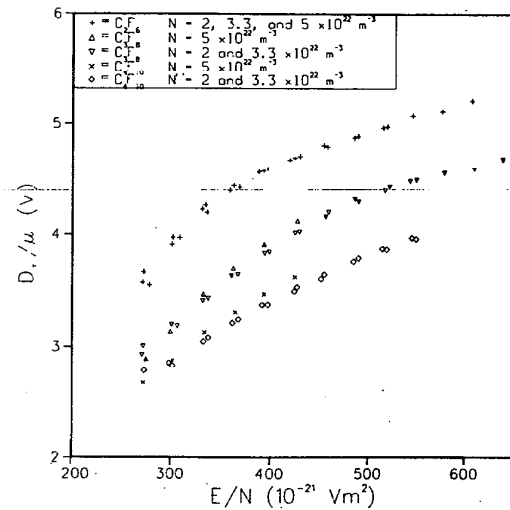


FIGURE 2.5. D_T/μ in C_2F_6 , C_3F_8 , and C_4F_{10} as functions of E/N . All data were taken from Naidu and Prasad (Ref. 73).

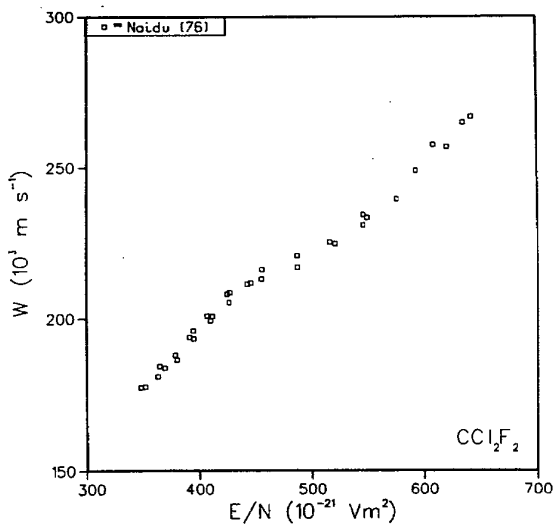


FIGURE 2.3. W for electrons in CCl_2F_2 as a function of E/N .

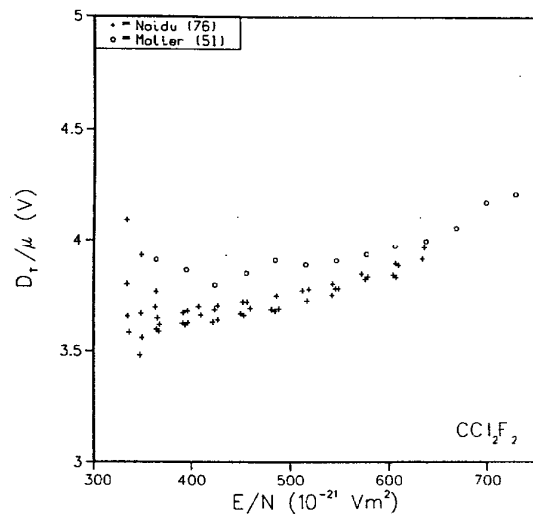


FIGURE 2.6. D_T/μ in CCl_2F_2 as a function of E/N .

c. Electron Gain and Loss Processes, Halogenated Hydrocarbons

Perfluoroalkanes

In 1958 Howard⁷⁸ reported the first data on electron gain and loss processes in the perfluoroalkanes. These were values of λ/N in CF_4 obtained for $N = 760 \times 10^{22} \text{ m}^{-3}$ using spatial current growth techniques. In 1963 Moruzzi and Craggs⁷⁹ reported η/N , α/N , and λ/N in C_3F_8 obtained for gas densities between 3.3 and $33 \times 10^{22} \text{ m}^{-3}$ also using spatial current growth techniques. For a given E/N and N between 3.3 and $8 \times 10^{22} \text{ m}^{-3}$, these authors reported an increase in η/N and a decrease in α/N with increasing N . Subsequently, in a conference proceedings, Devins and Wolff⁸⁰ reported attachment and ionization coefficients for all of the first four perfluoroalkanes obtained using similar experimental methods, again for gas densities between 3.3 and $33 \times 10^{22} \text{ m}^{-3}$. An increase of η/N with increasing gas density was reported for C_4F_{10} only.

Bozin and Goodyear⁸¹ also used spatial current growth techniques to repeat measurements of η/N , α/N , and λ/N in CF_4 and C_2F_6 with an interest in identifying detachment effects. The coefficients obtained for CF_4 for N between 16 and $70 \times 10^{22} \text{ m}^{-3}$ and for C_2F_6 for N between 8 and $30 \times 10^{22} \text{ m}^{-3}$ showed no systematic trend with N , but displayed a scatter of 25% for data taken at different N . These authors detected no detachment for CF_4 in the gas density range studied, but suggested a detachment coefficient (δ/N) of the order of $0.01 \times 10^{-22} \text{ m}^2$ may be appropriate for C_2F_6 in the range of experimental conditions studied. Mass spectrometric studies which would have identified the detaching ion were not made.

Using the same apparatus, Razzak and Goodyear⁸² made similar measurements in C_4F_{10} and confirmed the gas density dependence of η/N reported by Devins and Wolff. The observed increase in η/N with gas density is interpreted as due to an ion-molecule reaction which was not identified. No evidence for detachment was found.

Bortnik and Panov⁶⁷ also used spatial current growth techniques to obtain η/N and α/N in CF_4 and C_2F_6 for gas densities between 6 and $106 \times 10^{22} \text{ m}^{-3}$.

Using the experimental and analytic techniques described in Sec. 5.2.b, Naidu and Prasad⁷³ superseding Ref. 74 measured η/N , α/N , and λ/N for all the perfluoroalkanes at low gas densities (between 2 and $7 \times 10^{22} \text{ m}^{-3}$). Their purpose was to clarify gas density effects and compare measured attachment coefficients with those calculated from measured cross sections for electron-impact formation of F^- , assuming a Maxwellian energy distribution function. No systematic dependence on gas density was observed for CF_4 and C_2F_6 but a scatter of up to 20% existed in the data reported. An increase of η/N with N was observed for C_3F_8 and C_4F_{10} , in agreement with earlier work. No gas density dependence of α/N was observed for any of these gases. The calculated attachment coefficients were higher by approximately a factor of 4 than those measured, indicating either a non-Maxwellian electron distribution function or a more complex negative ion reaction scheme than incorporated in the calculation.

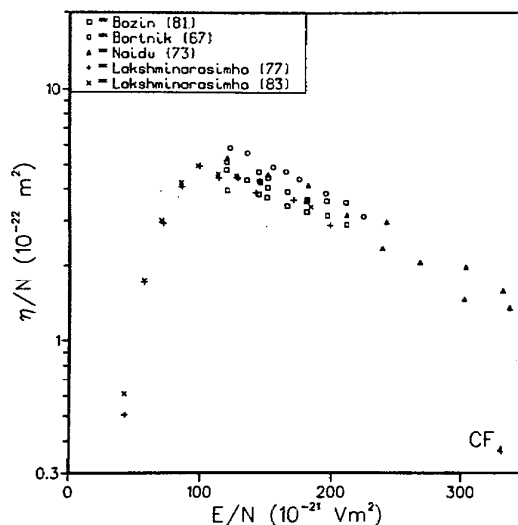


FIGURE 2.7. η/N in CF_4 as a function of E/N .

Lakshminarasimha, Lucas, and Price⁷⁷ used their analysis of current amplification and radial distribution profile of the anode current in a dc discharge to obtain η/N and α/N in CF_4 for E/N between 50 and $350 \times 10^{-21} \text{ V m}^{-2}$.

Lakshminarasimha, Lucas, and Snelson⁸³ used temporal current growth techniques in CF_4 to separate the current due to the primary electrons from that due to negative ions formed by attachment and delayed currents due to detaching electrons and thus obtained more reliable values of α/N and η/N .

The data for η/N , α/N , and λ/N in CF_4 are collected in Figs. 2.7, 2.8, and 2.9, respectively, with the exception of the early data reported by Devins and Wolff which show no remarkable contrast to data reported subsequently. For the attachment data shown in Fig. 2.7 there is reasonable agreement between the various reported values. The data of Lakshminarasimha and co-workers are recommended for E/N up to $200 \times 10^{-21} \text{ V m}^{-2}$. Above this value, those of

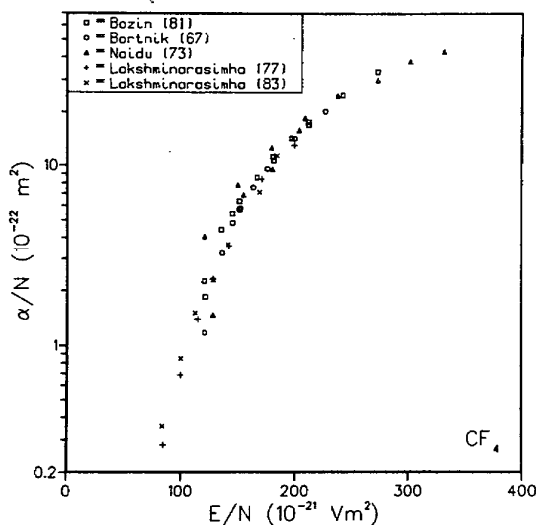
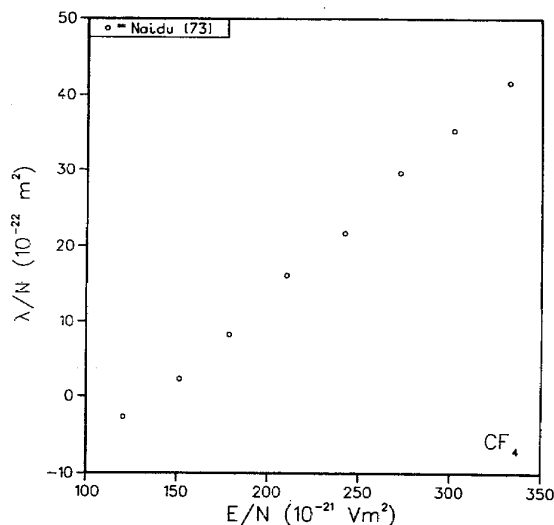


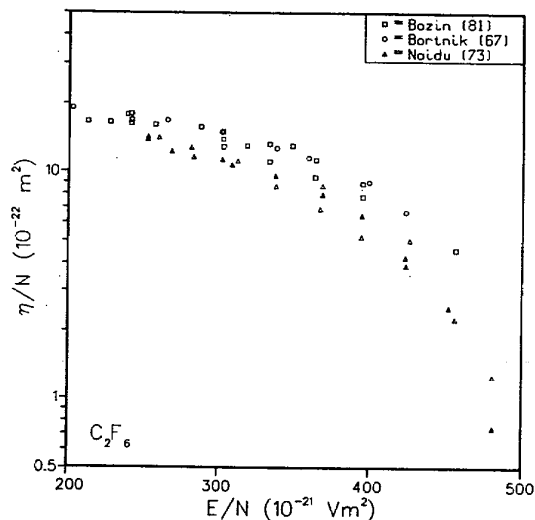
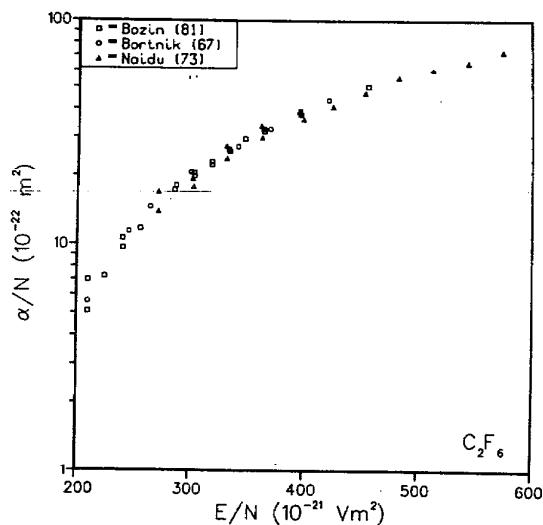
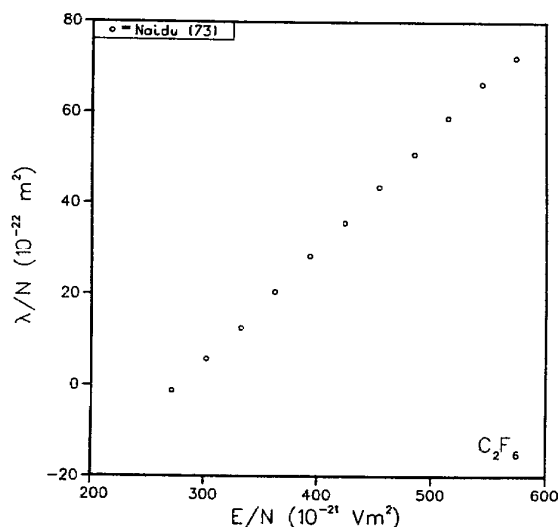
FIGURE 2.8. α/N in CF_4 as a function of E/N .

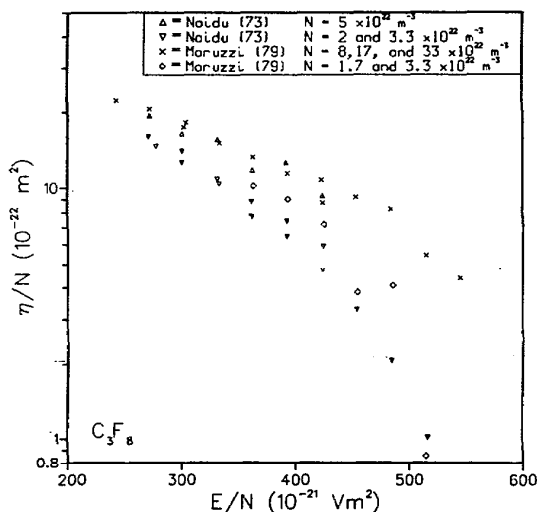
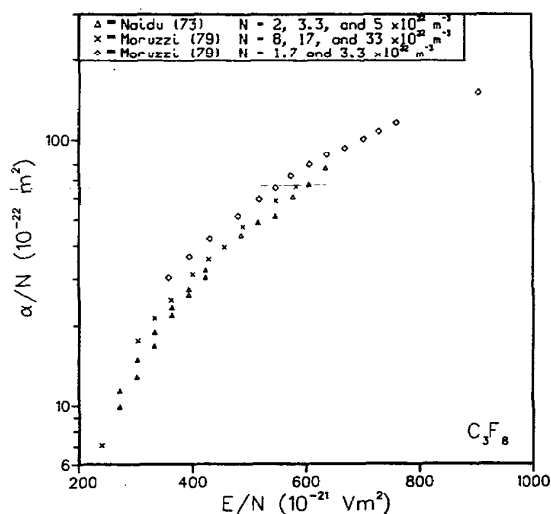
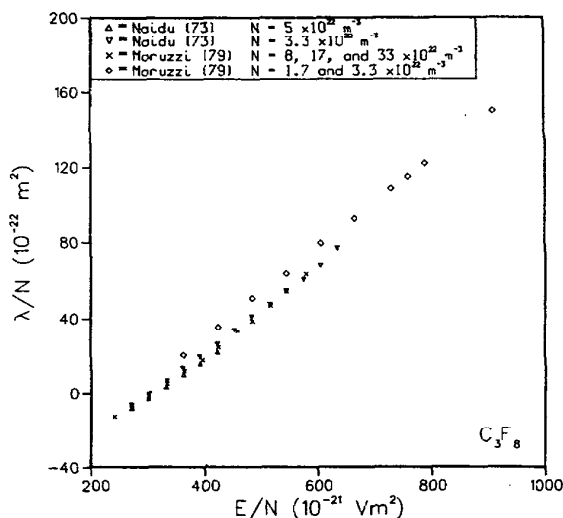
FIGURE 2.9. λ/N in CF_4 as a function of E/N .

Naidu and Prasad are recommended, although the scatter in these data introduced an uncertainty of $\pm 12\%$. The ionization data are shown in Fig. 2.8. The more recent data of Lakshminarasimha and co-workers⁸³ are recommended for E/N up to $180 \times 10^{-21} \text{ V m}^2$. For low E/N , the Naidu and Prasad data taken at $N = 2$ and $5 \times 10^{22} \text{ m}^{-3}$ differ by a factor of 3, but this effect becomes negligible for E/N above $200 \times 10^{-21} \text{ V m}^2$, where these data are recommended. The values of λ/N measured by Naidu and Prasad are shown in Fig. 2.9.

For C_2F_6 , the data on η/N and α/N obtained in three different investigations are displayed in Figs. 2.10 and 2.11, respectively. For η/N , there is considerable scatter in the data. Although the results of Bozin and Goodyear are recommended as a reasonable working set, a large uncertainty ($\pm 25\%$) should be assigned to these data. For α/N , the scatter is less. The data of Bortnik and Panov are recommended for E/N below $400 \times 10^{-21} \text{ V m}^2$, and those of Naidu and Prasad, for higher E/N . The only reported data for λ/N in C_2F_6 are given in Fig. 2.12.

For C_3F_8 the values of η/N reported by Naidu and Prasad and by Moruzzi and Craggs are compared in Fig. 2.13. Moruzzi and Craggs report an N dependence of η/N for N below $8 \times 10^{22} \text{ m}^{-3}$. In this range, their data are approximately 25% higher than those of Naidu and Prasad. Moruzzi and Craggs report no N dependence for N between 8 and $33 \times 10^{22} \text{ m}^{-3}$, and their data for this range agree well with those of Naidu and Prasad for $N = 5 \times 10^{22} \text{ m}^{-3}$. The data of Moruzzi and Craggs, which extend over broader ranges of N and E/N , are recommended. The values of α/N in C_3F_8 taken from these two works are compared in Fig. 2.14. Moruzzi and Craggs reported a slight decrease with increasing N for N between 3 and $8 \times 10^{22} \text{ m}^{-3}$ and no change with N for N between 8 and $33 \times 10^{22} \text{ m}^{-3}$. These effects are not large, and no interpretation of the ion-molecule reaction scheme using mass spectrographic techniques has been made to explain them. An uncertainty of $\pm 20\%$ should be applied to any of these data. Data on λ/N in C_3F_8 determined from these two investigations, shown in Fig.

FIGURE 2.10. η/N in C_2F_6 as a function of E/N .FIGURE 2.11. α/N in C_2F_6 as a function of E/N .FIGURE 2.12. λ/N in C_2F_6 as a function of E/N .

FIGURE 2.13. η/N in C_3F_8 as a function of E/N .FIGURE 2.14. α/N in C_3F_8 as a function of E/N .FIGURE 2.15. λ/N in C_3F_8 as a function of E/N .

2.15, are subject to the same confusion concerning gas density dependence, and the same uncertainty should be applied to them.

Figure 2.16 compares data for η/N for C_4F_{10} measured by Naidu and Prasad and by Razzak and Goodyear. The results reported by Razzak and Goodyear were taken over a broader gas density range (3 to $70 \times 10^{22} \text{ m}^{-3}$) and clearly display the increase of η/N with increasing gas density. For $N = 3.3 \times 10^{22} \text{ m}^{-3}$, the two data sets show considerable disagreement, and no recommendations can be made. For $N = 6.7 \times 10^{22} \text{ m}^{-3}$, the two sets agree reasonably well, and those of Razzak and Goodyear, which extend over a wider range of E/N , are recommended. For higher N , the user should keep in mind that η/N changes with N .

Figure 2.17 compares α/N determined by these two investigations, neither of which reported an N dependence. The two sets for η/N taken at the same gas density are in reasonable agreement, as are those for α/N which display no N dependence. Figure 2.18, which gives λ/N , clearly reflects the increase of η/N and, hence, the decrease of λ/N with N . The two sets of data taken at $N = 6.7 \times 10^{22} \text{ m}^{-3}$ agree well.

CCl_2F_2

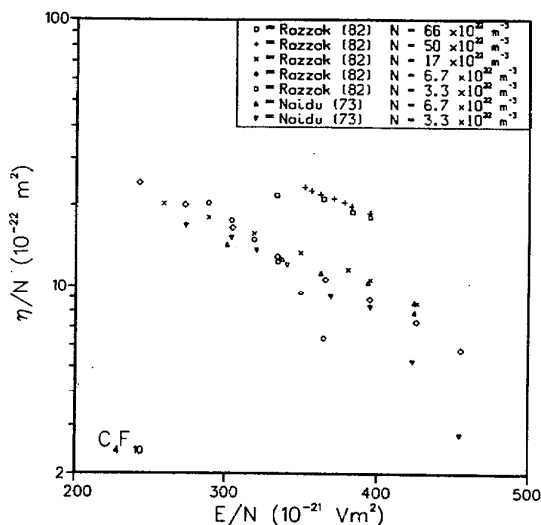
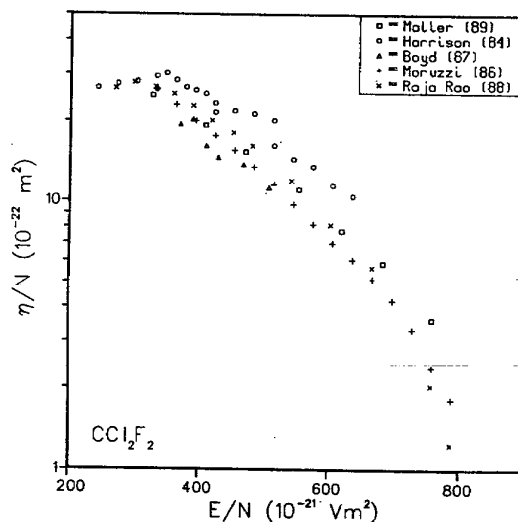
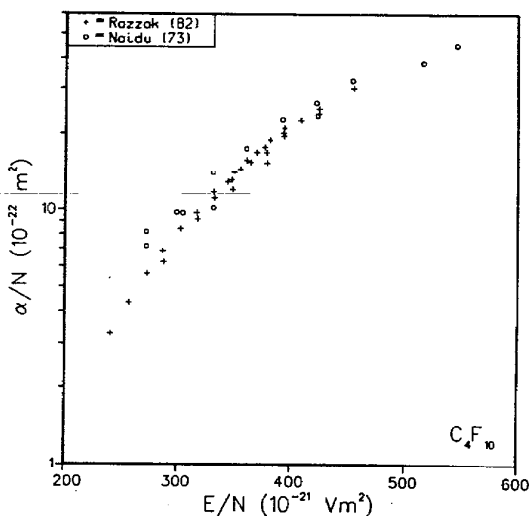
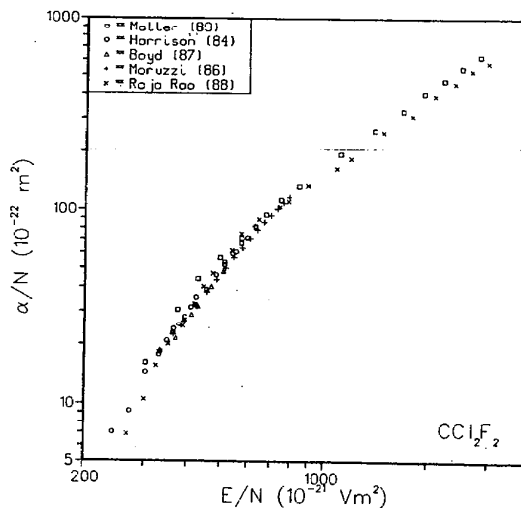
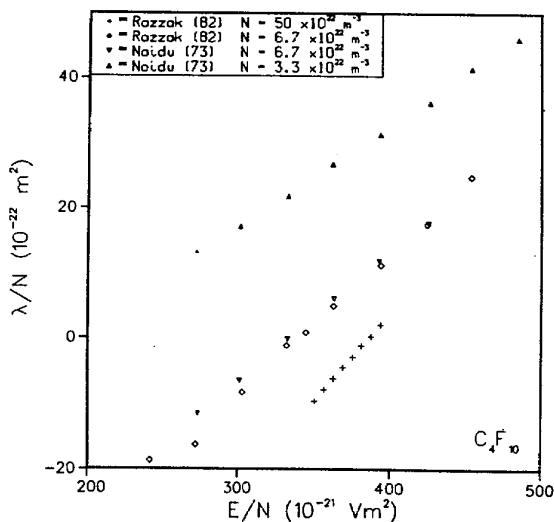
In CCl_2F_2 , the earliest measurements of the attachment and ionization coefficients were made by Harrison and Geballe⁸⁴ in 1953 using spatial current growth techniques. Subsequently, Schlumbohm⁸⁵ analyzed the temporal growth of prebreakdown currents to obtain the electron growth constant, λ/N . Moruzzi⁸⁶ also measured the ionization and attachment coefficients using spatial current growth techniques for gas densities between 16 and $70 \times 10^{22} \text{ m}^{-3}$.

Boyd, Crichton, and Munknielsen⁸⁷ used current growth techniques to determine ionization and attachment coefficients for N between 16 and $70 \times 10^{22} \text{ m}^{-3}$, but also extended measurements of λ/N up to $N = 2000 \times 10^{22} \text{ m}^{-3}$. A decrease of λ/N with increasing gas density was observed.

Raja Rao and Govinda Raju⁸⁸ also used spatial current growth techniques to determine ionization and attachment coefficients in pure CCl_2F_2 in connection with their studies of CCl_2F_2 -air mixtures. They extended their measurements to much higher values of E/N (up to $3000 \times 10^{-21} \text{ V m}^{-2}$). For E/N above $900 \times 10^{-21} \text{ V m}^{-2}$, attachment could not be separated accurately from the ionization coefficient measurements, and λ/N was reported. Between 500 and $800 \times 10^{-21} \text{ V m}^{-2}$, η/N was found to be slightly dependent on gas density, a result consistent with the findings of Boyd and co-workers.

In their study of swarm coefficients in mixtures of CCl_2F_2 and nitrogen, Maller and Naidu⁸⁹ obtained values of α/N and η/N in pure CCl_2F_2 , using spatial current growth techniques for $300 < E/N < 750 \times 10^{-21} \text{ V m}^{-2}$ and the similar pressure current growth technique (see Huxley and Crompton's book, Ref. 2, p. 500) for E/N up to $3000 \times 10^{-21} \text{ V m}^{-2}$. Risbud and Naidu⁹⁰ also fit the experimental data of Maller and Naidu.

Figure 2.19 compares the data for η/N in CCl_2F_2 . With the exception of the early measurements, the experimental data agree to within $\pm 15\%$. Those of Raja Rao are recommended as a reasonable working set which extends over the

FIGURE 2.16. η/N in C_4F_{10} as a function of E/N .FIGURE 2.19. η/N in CCl_2F_2 as a function of E/N .FIGURE 2.17. α/N in C_4F_{10} as a function of E/N .FIGURE 2.20. α/N in CCl_2F_2 as a function of E/N .FIGURE 2.18. λ/N in C_4F_{10} as a function of E/N .

widest range of E/N . The data for α/N , compared in Fig. 2.20, are in good agreement. Those of Raja Rao are recommended for E/N up to $900 \times 10^{-21} \text{ V m}^2$. For higher E/N those of Moller and Naidu are recommended because Raja Rao did not correct for detachment.

Other Halogenated Hydrocarbons

A research group at Oak Ridge led by L. G. Christophorou has studied attachment in an extensive series of halogenated hydrocarbons mixed in trace quantities in nonattaching "carrier," or "buffer" gases, typically Ar, N_2 , or C_2H_4 . Sampling techniques are used to determine the electron drift velocity, and the pulse-shape method is used to determine the attachment coefficient (see Christophorou's book, Ref. 3, p. 441). The product of these quantities $\eta W/N$,

the rate of electron attachment, is thus determined as a function of E/N . The reader is referred to the original references identified below for details of these mixture studies.

In the swarm-beam technique Christophorou and co-workers⁹¹ combined these data with results of electron beam measurements to determine the cross section for dissociative attachment in the buffer gas. Subsequently Christophorou and co-workers⁹² developed a method for determining cross sections from the swarm data alone in cases where electron attachment resonances peak sharply at thermal energies. Christophorou, McCorkle, and Anderson⁹³ also developed a procedure whereby the electron attachment cross section as a function of electron energy could be unfolded from the attachment rates taken in a carrier gas of known distribution function, such as nitrogen or argon. To apply these data to mixtures with more than a trace of the halogenated hydrocarbons would require a knowledge of elastic and inelastic electron scattering cross sections for the halogenated hydrocarbons.

The distribution function of the carrier gas is normally determined from solutions of the Boltzmann equation using experimentally determined cross sections for electron collision processes. As shown in Christophorou's book, Ref. 3, Chap. 4, the nitrogen and argon distribution functions are large over adjacent energy ranges. The distribution functions for these two gases have been redetermined recently using newly available cross sections.^{94,95} Thus, these are suitable as carrier gases. The data for an attaching component are found to be independent of carrier gas in the region of overlapping energy in most cases.

In a continuing program to identify gaseous dielectrics with desirable breakdown characteristics, the Oak Ridge group has applied these techniques to an extensive series of halogenated hydrocarbons.^{94,96-100} Christophorou¹⁰¹ has recently reviewed the processes occurring in these systems, the data resulting from these studies, and related data. The data for the halogenated hydrocarbons, presented as originally reported as attachment rates as functions of mean electron energy, are given in Figs. 2.21 and 2.31.

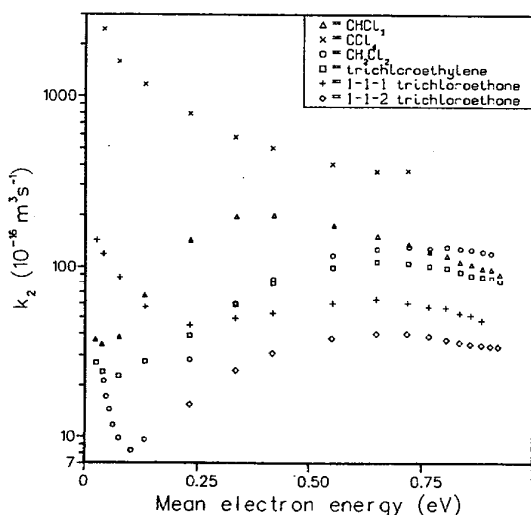


FIGURE 2.21. k_2 in CHCl_3 , CCl_4 , CH_2Cl_2 , trichloroethylene, 1-1-1 trichloroethane, and 1-1-2 trichloroethane as functions of the mean electron energy. All data were taken from Christodoulides and Christophorou (Ref. 96).

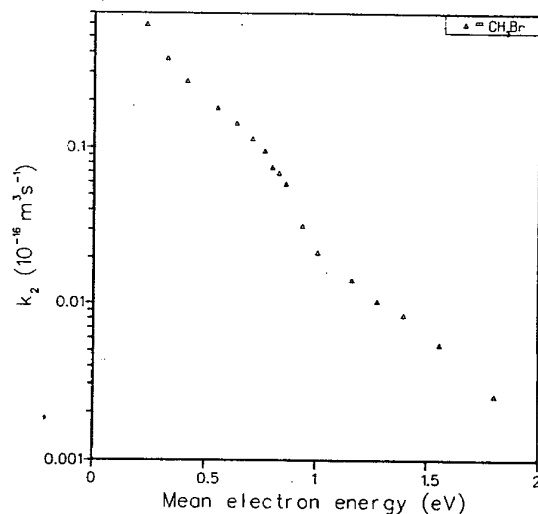


FIGURE 2.22. k_2 in CH_3Br as a function of mean electron energy. The data were taken from Christodoulides and Christophorou (Ref. 96).

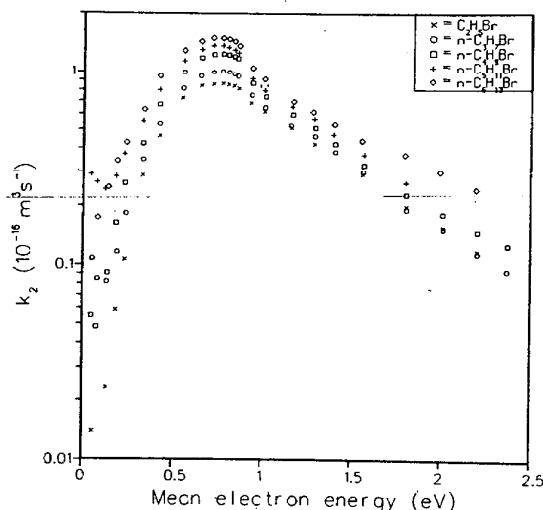


FIGURE 2.23. k_2 in $\text{C}_2\text{H}_5\text{Br}$, $n\text{-C}_3\text{H}_7\text{Br}$, $n\text{-C}_4\text{H}_9\text{Br}$, $n\text{-C}_5\text{H}_{11}\text{Br}$, and $n\text{-C}_6\text{H}_{13}\text{Br}$ as functions of the mean electron energy. All data were taken from Christodoulides and Christophorou (Ref. 96).

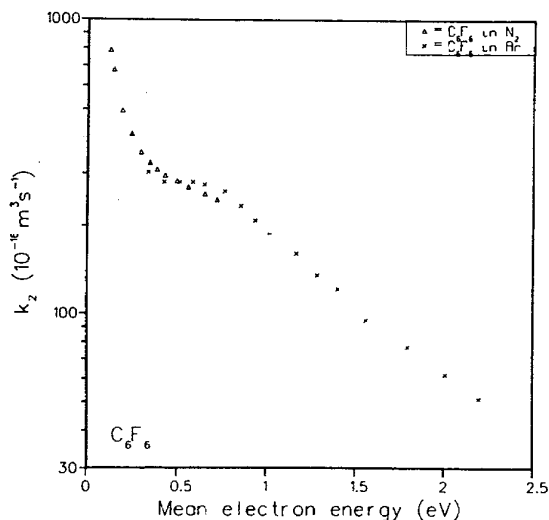


FIGURE 2.24. k_2 in C_6F_6 as a function of the mean electron energy. All data were taken from Gant and Christophorou (Ref. 97).

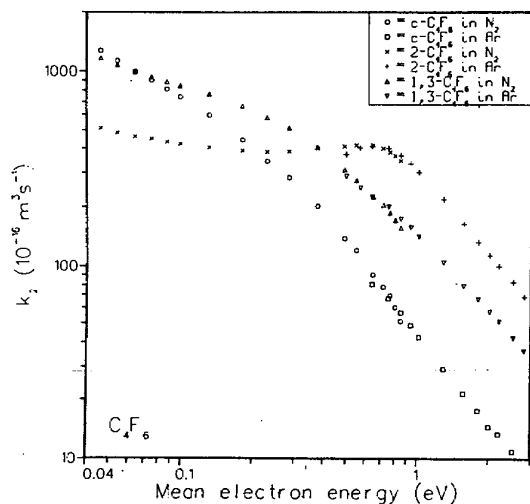


FIGURE 2.25. k_2 in $c\text{-C}_4\text{F}_6$, $2\text{-C}_4\text{F}_6$ and $1,3\text{-C}_4\text{F}_6$ as functions of the mean electron energy. All data were taken from Christodoulides and co-workers (Ref. 98).

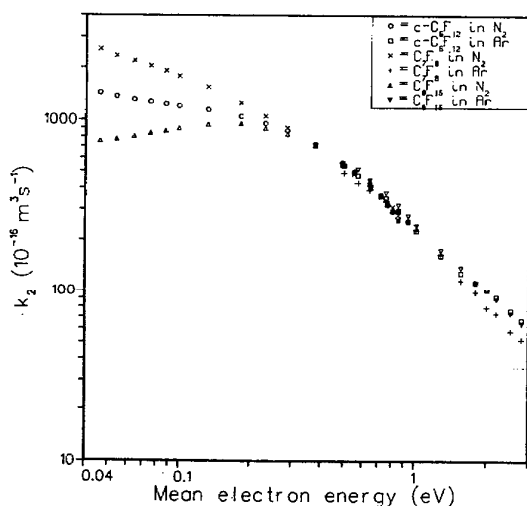


FIGURE 2.28. k_2 in $c\text{-C}_6\text{F}_{12}$, C_7F_8 , and C_8F_{16} as functions of mean electron energy. The data were taken from Pai and co-workers (Ref. 99).

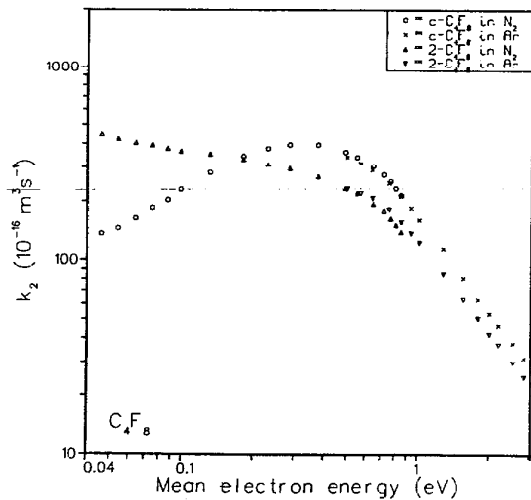


FIGURE 2.26. k_2 in $c\text{-C}_4\text{F}_8$ and $2\text{-C}_4\text{F}_8$ as functions of mean electron energy. All data were taken from Christodoulides and co-workers (Ref. 98).

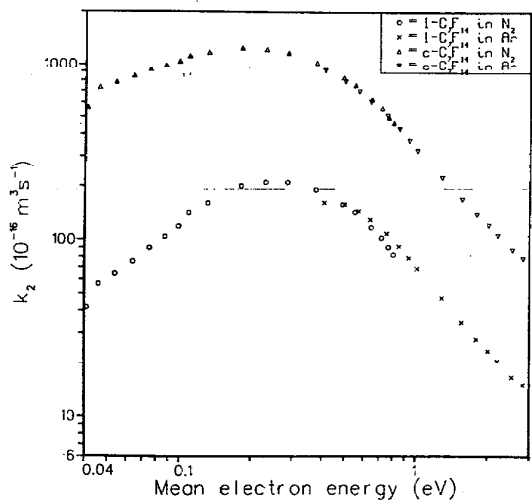


FIGURE 2.29. k_2 in $1\text{-C}_7\text{F}_{14}$ and $c\text{-C}_7\text{F}_{14}$ as functions of mean electron energy. The data were taken from Christodoulides and Christophorou (Ref. 100).

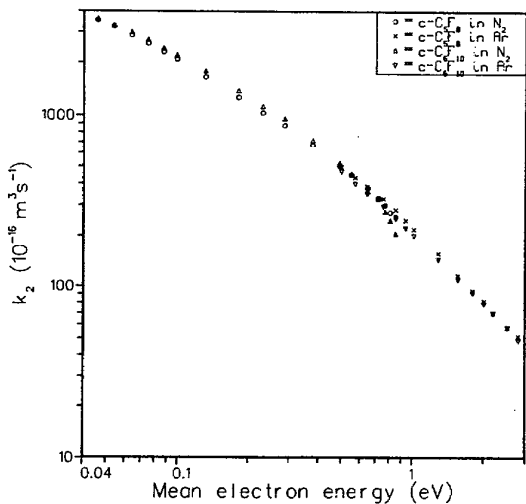


FIGURE 2.27. k_2 in $c\text{-C}_5\text{F}_8$ and $c\text{-C}_6\text{F}_{10}$ as functions of mean electron energy. All data were taken from Pai and co-workers (Ref. 99).

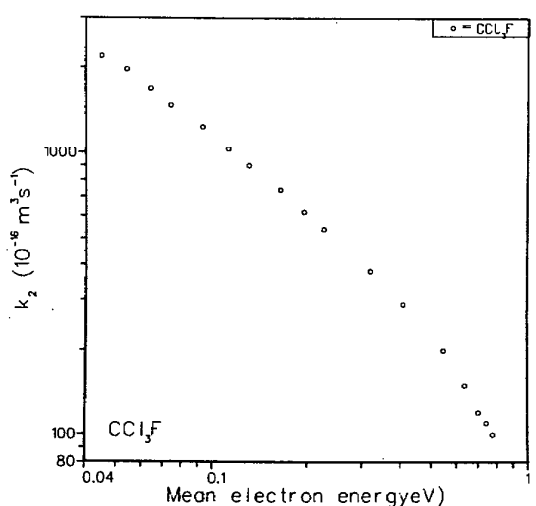


FIGURE 2.30. k_2 in CCl_3F as a function of mean electron energy. The data were taken from McCorkle and co-workers (Ref. 94).

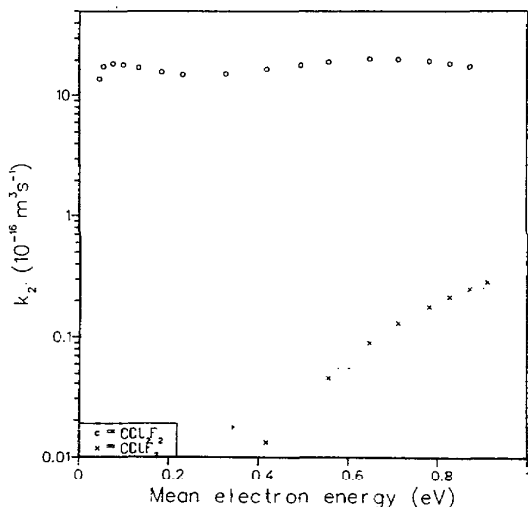


FIGURE 2.31. k_2 in CCl_2F_2 and CClF_3 as functions of E/N . The data were taken from McCorkle and co-workers (Ref. 94).

5.3. Oxygen

Oxygen is of particular interest as a major constituent of the most common insulator, air, and has been the subject of extensive research. It is one of the gases discussed by Dutton,¹ and electron swarm data in oxygen have also been reviewed by Huxley and Crompton,² Parkes²⁵ and Rees.²¹ Oxygen is experimentally difficult because the interaction of the electron swarm with the gas molecules is superimposed on a complex ion-molecule chemistry, making observations difficult to interpret. It is useful to define three regions of E/N , characterized by the relative importance of various electron density-changing processes, in discussing swarm data in oxygen. In the low E/N region ($E/N \leq 12 \times 10^{-21} \text{ V m}^2$), three-body attachment is the dominant electron density-changing process, and the rapid decrease in n for low E/N limits the range of experimental parameters for which W and DN can be measured.¹⁰² In the intermediate E/N range, between 12 and $60 \times 10^{-21} \text{ V m}^2$, two-body dissociative attachment becomes significant. For high E/N ($\geq 60 \times 10^{-21} \text{ V m}^2$), detachment occurs and ionization is a major effect.

a. Drift Velocity, O_2

Both Dutton¹ and Huxley and Crompton² report the results of many measurements of the electron drift velocity in oxygen made prior to 1973. For these data in the low E/N region, Nelson and Davis³⁴ used the drift-dwell-drift technique to extend measurements down to $E/N = 0.01 \times 10^{-21} \text{ V m}^2$, obtaining values of W considerably larger than those calculated by Hake and Phelps,¹⁰³ the only other data available for comparison for E/N below $0.1 \times 10^{-21} \text{ V m}^2$. Many measurements have been made for E/N between 0.2 and $10 \times 10^{-21} \text{ V m}^2$, typically using the shutter techniques described in Sec. 3.1. Although there is some dispersion, the results of these are in reasonable agreement (see Dutton¹), and values of W calculated by Hake and Phelps¹⁰³ compare well with the measurements. Dutton also reports drift veloc-

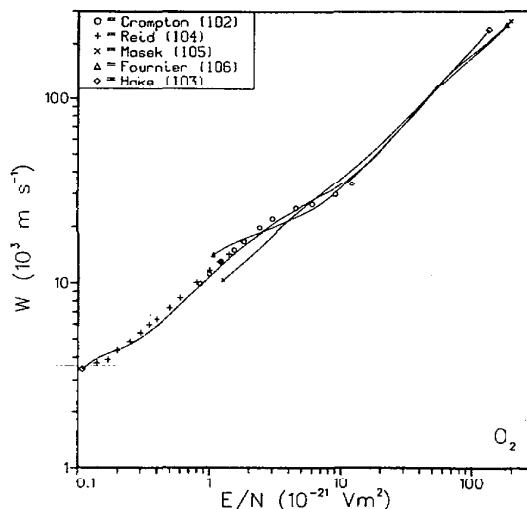


FIGURE 3.1. W for electrons in O_2 as a function of E/N .

ities for the region of high E/N obtained with shutter techniques and from studies of pulsed avalanches.

Recent measurements have concentrated entirely on the region of low E/N . Crompton and Elford¹⁰² used conventional shutter techniques to measure W for E/N between 0.8 and $12 \times 10^{-21} \text{ V m}^2$. They also discuss limitations imposed by this technique on the range of experimental parameters for which accurate measurements of the drift velocity in oxygen can be made. They corrected their measurements for the effects of both attachment and diffusion with an estimated error of $\leq 2\%$ for the higher values of E/N and somewhat greater for $E/N \leq 1 \times 10^{-21} \text{ V m}^2$. Reid and Crompton,¹⁰⁴ using an rf technique that detects only electrons (and not the background negative ions), extended these measurements down to $0.14 \times 10^{-21} \text{ V m}^2$. The uncertainty claimed is 5% at the lowest values of E/N and 2% at higher E/N . The only other experimental values of W in O_2 reported for $E/N \leq 1.0 \times 10^{-21} \text{ V m}^2$, those of Nelson and Davis,³⁴ are somewhat higher than the recent values of Reid and Crompton.

Both Masek and co-workers¹⁰⁵ and Fournier and co-workers,¹⁰⁶ using conventional two-term expansions, have completed numerical solutions of the Boltzmann equation to obtain the drift velocity in oxygen. These are compared with data of Crompton and Elford and of Reid and Crompton in Fig. 3.1. The values calculated by Hake and Phelps¹⁰³ are also shown to aid in making comparisons with earlier data.

The recommended data are those measured by Reid and Crompton for E/N between 0.1 and $1.4 \times 10^{-21} \text{ V m}^2$ and by Crompton and Elford for E/N between 1 and $12 \times 10^{-21} \text{ V m}^2$. For E/N between 12 and $200 \times 10^{-21} \text{ V m}^2$, the calculated data agree closely. For E/N above $200 \times 10^{-21} \text{ V m}^2$, the measured data presented by Dutton¹ are recommended.

b. (Diffusion Coefficient)/Mobility, O_2

The data available prior to 1973 on D_T/μ and D_L/μ in oxygen have been reviewed by both Dutton¹ and Huxley and Crompton.² Values of D_T/μ measured by Huxley and co-

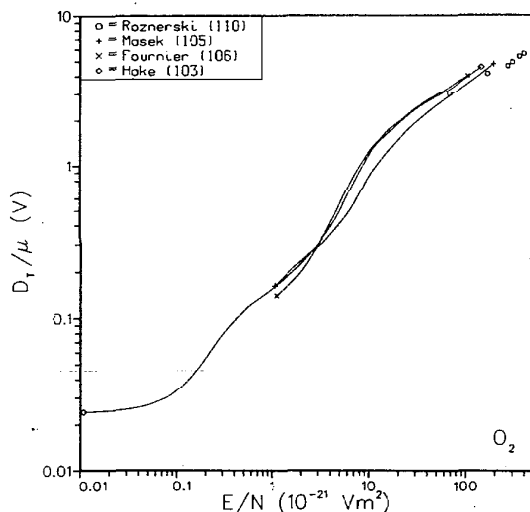


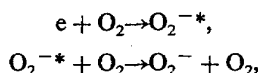
FIGURE 3.2. D_1/μ in O_2 as a function of E/N .

workers,¹⁰⁷ Rees,¹⁰⁸ and Naidu and Prasad¹⁰⁹ which have a quoted error of less than 3% are in good agreement with values calculated by Hake and Phelps.¹⁰³ The only data reported recently are those measured by Roznerski and Mechlinska-Drewko¹¹⁰ and those calculated by Masek and co-workers¹⁰⁵ and by Fournier and co-workers¹⁰⁶ using standard Boltzmann equation techniques. These are compared in Fig. 3.2, which also includes values calculated by Hake and Phelps¹⁰³ for comparison. Dutton shows that Hake and Phelps' calculations give a good representation of the measured data over an extensive range of E/N (0.01 to 100×10^{-21} V m²). The data measured by Roznerski and Mechlinska-Drewko are somewhat lower than the earlier measured values. The recent calculations agree reasonably well with those of Hake and Phelps, which are recommended as reliable approximations over a broad energy range.

Dutton¹ reports a rather large disagreement between measured and calculated values of D_1/μ for low E/N and suggests that a revision in the cross sections used to obtain the calculated data may be necessary. No new data are available to clarify the situation.

c. Electron Gain and Loss Processes, O_2

As discussed at the beginning of Sec. 5.3, three regions of E/N characterize electron gain and loss processes in oxygen. For E/N below 1.2×10^{-21} V m², experimental results clearly document three-body attachment, and these are reported and discussed by Dutton.¹ Taniguchi and co-workers¹¹¹ calculated the attachment coefficient for the three-body Block-Bradbury process,



using a Boltzmann equation method. The results, shown in Ref. 111, Fig. 1, are in reasonable agreement with the observations at low gas number densities. More complex high gas-density effects and attachment cooling are discussed in papers by Crompton and co-workers,¹¹² Goans and Christophorou,¹¹³ Buursen and co-workers,¹¹⁴ and Grünberg.¹¹⁵

In the range of intermediate E/N many measurements of η/N or quantities from which η/N can be derived, given adequate associated data, were made prior to 1973 and are documented by Dutton.¹ There is appreciable scatter in these data, some of which can be attributed to experimental error or incomplete documentation. Dutton concluded that for $E/N > 30 \times 10^{-21}$ V m² the most reliable η/N data were those of Grünberg¹¹⁵ and Chatterton and Craggs.¹¹⁶ Although early data by Huxley¹⁰⁷ was also recommended, it has been determined subsequently that a correction for anisotropic diffusion should be made to correctly obtain η/N from these data (see Huxley and Crompton, Ref. 2, pp. 492-495).

The analysis of the measurements is even more complex in the region of high E/N ($\geq 60 \times 10^{-21}$ V m²) where ionization, detachment, and charge transfer as well as attachment occur. In 1974 Dutton¹ pointed out that large uncertainties accompanied most reported values of η/N which has been determined by fitting spatial current growth curves. He concluded that in the region where ionization is significant, the attachment coefficient is known only to an order of magnitude.

The situation Dutton describes for detachment is even more indefinite. Fitting procedures provided a wide range of values including $\delta = 0$, although several references¹¹⁷⁻¹¹⁹ established the existence of a small, but finite δ/N . For both attachment and detachment determinations, analyses generally used incomplete reaction schemes, and negative ion concentrations were not monitored.

Dutton reported many values of the electron growth constant, which show general agreement. He also discussed the measurements of the ionization coefficient made by Price, Lucas, and Moruzzi,¹²⁰ who utilized the fact that the addition of small percentages of hydrogen to oxygen gives a mixture which, because of the fast associative detachment reaction $O^- + H_2 \rightarrow H_2O + e$, behaves as an electropositive gas. Calculations showed that changes in the energy distribution of the mixture due to the hydrogen component were negligible, so that an ionization coefficient closely approximating that for pure oxygen could be accurately determined by spatial current growth techniques.

Several recent studies have been directed toward clarification of the confused picture of electron gain and loss processes in oxygen at intermediate and high E/N . These studies have typically used analyses incorporating extensive reaction schemes. In some cases systems have been monitored for various ion concentrations using mass spectrometers. Also, efforts to distinguish detachment for different oxygen ions have led to more detailed notation where δ_1 , δ_2 , δ_3 refer to detachment from O^- , O_2^- , and O_3^- , respectively.

As mentioned above, Price, Lucas, and Moruzzi¹²⁰ made spatial current-growth measurements in O_2 containing small amounts of H_2 to obtain the ionization coefficient (α/N) closely corresponding to that for pure O_2 . These authors also obtained ionization coefficients for O_2 using O_2 - CO_2 mixtures and even higher values of E/N .¹²¹ For these measurements the claimed uncertainty is $\pm 2\%$. Subsequently, Price, Lucas, and Moruzzi¹²² measured spatial current growth in pure O_2 for E/N between 90 and 150×10^{-21}

V m^{-2} . Their analysis of data taken at $N = 33 \times 10^{22} \text{ m}^{-3}$ assumes ionization and attachment, charge transfer ($\text{O}^- + \text{O}_2 \rightarrow \text{O}_2^- + \text{O}$), detachment from O^- ($\text{O}^- + \text{O}_2 \rightarrow \text{O}_2 + \text{O} + \text{e}$), and the ion-conversion reaction ($\text{O}^- + 2\text{O}_2 \rightarrow \text{O}_3^- + \text{O}_2$), but utilizes the fact that the reaction rate for the latter process is much less than that for charge transfer. They invoke various arguments to support their assumption that detachment from O_2^- is negligible at $N = 60 \times 10^{22} \text{ m}^{-3}$. They utilized the values of α/N obtained with the mixture technique to fit the current growth curves and obtain an "effective attachment coefficient" η^* . Under these experimental conditions, η^* can be expressed as a function of the true attachment coefficient, the rate of charge transfer between O^- and O_2 , and δ_1/N . Taking the values calculated by Lucas and co-workers¹²³ as the true attachment coefficient and charge-transfer and ion-conversion rates measured by Kinsman and Rees,¹²⁴ these authors also obtained values of δ_1/N . However, similar measurements at $N = 330 \times 10^{22} \text{ m}^{-3}$ revealed an increase in $(\alpha - \eta^*)/N$ which they attribute to a detachment from O_3^- . This explanation is speculative in the absence of ion mass spectra. Davies²⁹ reanalyzed the data of Price, and co-workers¹²² for $E/N = 106 \times 10^{-21} \text{ V m}^{-2}$ and obtained good agreement with their value of δ_1/N .

In connection with measurements of the excitation discussed in Sec. 5.3.d below, Lawton and Phelps¹²⁵ used drift tube techniques to measure both η/N and α/N for E/N between 15 and $80 \times 10^{-21} \text{ V m}^{-2}$. In their analysis each coefficient required knowledge of the value of the other. The complementary coefficients were, in each case, calculated from a set of recommended cross sections chosen so that the calculated transport coefficients would be consistent with experiment and would have an energy dependence consistent with electron beam experiments.

In an effort to obtain more credible detachment data, O'Neill and Craggs¹²⁶ used a double-gap drift tube arrangement in which negative ions were formed in the first chamber and detached in the second. The relative concentrations of negative oxygen ions entering the second gap could be selected to be primarily O_2^- or O_3^- . These authors incorporated a mass spectrometer in their apparatus to monitor both negative ion and impurity concentrations, and determined that most of the O_3^- was depleted by charge transfer from O_3^- to O . They invoked an extensive reaction scheme in their fit to spatial current growth curves to obtain a self-consistent set of swarm coefficients for ionization (α/N), charge transfer ($\text{O}^- + \text{O}_2 \rightarrow \text{O}_2^- + \text{O}$ and $\text{O}_3^- + \text{O} \rightarrow \text{O}_3 + \text{O}^-$) and collisional detachment from O_2^- and O^- , assuming a constant value of η/N of $1.8 \times 10^{-22} \text{ m}^2$ over the range of E/N considered (123 to $169 \times 10^{-21} \text{ V m}^{-2}$). As shown in Fig. 3.3 and the discussion below, the latter approximation is reasonable. Measurements showed no dependence on gas density over the range from 65 to $195 \times 10^{22} \text{ m}^{-3}$. The detachment coefficient for O_2^- was reported to be more than 20 times less than that for O^- .

From studies of electron avalanches in oxygen, at gas densities between 3.3 and $26 \times 10^{22} \text{ m}^{-3}$, Frommhold¹²⁷ obtained rates for detachment from an ion which he identified as O^- . Subsequently Goodson, Corbin, and Frommhold¹²⁸ used electron avalanche methods to study detachment in oxygen for E/N between 80 and $400 \times 10^{-21} \text{ V m}^{-2}$. The reac-

tion scheme used in their analysis excludes O^- , but includes the effects of ionization, attachment and detachment for O_2^- , O_3^- , and O_4^- and assumes the presence of positive ions. These authors claim that the initial dominant concentration of O^- is depleted very rapidly by detachment, and the measurements observe a second, slower detachment which the authors attribute to the reaction $\text{O}_2^- + \text{O}_2 \rightarrow \text{e} + 2\text{O}_2$.

Corbin and Frommhold¹²⁹ used the method of time-resolved avalanche pulses in $\text{H}_2\text{-O}_2$ mixtures to obtain values of α/N in O_2 for E/N between 100 and $200 \times 10^{-21} \text{ V m}^{-2}$. The reaction scheme used in their analysis assumed the presence of four negative ions O^- , O_2^- , O_3^- , and O_4^- and of positive ions. Although the rates of various reactions involving these ions are not well established, these authors quote an uncertainty of $\pm 5\%$ for the α/N reported.

In his review of negative ion/molecule reactions, Parkes²⁵ calculated the detachment rate for O^- using two different energy distribution functions for the negative oxygen ions: the first was a simple Maxwellian distribution function and the second, a distribution shifted to higher energies, as suggested by Rebentrost.¹³⁰ He questions Goodson, Corbin, and Frommhold's interpretation of their experiment as yielding detachment data for O_2^- .

In connection with measurements of breakdown voltages in oxygen, Blair and Whittington¹³¹ measured λ/N by the Townsend current growth technique and for E/N between 100 and $200 \times 10^{-21} \text{ V m}^{-2}$ and gas densities up to $1000 \times 10^{22} \text{ m}^{-3}$, but did not attempt to separate coefficients describing the various contributing processes (attachment, ionization, detachment). For N below $300 \times 10^{22} \text{ m}^{-3}$ and at a given E/N , a slight increase of λ/N with decreasing N was reported.

Masek and co-workers,^{132,133} using the traditional two-term Boltzmann analysis and a selected set of cross sections, calculated the two-body attachment coefficient and the ionization coefficient.

Lucas, Price, and Morruzzi¹²³ used a somewhat modified technique employing a less extensive set of cross sections to solve the Boltzmann equation for the distribution function and iterative fits to various transport and swarm coefficients. As the drift velocities available to Lucas and co-workers exhibited a wide dispersion, the calculations were done for two different sets of drift velocities; first, those of Naidu and Prasad¹⁰⁹ and second, a combined set using low E/N values of Nielsen and Bradbury¹³⁹ and high E/N values of Frommhold.¹²⁷ Thus, attachment coefficients corresponding to both sets of drift velocities were calculated, and define a band of values of η/N for E/N in the intermediate and high range.

Wagner¹³⁵ incorporated an extended reaction scheme to reanalyze the spatial current growth measurements of Prasad and Craggs¹³⁶ and Sukhum, Prasad, and Craggs¹³⁷ to obtain η/N , α/N , and δ_1/N for E/N between 90 and $155 \times 10^{-21} \text{ V m}^{-2}$. Detachment from O_2^- and O_3^- were not included, although charge transfer was included, in this analysis and the detachment coefficient probably represents a composite of all detachment processes.

Figures 3.3–3.6 display the results of these recent studies on electron gain and loss processes in oxygen.

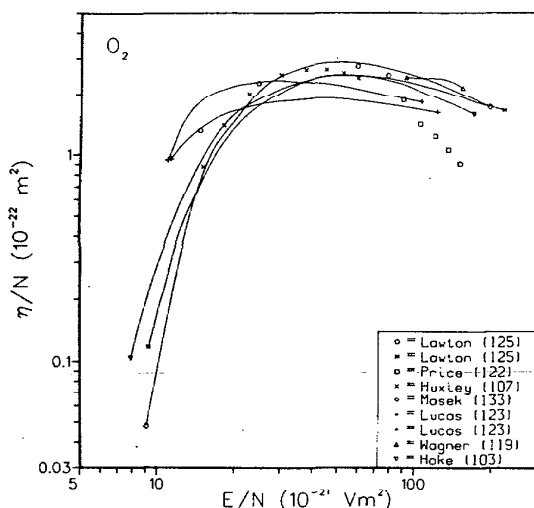


FIGURE 3.3. η/N in O_2 as a function of E/N . The upper curve attributed to Lucas (Ref. 123) was calculated using drift velocities of Naidu and Prasad (Ref. 109); the lower curve, those of Nielsen and Bradbury (Ref. 139) and Frommhold (Ref. 127).

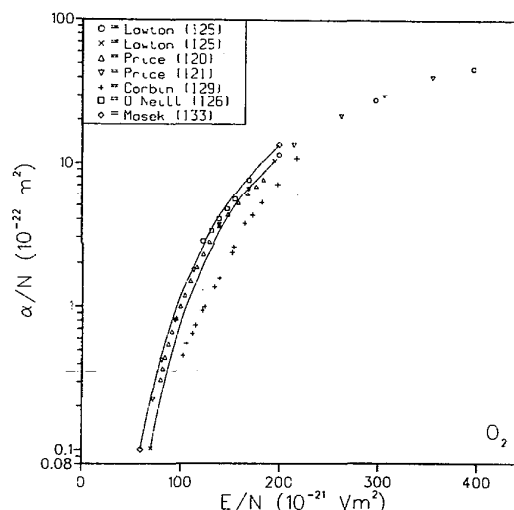


FIGURE 3.6. α/N in O_2 as a function of E/N .

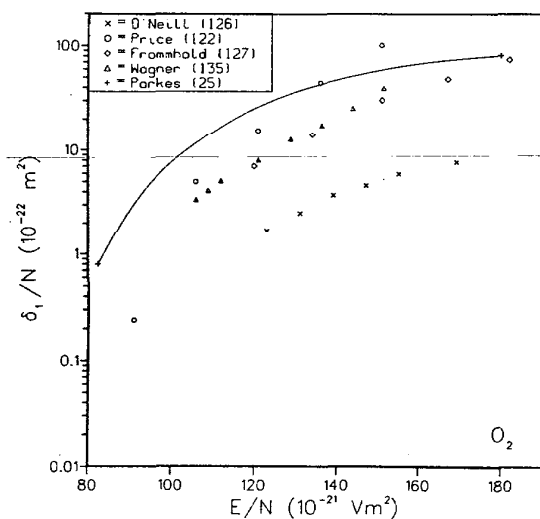


FIGURE 3.4. δ_1/N for O^- in O_2 as a function of E/N .

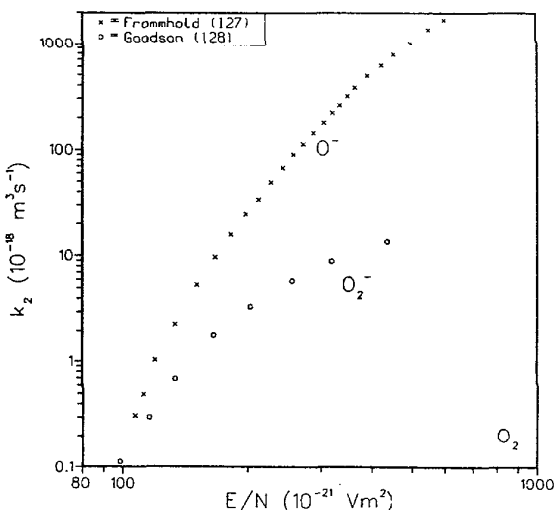


FIGURE 3.5. Detachment rates for O^- and O_2^- in O_2 as functions of E/N .

Figure 3.3 compares attachment data in the intermediate and high E/N regions obtained from the recent studies discussed in the preceding paragraphs. These include η/N measured and calculated by Lawton and Phelps,¹²⁵ η^*/N measured by Price and co-workers,¹²² η/N calculated by Masek and co-workers,¹³³ η/N calculated by Lucas and co-workers¹²³ using the drift velocity data of Naidu and Prasad,¹⁰⁹ η/N calculated by Lucas and co-workers using the drift velocity data of Nielsen and Bradbury¹³⁹ and Frommhold,¹²⁷ and finally, those obtained by Wagner¹³⁵ in his reanalysis of earlier data. To serve as a guide in making comparisons with earlier work reported by Dutton,¹ the data of Hake and Phelps¹⁰³ are also included in this figure.

Because η^*/N reported by Price and co-workers represents a composite of attachment and detachment, it is expected to be lower than the data for η/N reported by the other workers, as shown in the figure. The rapid drop in η/N for E/N above $90 \times 10^{-21} \text{ V m}^2$ is, however, inconsistent with theory and cannot be attributed to detachment. The data calculated by Lucas and co-workers are high for E/N below 20 and low for E/N above $20 \times 10^{-21} \text{ V m}^2$. With the exception of these data sets, the other results shown are in reasonable agreement for E/N above $20 \times 10^{-21} \text{ V m}^2$ and any one (for example, the data calculated by Masek since it extends over the broadest range of E/N) may be recommended in this region of E/N with an estimated uncertainty of 20%. For E/N below $20 \times 10^{-21} \text{ V m}^2$, the various calculated data exhibit broad dispersion, as does the earlier experimental data reported by Dutton.¹ Clearly, no recommendations can be made on data for η/N in this region of E/N , and measurements are needed to determine reliable values.

Figure 3.4 compares the swarm coefficients for detachment from O^- (δ_1/N) derived by Price and co-workers¹²² and by Wagner¹³⁵ with those measured by O'Neill and Craggs¹²⁶ and calculated by Parkes.²⁵ A few points from the early data of Frommhold¹²⁷ who obtained the inverse of the detachment rate from an ion which he identifies as O^- are also included in this figure. The conversion of the original

Frommhold data to this representation used the relationship $\delta_1/N = k_2/W_{O^-}$. Here W_{O^-} is the O^- drift velocity obtained from the reduced mobilities measured by Snuggs and co-workers¹³⁸ at low gas densities (between 0.17 and $0.24 \times 10^{22} \text{ m}^{-3}$) and extrapolated to E/N values compatible with Frommhold's measurements. The rate constants calculated by Parkes for a non-Maxwellian energy distribution were also converted to swarm coefficients using O^- drift velocities determined from Snuggs' data. The data of O'Neill and Craggs are considerably lower than the others. Parkes²⁵ points out that these values would be increased if the charge-transfer process $O_3^- + O_2 \rightarrow O_3 + O_2^-$ were included in the analysis used to obtain them. Figure 3.4 demonstrates the broad dispersion in the δ_1/N data.

Figure 3.5 compares the detachment rates measured by Frommhold¹²⁷ and interpreted as due to detachment from O^- with those measured by Goodson, Corbin, and Frommhold¹²⁸ and interpreted as due to detachment from O_2^- .

The picture of detachment in oxygen is still cloudy and can be clarified only with more work incorporating identification of the specific ions present, their concentrations, energy distributions, and the reactions in which they participate. No recommendations concerning reliable data can be made at this time.

Figure 3.6 compares the recent data on α/N in oxygen, i.e., measured by Price and co-workers,^{120,121} Lawton and Phelps,¹²⁵ Corbin and Frommhold,¹²⁹ O'Neill and Craggs,¹²⁶ and calculated by Lawton and Phelps¹²⁵ and by Masek and co-workers.¹³³ These data are in reasonable agreement with the exception of those of Corbin and Frommhold, which are considerably lower than the others. Corbin and Frommhold suggest that while their measurements include only the effect of instantaneous ionization (which occurs in times $< 10^{-8}$ s), a Penning-type process between excited and ground-state oxygen molecules (which takes about 10^{-6} s) may enhance the values of α/N obtained by steady-state techniques. The data reported by Price and

co-workers, which are the most complete and consistent, are recommended to the user as a reasonable working set.

Figure 3.7 compares values of λ/N measured by Blair and Whittington¹³¹ for N between 82.5 and $660 \times 10^{22} \text{ m}^{-3}$ with those calculated by Masek and co-workers.¹³³ These experimental data are recommended as a reasonable approximation to λ/N in oxygen, but the reader should be aware that comparable data compiled by Dutton¹ displayed considerable scatter for E/N between 100 and $150 \times 10^{-21} \text{ V m}^{-2}$. Uncertainties of the order of $\pm 20\%$ should be assigned to these data.

d. Excitation Coefficient, O_2

Using drift tube techniques and measuring the absolute intensity of the 762 nm band emission, Lawton and Phelps¹²⁵ obtained the excitation coefficient for the $b^1\Sigma_g^+$ state of O_2 , i.e., the number of $b^1\Sigma_g^+$ molecules produced per centimeter of electron drift per O_2 molecule. This coefficient includes excitation of the $b^1\Sigma_g^+$ state via cascading from higher molecular states. In comparing these with excitation coefficients calculated using cross sections measured by beam techniques, the authors find the values measured by drift tube techniques are much higher except for $E/N < 8 \times 10^{-21} \text{ V m}^{-2}$. They find that the excitation coefficient for the $b^1\Sigma_g^+$ state is very nearly equal to the sum of the excitation coefficients for the $b^1\Sigma_g^+$ and all higher states, i.e., apparently all of these excited states collisionally relax to the $b^1\Sigma_g^+$ state. Masek and co-workers¹³³ also calculated the rate for direct excitation to the $b^1\Sigma_g^+$ state with no cascading using known cross sections. These have been converted to ϵ/N using the drift velocities calculated by Masek and co-workers¹⁰⁵ and are compared with the Lawton and Phelps data in Fig. 3.8.

5.4. Air

Spatial transport and swarm parameters that describe the behavior of electron swarms in air, the most common of

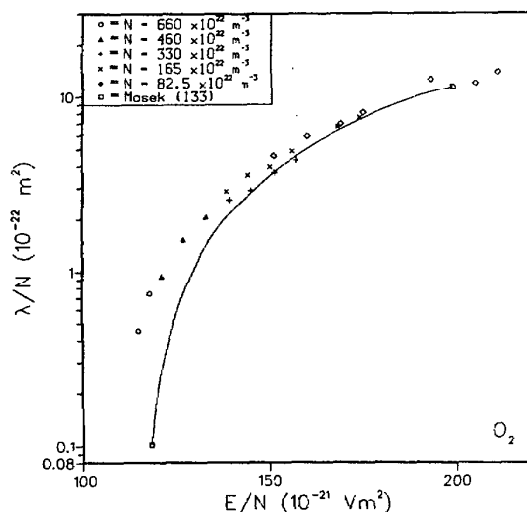


FIGURE 3.7. λ/N in O_2 as a function of E/N . With the exception of those reported by Masek, all data were taken from Blair and Whittington (Ref. 131).

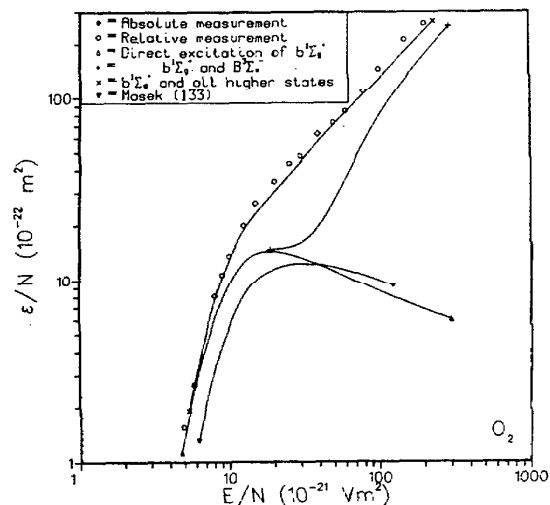


FIGURE 3.8. Excitation coefficient for the $b^1\Sigma_g^+$ state of O_2 as a function of E/N . With the exception of those reported by Masek, all data were taken from Lawton and Phelps (Ref. 125).

gaseous insulators, are important in understanding its breakdown properties as well as in modeling the upper atmosphere. However, these data have not been systematically studied, partly because the composition of "air" is not always clearly defined but may vary in water vapor and carbon dioxide content. For the remainder of this discussion, dry CO_2 -free air is defined as 21% oxygen and 79% nitrogen, and much of the data presented here refer to this mixture. We have included some data which qualitatively describe the effect of the addition of water on the transport properties of air.

The electronegative properties of air arise from dissociative attachment to its oxygen component, but differ from those in pure oxygen because subsequent detachment and ion-molecule reactions are strongly influenced by the nitrogen component of the air. Thus, as in oxygen (see Sec. 5.3), three regions of E/N are defined: below $12 \times 10^{-21} \text{ V m}^2$, three-body attachment to O_2 is the dominant process; between $E/N = 12$ and $100 \times 10^{-21} \text{ V m}^2$, two-body dissociative attachment to O_2 occurs; and above $100 \times 10^{-21} \text{ V m}^2$, ionization of both O_2 and N_2 are also large effects. In the intermediate and high E/N regions, interactions of the negative oxygen ions with other gas constituents occur. The swarm data for air compiled by Dutton¹ are not extensive and show considerable scatter in the electron growth constant and, especially, the attachment coefficient.

Few additional data have been reported since 1973.

a. Drift Velocity, Air

The data compiled by Dutton¹ include drift velocities in air reported by Nielsen and Bradbury¹³⁹ and by Hessenauer¹⁴⁰ in the region of E/N below $10 \times 10^{-21} \text{ V m}^2$, and by Ryzko¹⁴¹ and Frommhold¹²⁷ in the region of E/N above $100 \times 10^{-21} \text{ V m}^2$, but no data measured for intermediate E/N . Also data calculated for the entire range of E/N by Heylen,¹⁴² who assumed a Maxwellian energy distribution and an estimated energy dependence of the cross sections, were reported. These measurements and calculated data agree remarkably well.

In view of the broad interest in air and inconsistencies in other transport data in air, Rees¹⁴³ reexamined the electron drift velocity in dry CO_2 -free air for gas densities between 33 and $165 \times 10^{22} \text{ m}^{-3}$ and E/N between 0.4 and $12 \times 10^{-21} \text{ V m}^2$. The measured values were corrected for diffusion effects. Hegerberg and Reid¹⁴⁴ extended drift velocity measurements in dry CO_2 -free air to lower E/N ($0.1 \times 10^{-21} \text{ V m}^2$) for gas densities between 10 and $33 \times 10^{22} \text{ m}^{-3}$ and made corrections for attachment. The length of the drift tube excluded the need for a lateral diffusion correction.

The electron drift velocities in dry air measured by Nielsen and Bradbury, Hessenauer, Rees, and Hegerberg and Reid are compared in Fig. 4.1. The more recent data display somewhat lower values, possibly because the earlier investigators made no corrections for diffusion. The data of Hegerberg and Reid are slightly below those of Rees, presumably because the attachment correction was not made for the latter data. These two data sets agree, however, to within the combined error limits and taken together form the data set recommended as most reliable.

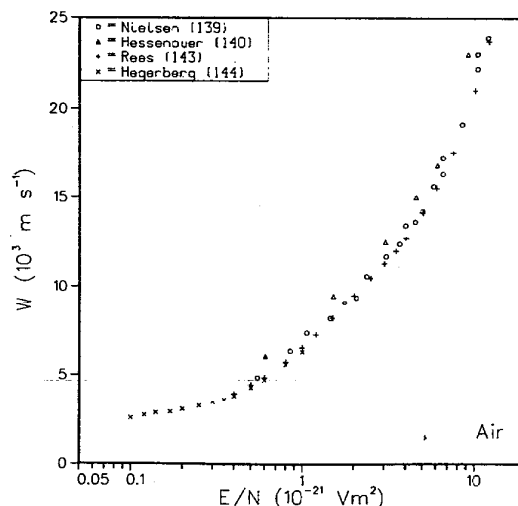


FIGURE 4.1. W for electrons in air as a function of E/N .

Milloy and co-workers¹⁴⁵ used shutter techniques to study the effect on the drift velocity of the addition of 1.5% water vapor (50% relative humidity) to dry CO_2 -free air. Figure 4.2 compares their measurements with those of Rees for dry air (repeating Rees' data from Fig. 4.1). The presence of water resulted in a large increase in the drift velocity for low E/N . Milloy also measured the drift velocity in dry air containing 5% CO_2 ; a large increase in W for E/N below $1.0 \times 10^{-21} \text{ V m}^2$ was reported.

For E/N between 130 and $160 \times 10^{-21} \text{ V m}^2$, Ryzko¹⁴¹ measured the drift velocity in air containing 16% water vapor as well as in dry air and found the drift velocity approximately 7% higher in the moist air.

From the data of Milloy and of Ryzko, the conclusion is that the presence of water vapor increases the drift velocity in air. The increase is, however, specific to the particular mixtures studied and cannot be used for quantitative predictions for other cases.

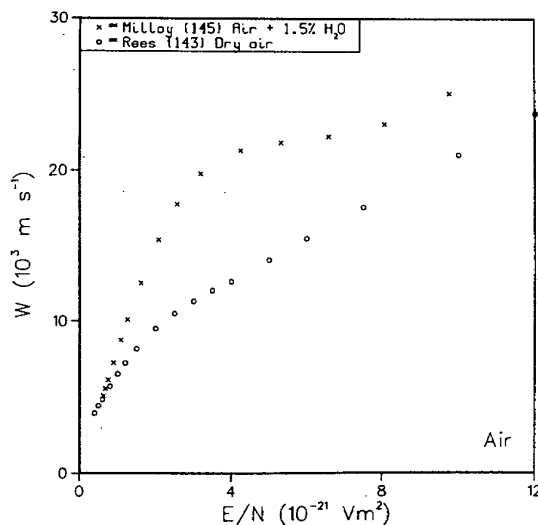


FIGURE 4.2. W for electrons in mixtures of air and water vapor as a function of E/N .

b. (Diffusion Coefficient)/Mobility, Air

Early measurements of D_T/μ in air were reported by Townsend and Tizard,¹⁴⁶ Bailey,¹⁴⁷ and Huxley and Zazou.¹⁴⁸ These measurements were somewhat suspect due to gas composition and also because at low gas densities and a given E/N , values varied with N . Crompton, Huxley, and Sutton¹⁴⁹ suggested that this effect was due to negative ions which contributed to the current in the central disk of the anode. To correct for this effect, they derived D_T/μ from ratios of currents on adjacent rings of the anode, excluding the center disk, and found their results to be self-consistent as the gas density was varied for E/N between 0.3 and $60 \times 10^{-21} \text{ V m}^2$. Rees and Jory¹⁵⁰ used a similar technique to extend measurements to higher E/N ($110 \times 10^{-21} \text{ V m}^2$). Dutton¹ compared the results of Crompton and co-workers with those of Rees and Jory and of Townsend and Tizard. The first two data sets are in good agreement, but somewhat higher at low E/N , than the third data set which was taken in air containing CO_2 .

Raja Rao and Govinda Raju¹⁵¹ repeated measurements over a range of experimental parameters similar to those chosen by Crompton and co-workers, but used an analysis depending on the current to the center disk of the anode as well as to the annular rings.

In view of the absence of any measured values of D_T/μ for E/N above $110 \times 10^{-21} \text{ V m}^2$, Maller and Naidu¹⁵² used the Townsend-Huxley technique (see Sec. 3.2) to extend measurements of D_T/μ in dry air up to $1500 \times 10^{-21} \text{ V m}^2$.

The analysis used in the works discussed so far did not allow for the presence of secondary electrons due to ionization for high E/N . In fact, Rees and Jory¹⁵⁰ demonstrated that the error due to omission of ionization from the analysis is negligible for $E/N < 110 \times 10^{-21} \text{ V m}^2$. Lakshminarasimha and Lucas¹⁵⁴ measured the radial distribution of the anode current and used a computer analysis which includes secondary electrons to obtain D_T/μ . These results, which were reported at approximately the same time as those of Maller and Naidu, also extended the range of E/N to much higher values than previous measurements.

With the exception of the very early work, the measured values of D_T/μ in dry air are compared in Fig. 4.3. The data of Raja Rao for E/N below $10 \times 10^{-21} \text{ V m}^2$ are somewhat lower than those of Crompton and co-workers; the data of Maller and Naidu and those of Lakshminarasimha and Lucas diverge slightly for E/N above $800 \times 10^{-21} \text{ V m}^2$. Otherwise, the data displayed are in good agreement. The data of Crompton and co-workers are recommended for E/N between 0.3 and $60 \times 10^{-21} \text{ V m}^2$, and the data of Rees and Jory, for E/N between 60 and $110 \times 10^{-21} \text{ V m}^2$. For higher E/N , the data of Lakshminarasimha and Lucas are recommended.

Maller and Naidu¹⁵² also measured D_T/μ for humid air (relative humidity = 55% at 293 K) for E/N between 30 and $1500 \times 10^{-21} \text{ V m}^2$. These data show that D_T/μ is somewhat higher for the humid air for low E/N , but above $250 \times 10^{-21} \text{ V m}^2$ the results are the same for both mixtures. These data give some indication of the influence of humidity on D_T/μ , but are insufficient to provide the basis for general conclusions.

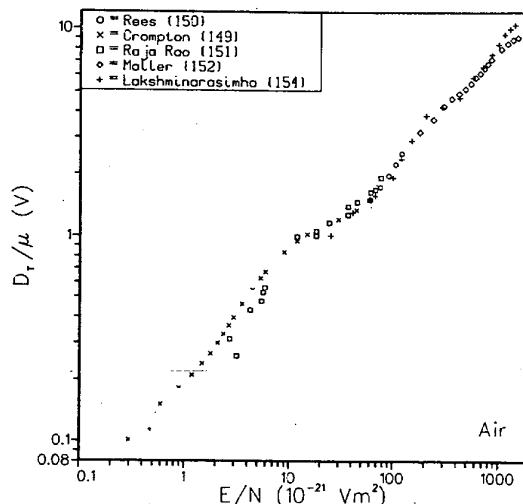


FIGURE 4.3. D_T/μ in air as a function of E/N .

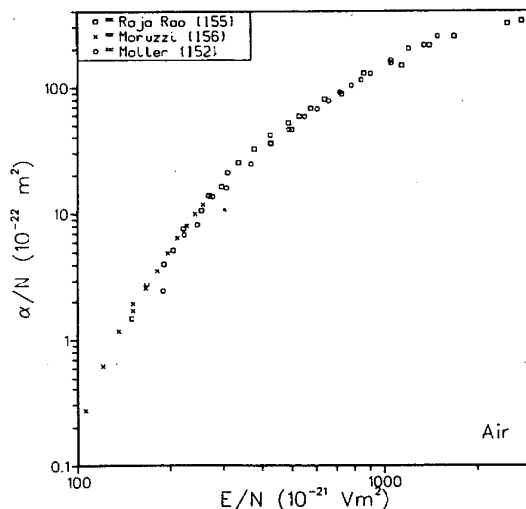
c. Electron Gain and Loss Processes, Air

The early work on electron gain and loss processes in air discussed by Dutton¹ includes many measurements of the attachment coefficient and electron growth constant. Most of this work was carried out using ambient air heated to remove H_2O , but not CO_2 . The attachment data for all values of E/N display considerable scatter. A density dependence indicative of three-body attachment for E/N below $12 \times 10^{-21} \text{ V m}^2$, such as is observed in pure oxygen, was reported by Hessenauer,¹⁴⁰ although the effect was not as clearly demonstrated as in pure oxygen. In the region of E/N above $85 \times 10^{-21} \text{ V m}^2$, most of the work has indicated some detachment, but the reported values of δ/N range from zero to $15 \times 10^{-22} \text{ m}^2$.

The electron growth constant data are also scattered, particularly for E/N between 100 and $150 \times 10^{-21} \text{ V m}^2$. This scatter is attributed to an N dependence of λ/N . For higher E/N , values of λ/N taken in mercury-contaminated air agree with the data of Raja Rao and Govinda Raju,¹⁵⁵ who extended measurements of the ionization coefficient in mercury-free dry air to high values of E/N ($2825 \times 10^{-21} \text{ V m}^2$). Attachment was assumed negligible in their analysis, and no consistent results indicating finite detachment coefficients were obtained.

Only two recent papers have reported electron swarm coefficients in dry air. Maller and Naidu¹⁵² extended transport coefficient measurements to high E/N and reported values of α/N as a by-product, although they did not discuss attachment or detachment.

Moruzzi and Price¹⁵⁶ reported observations of current growth curves in dry air. An expected departure of these curves from exponential due to electron attachment was not observed. They interpret this as being due to a rapid detachment mechanism which masks the presence of attachment and suggest the reaction $\text{O}^- + \text{N}_2^* \rightarrow \text{products} + \text{e}$ (where N_2^* indicates an excited nitrogen molecule) as the detachment process. These authors conclude an "effective" attachment coefficient (incorporating both attachment and detachment) of $\eta^*/N < 3 \times 10^{-24} \text{ m}^2$. Attempts by Comer and

FIGURE 4.4. α/N in air as a function of E/N .

Schulz¹⁵⁷ and by Fehsenfeld and co-workers¹⁵⁸ to observe this ion-molecule reaction directly using ground state N_2 at room temperature have led to apparently conflicting results. If the excited species proposed by Moruzzi and Price is produced by electron impact excitation, then the detachment rate would be a function of the electron current used in the drift-tube measurements, but these authors did not investigate the current dependence of their observations.

As no new data for η/N in air have been reported since Dutton¹ published his review, no associated figure is included here. The data on α/N in dry air measured by Raja Rao and Govinda Raju,¹⁵⁵ Maller and Naidu,¹⁵² and Moruzzi and Price,¹⁵⁶ compared in Fig. 4.4, agree with the exception of the Maller data which are somewhat low for E/N below $500 \times 10^{-21} \text{ V m}^{-2}$. The Raja Rao data are recommended as a consistent working set for E/N above $300 \times 10^{-21} \text{ V m}^{-2}$; the Moruzzi data are recommended for E/N below $300 \times 10^{-21} \text{ V m}^{-2}$. No calculations for the electron growth constant in air have been published.

Kuffel¹⁵⁹ used spatial current growth techniques to study the effect of humidity on the breakdown voltage in air. For air containing 2.8% water vapor, an increase in η/N of between 1.5 and 7 for E/N between 50 and $100 \times 10^{-21} \text{ V m}^{-2}$ was observed.

Prasad and Craggs,¹⁶⁰ also investigating the effect of humidity on the breakdown properties of air, determined η/N and α/N for mixtures of water vapor in air by observing spatial growth of prebreakdown currents. They also reported a definite increase in η/N and a small increase in α/N with increasing water vapor content.

5.5. Water

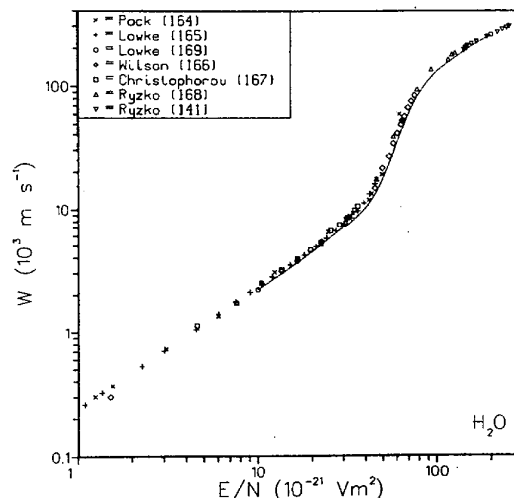
Although water is an important constituent of mixtures, e.g., of air as an insulating gas and of the atmosphere, properties of swarms in pure water vapor have not been extensively studied nor has the existing data been previously collected. Water is characterized by three regions of E/N . The region below $30 \times 10^{-21} \text{ V m}^{-2}$ has been the subject of some controversy which is discussed in Sec. 5.5.3. A narrow intermediate region for E/N between 30 and 60×10^{-21}

V m^{-2} is characterized by the two-body dissociative attachment process $e + \text{H}_2\text{O} \rightarrow \text{H}^- + \text{OH}$. In the high E/N region beginning at $60 \times 10^{-21} \text{ V m}^{-2}$, relatively weak ionization as well as attachment occurs.

Early studies by Bailey and Duncanson¹⁶² used the indirect magnetic and electric field technique to measure the drift velocity (see Dutton, Ref. 1, Sec. 3.1), the Townsend energy factor k_T , and the attachment coefficient. These data are subsequently found to be in serious disagreement with later measurements of these swarm parameters and were also demonstrated to be inconsistent with electron beam data on attachment (see for example, Ref. 163). Consequently, these data will not be considered further in this article.

a. Drift Velocity, H_2O

After the work of Bailey and Duncanson, the first measurements of the electron drift velocity in water were made by Pack, Voshall, and Phelps,¹⁶⁴ who used drift tube sampling techniques for E/N between 1 and $60 \times 10^{-21} \text{ V m}^{-2}$. Shortly thereafter, in connection with their measurements on mixtures, Lowke and Rees¹⁶⁵ reported measurements for pure water using similar techniques over approximately the same range of E/N . In an extensive study comparing transport properties in water vapor and deuterated water vapor, Wilson and co-workers,¹⁶⁶ also reported drift velocities obtained using sampling techniques. In his studies relating the dipole moment to scattering cross-sections, Christophorou¹⁶⁷ measured drift velocities of 34 polar molecules, including water. Ryzko^{141,168} used avalanche techniques to extend these measurements to higher values of E/N . These various data are given in Fig. 5.1 and are in good agreement. In calculations of the longitudinal diffusion coefficient using the gradient expansion method, Lowke and Parker (Ref. 169, Appendix II) also obtained drift velocities in water. As shown in Fig. 5.1, these values of W are in good agreement with the experimental data. The data measured by Lowke and Rees are recommended for E/N between 1 and $60 \times 10^{-21} \text{ V m}^{-2}$. For higher E/N , the data of Ryzko, which are consistent with other measurements and most complete, are recommended.

FIGURE 5.1. W for electrons in H_2O as a function of E/N .

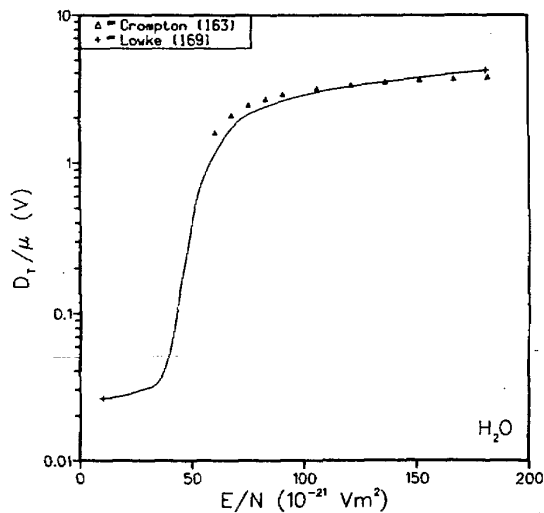


FIGURE 5.2. D_T/μ in H_2O as a function of E/N .

b. (Diffusion Coefficient)/Mobility, H_2O

With the exception of the data of Bailey and Duncanson, the only measurements of D_T/μ in water vapor were made by Crompton, Rees, and Jory^{163,170} using the radial diffusion techniques (described in Sec. 3.2) for E/N between 60 and $180 \times 10^{-21} \text{ V m}^2$. In the only measurements of D_L/μ , Wilson and co-workers¹⁶⁶ employed drift tube techniques for E/N between 4 and $75 \times 10^{21} \text{ V m}^2$. Lowke and Parker¹⁶⁹ used for the first time the gradient expansion method of solution of the Boltzmann equation, which requires the solution of additional equations, with the unpublished cross sections of Cohen and Phelps to calculate D_T/μ and D_L/μ . Further analysis of H_2O using recently developed techniques for solution of the Boltzmann equation¹³ is desirable.

These data are presented in Figs. 5.2 and 5.3. For the transverse case, the measured and calculated values agree reasonably well over their common range of E/N , but the calculated data extend to much lower E/N . The measured

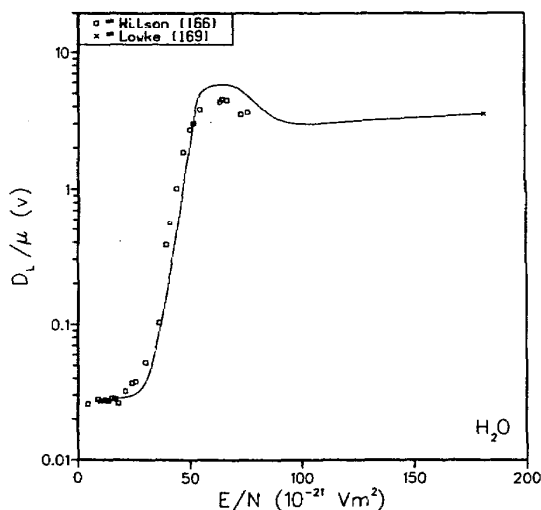


FIGURE 5.3. D_L/μ in H_2O as a function of E/N .

data of Crompton and co-workers are recommended for E/N between 60 and $180 \times 10^{-21} \text{ V m}^2$. For E/N below $20 \times 10^{-21} \text{ V m}^2$, both theory and experiment indicate that electrons are thermal. Theory may not give an accurate description of D_T/μ as a function of E/N for E/N between 20 and $60 \times 10^{-21} \text{ V m}^2$ because of an inadequate knowledge of electron collision cross sections. There is clearly a need for measurements in this region. For the longitudinal case, agreement between the measured and calculated data is also reasonable in the region of E/N where they overlap, both indicating a maximum around $E/N = 65 \times 10^{-21} \text{ V m}^2$. The measured data are recommended for the E/N range where available.

c. Electron Gain and Loss Processes, H_2O

Early work by Bradbury and Tatel¹⁷¹ included a general investigation of negative-ion formation in water vapor. Below $39 \times 10^{-21} \text{ V m}^2$, these authors detected an attachment process, the probability of which increased with gas density. They attributed this to attachment to the small aggregates of water molecules which form as condensation approaches. At $30 \times 10^{-21} \text{ V m}^2$, they detected the threshold for a second attachment process that increased rapidly with E/N , which they attributed to the two-body dissociative process, $e + H_2O \rightarrow H^- + OH$.

In studies on the effect of humidity on the breakdown voltage in air, Kuffel¹⁵⁹ employed spatial current growth techniques to determine the attachment coefficient in water vapor for E/N between 2 and $75 \times 10^{-21} \text{ V m}^2$. As Kuffel did not consider ionization in his analysis, the quantity reported was $(\eta - \alpha)/N$ or $-\lambda/N$. In the low E/N region (below $39 \times 10^{-21} \text{ V m}^2$), Kuffel reported an effect similar to that seen by Bradbury and Tatel, an apparent attachment which increased with gas density and decreased with E/N .

Moruzzi and Phelps¹⁷² surveyed negative ion formation in water vapor using an rf mass spectrometer coupled to an electron drift tube. Although many hydrated negative ions were observed, no negative ions were detected for E/N below $30 \times 10^{-21} \text{ V m}^2$. Similarly, Pack, Voshall and Phelps¹⁶⁴ found no evidence of attachment in water vapor at the saturation gas density below $30 \times 10^{-21} \text{ V m}^2$. Parr and Moruzzi¹⁷³ observed no attachment below $39 \times 10^{-21} \text{ V m}^2$, and Wilson and co-workers¹⁶⁶ observed no negative ions below $30 \times 10^{-21} \text{ V m}^2$. As demonstrated by Moruzzi and Phelps¹⁷² and Pack and Phelps,¹⁷⁴ when oxygen is present in water vapor, attachment processes leading to formation of complex negative ions occur at low E/N . Thus the presence of impurities is the probable explanation for the negative ion formation at E/N below $30 \times 10^{-21} \text{ V m}^2$ observed by Bradbury and Tatel and by Kuffel.

In connection with breakdown studies in water vapor, Prasad and Craggs¹⁶⁰ obtained attachment and ionization coefficients using spatial current growth techniques for E/N between 80 and $150 \times 10^{-21} \text{ V m}^2$. Subsequently, Crompton, Rees, and Jory^{163,170} completed measurements of D_T/μ discussed in the previous section, and from further analysis of their radial diffusion data, obtained the attachment coefficient for E/N between 70 and $180 \times 10^{-21} \text{ V m}^2$. Their analysis utilized ionization coefficients of Prasad and Craggs,¹⁶⁰

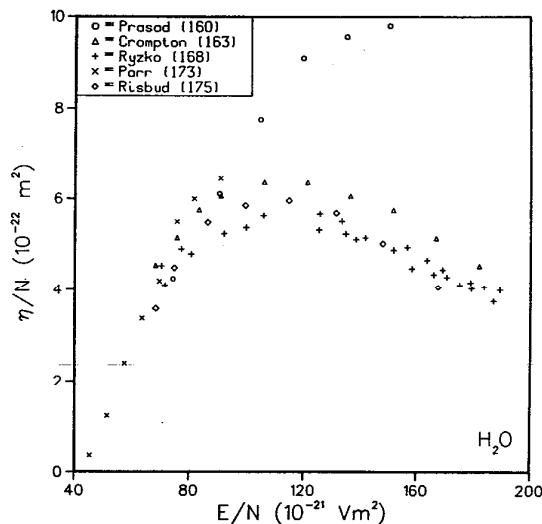


FIGURE 5.4. η/N in H_2O as a function of E/N .

which later work suggests may be in error. Reanalysis of the data of Crompton, Rees, and Jory using more reliable ionization data would be desirable.

In view of the large discrepancies between the data of Crompton and co-workers and those of earlier workers (Bailey and Duncanson, Kuffel, Prasad and Craggs) in the region of intermediate and high E/N , Ryzko¹⁶⁸ used the pulsed Townsend discharge technique to measure the attachment and ionization coefficients for E/N between 70 and $190 \times 10^{-21} \text{ V m}^{-2}$.

In a further attempt to establish the attachment coefficient, Risbud and Naidu¹⁷⁵ repeated measurements using a pulsed Townsend discharge for E/N between 60 and $180 \times 10^{-21} \text{ V m}^{-2}$ and report both η/N and α/N .

With the intention of clarifying the controversy on attachment in the low E/N region, Parr and Moruzzi¹⁷³ used a pulsed Townsend discharge to measure $-(\alpha - \eta)/N$ in water vapor for E/N between 0 and $90 \times 10^{-21} \text{ V m}^{-2}$. No attachment was observed below $39 \times 10^{-21} \text{ V m}^{-2}$. These authors used the ionization coefficients of Ryzko¹⁶⁸ for E/N above $60 \times 10^{-21} \text{ V m}^{-2}$ to obtain η/N from their data.

The attachment coefficients in water obtained by these authors are compared in Fig. 5.4. The data of Ryzko¹⁶⁸ and Risbud and Naidu¹⁷⁵ are in general agreement with regard to E/N dependence, but somewhat lower than those of Parr and Moruzzi, which are recommended for E/N between 40 and $70 \times 10^{-21} \text{ V m}^{-2}$. The data of Prasad and Craggs¹⁶⁰ are in serious disagreement with the other four data sets for $E/N > 100 \times 10^{-21} \text{ V m}^{-2}$.

The ionization coefficients measured by Prasad and Craggs,¹⁶⁰ Ryzko,¹⁷⁰ and Risbud and Naidu,¹⁷⁵ compared in Fig. 5.5, disagree in the region of common E/N . The data of Risbud and Naidu, which extend over a larger range of E/N than the others, are recommended as a good working set, but the reader is cautioned to assign to them an uncertainty of $\pm 20\%$.

5.6. Carbon Dioxide

Current interest in carbon dioxide is high due to its use in high power lasers, usually as a mixture constituent. Work

directed toward understanding laser mixtures has frequently included data for pure CO_2 . Swarm data available prior to 1973 have been compiled by both Dutton¹ and Huxley and Crompton.² Carbon dioxide is characterized by three regions of E/N . Below $50 \times 10^{-21} \text{ V m}^{-2}$, neither attachment nor ionization occur; between 50 and $90 \times 10^{-21} \text{ V m}^{-2}$, two-body dissociative attachment is the dominant process; and above $90 \times 10^{-21} \text{ V m}^{-2}$, both attachment and ionization occur.

a. Drift Velocity, CO_2

Dutton¹ compiled the extensive data on drift velocities in carbon dioxide available prior to 1973. For E/N below $30 \times 10^{-21} \text{ V m}^{-2}$ these can be represented by the measurements of Pack, Voshall, and Phelps¹⁶⁴ which extend from 0.05 to $20 \times 10^{-21} \text{ V m}^{-2}$ and are in excellent agreement with values calculated by Hake and Phelps¹⁰ using a set of cross sections taken from data available in 1967 and by the measurements of Elford¹⁷⁶ for which the error is estimated to be less than 1%. There were no data available in the range of E/N between 20 and $100 \times 10^{-21} \text{ V m}^{-2}$, but Dutton compiled measured drift velocities for higher values of E/N . Data were also presented which demonstrated that W decreases with increasing gas density at low E/N .

In view of the gap in drift velocity data for E/N between 20 and $100 \times 10^{-21} \text{ V m}^{-2}$, Elford and Haddad¹⁷⁷ extended earlier measurements of Elford¹⁷⁶ at 293 K up to $50 \times 10^{-21} \text{ V m}^{-2}$ and also made measurements at 193, 224, 256, and 573 K and over a range of gas number densities. They have confirmed that W decreases linearly with increasing gas density at temperatures below 293 K.

In connection with studies of gas laser mixtures, two recent measurements of the drift velocity in pure carbon dioxide were made by time-of-flight techniques. Those by Saelee and co-workers¹⁷⁸ encompass the region of E/N for which no data were previously available, i.e., for E/N between 5.6 and $700 \times 10^{-21} \text{ V m}^{-2}$. Those of Sierra and co-workers¹⁷⁹ were made for E/N between 3 and $90 \times 10^{-21} \text{ V m}^{-2}$.

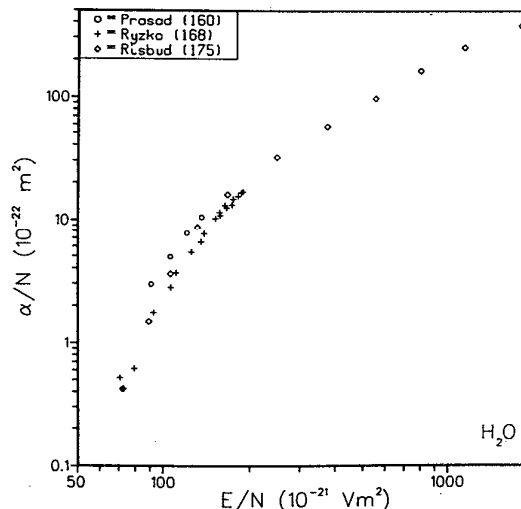
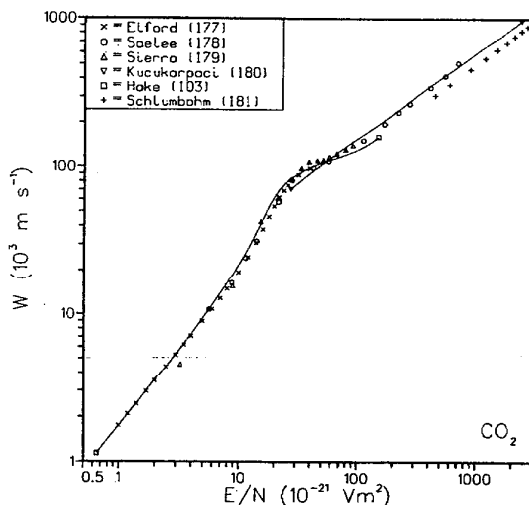


FIGURE 5.5. α/N in H_2O as a function of E/N .

FIGURE 6.1. W for electrons in CO_2 as a function of E/N .

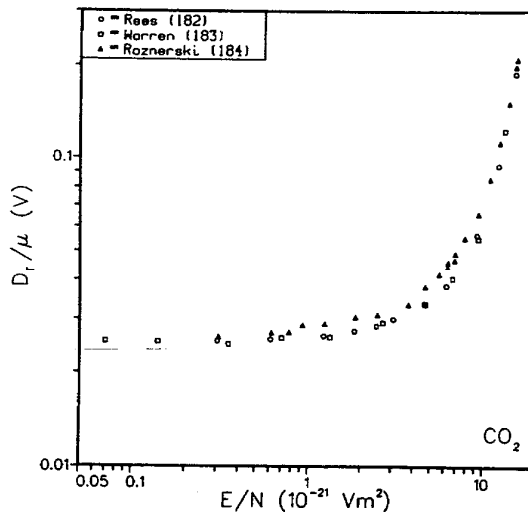
Kucukarpaci and Lucas¹⁸⁰ recently reported results of a Monte Carlo calculation of electron swarm parameters utilizing an extensive set of cross sections for electron collision processes in carbon dioxide. These calculations obtained the electron drift velocity for a very wide range of E/N ; $25 < E/N < 2500 \times 10^{-21} \text{ V m}^{-2}$.

Figure 6.1 compares the recent drift velocity data for carbon dioxide. Also included are the earlier data of Hake and Phelps¹⁰³ and of Schlumbohm¹⁸¹ to aid the user in making comparisons with the data compiled by Dutton. These data are in good agreement with the exceptions of those Sierra and co-workers for E/N between 3 and $10 \times 10^{-21} \text{ V m}^{-2}$ and of Schlumbohm for very high E/N . For low E/N , the data of Elford are recommended as the most reliable. For high E/N , the data calculated by Kucukarpaci and Lucas are recommended as a reasonable approximation with an uncertainty of $\pm 10\%$.

b. (Diffusion Coefficient)/Mobility, CO_2

In the region of $E/N < 20 \times 10^{-21} \text{ V m}^{-2}$, the data for D_T/μ considered as most reliable by Dutton¹ were those which extrapolated to approximate D_{Th}/μ as E/N decreased toward zero, where D_{Th} is the thermal diffusion coefficient. These data are from Rees¹⁸² and from Warren and Parker.¹⁸³ In the region of E/N between 10 and $60 \times 10^{-21} \text{ V m}^{-2}$, data for D_T/μ are expected to be reasonably accurate due to the absence of attachment and ionization, and the various data sets reported by Dutton are in good agreement. Above $60 \times 10^{-21} \text{ V m}^{-2}$, where attachment occurs but the attachment coefficient is not known accurately, the data are represented by the results of Rees¹⁸² who made corrections for ionization, but not attachment. Rees estimates the reported values of D_T/μ are low by from 4 to 9%. Dutton also reviewed investigations of the temperature dependence of D_T/μ in CO_2 where calculated and measured results are in agreement.

Data on D_L/μ in CO_2 included measurements over a limited range of low E/N by Wagner and co-workers¹⁵³ and for high E/N by Schlumbohm,¹⁶¹ as well as values calculated

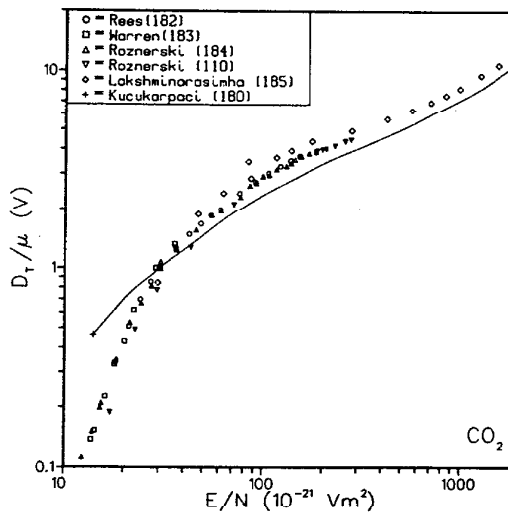
FIGURE 6.2. D_T/μ in CO_2 as a function of E/N (low E/N).

by Lowke and Parker¹⁶⁹ which agree with the measured data for E/N below $30 \times 10^{-21} \text{ V m}^{-2}$.

Roznerski and Mechlinska-Drewko¹⁸⁴ used standard steady-state Townsend techniques to measure D_T/μ in carbon dioxide. In the region of $E/N > 50 \times 10^{-21} \text{ V m}^{-2}$, the analysis requires ionization and attachment coefficients and D_L/μ to determine D_T/μ from the raw data. These authors completed a thorough analysis for E/N between 0.3 and $185 \times 10^{-21} \text{ V m}^{-2}$ ¹⁸⁴ and subsequently published measured values for E/N up to $277 \times 10^{-21} \text{ V m}^{-2}$ ¹¹⁰.

Lakshminarasimha and co-workers¹⁸⁵ extended measurements from E/N of 28 up to $1500 \times 10^{-21} \text{ V m}^{-2}$ using a limiting case analysis which excludes the need for accurate values of the other parameters ($\eta, \alpha, D_L/\mu$). They claim their obtained values of D_T/μ are uncertain by $\pm 5\%$.

Kucukarpaci and Lucas,¹⁸⁰ in their Monte Carlo calculations which assume that inelastic collisions result in anisotropic scattering, obtained both D_T/μ and D_L/μ for E/N between 12 and $3000 \times 10^{-21} \text{ V m}^{-2}$. These calculations were not extended to very low E/N .

FIGURE 6.3. D_T/μ in CO_2 as a function of E/N .

In their time-of-flight experiments, Saelee and co-workers¹⁷⁸ measured D_L/μ for E/N between 28 and $700 \times 10^{-21} \text{ V m}^2$, partially bridging the gap in earlier data.

Figure 6.2 compares data for D_T/μ in the region of E/N below $10 \times 10^{-21} \text{ V m}^2$. The recent data of Roznerski and Mechliniska-Drewko are slightly higher than the earlier data of Rees and of Warren and Parker. The latter two data sets, recommended by Dutton,¹ are still considered the most reliable.

Figure 6.3, which compares data discussed above for D_T/μ for a wider range of E/N , shows that the experimental data for D_T/μ are in good agreement. Those of Warren and Parker are recommended for E/N between 12 and $30 \times 10^{-21} \text{ V m}^2$; those of Rees for E/N between 30 and $150 \times 10^{-21} \text{ V m}^2$. Above $150 \times 10^{-21} \text{ V m}^2$, the data of Roznerski and Mechliniska-Drewko and of Lakshminarasimha and co-workers form a consistent set and are recommended.

The data for D_L/μ are shown in Fig. 6.4. For E/N between 0.2 and $3 \times 10^{-21} \text{ V m}^2$, the data measured by Wagner agree with those calculated by Lowke and Parker and are recommended. Above $30 \times 10^{-21} \text{ V m}^2$ the data measured by Saelee and co-workers and by Schlumbohm are fairly consistent and are reasonably fit by the calculations of Lowke and Parker. The measured data are recommended with an uncertainty of $\pm 20\%$ for this region of E/N . Measurements are needed to establish D_L/μ for E/N between 3 and $30 \times 10^{-21} \text{ V m}^2$.

Data calculated by Kucukarpaci and Lucas are lower than those measured for D_T/μ and higher than those measured for D_L/μ . For their common range of E/N , values of D_L/μ calculated by these authors and by Lowke and Parker are in reasonable agreement.

c. Electron Gain and Loss Processes, CO_2

Dutton¹ compiled the data available prior to 1974 on the attachment coefficient and electron growth constant in carbon dioxide.

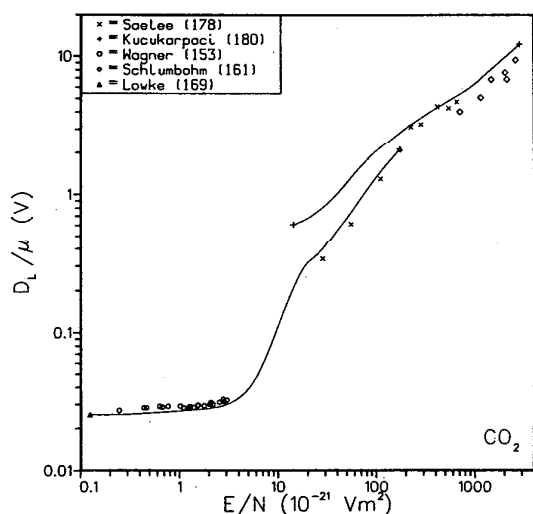


FIGURE 6.4. D_L/μ in CO_2 as a function of E/N .

The discussion of recent results requires comparisons to some of these earlier data, specifically the following: early measurements of η/N and α/N by Bhalla and Craggs¹⁸⁶ were obtained using standard spatial current growth techniques for E/N between 78 and $150 \times 10^{-21} \text{ V m}^2$. Chatterton and Craggs¹⁸⁷ used sampling techniques to extend measurements of η/N down to $E/N = 45 \times 10^{-21} \text{ V m}^2$. Schlumbohm⁸⁵ used an alternate technique, temporal current growth, to derive η/N and λ/N for E/N between 120 and $200 \times 10^{-21} \text{ V m}^2$. None of these early studies considered the influence of successive ion-molecule reactions initiated by the O^- ions released in the dissociative attachment process. Dutton noted that the attachment coefficient data display considerable dispersion, especially for E/N above $90 \times 10^{-21} \text{ V m}^2$ where ionization takes place, and points out that these data should be taken as approximate because of the uncertainties introduced by the curve-fitting procedures typically used to obtain them. In contrast, several sets of data on the electron growth constant for E/N between 90 and $360 \times 10^{-21} \text{ V m}^2$ were in excellent agreement. No data on the ionization coefficient were reported by Dutton. Several studies of electron gain and loss processes have been reported since 1974, with the general intent of better defining the attachment coefficient.

Alger and Rees,¹⁸⁸ using a drift tube/quadrupole mass spectrometer, measured the ion current ratio for the dominant negative ion species present, CO_3^- and O^- , the total ion current, and the electron current growth curves as a function of gas density. These curves were simultaneously fitted using an extensive reaction scheme which assumed ionization, two-body dissociative attachment ($e + \text{CO}_2 \rightarrow \text{O}^- + \text{CO}$), detachment from O^- , and the reaction: $\text{O}^- + 2\text{CO}_2 \rightarrow \text{CO}_3^- + \text{CO}_2$. These authors obtained η/N , for which they claim an uncertainty of $\pm 2\%$, and λ/N , for which they claim an uncertainty of $\pm 3\%$. Their analysis showed detachment to be negligible, in agreement with earlier work (Moruzzi and Phelps,¹⁷² Frommhold¹²⁷).

Conti and Williams,¹⁸⁹ in an extension of earlier work,¹⁹⁰ used steady-state techniques to extend measurements up to atmospheric gas density for the first time. Spatial current-growth curves were fitted assuming only ionization and attachment. The detachment is negligible is clearly established by work discussed below. The electron growth constant was found to be independent of N , confirming that the initial attachment process is a two-body, rather than a three-body, process. Their discussion indicates a large uncertainty in the values of η/N .

In connection with investigations of $\text{CO}_2:\text{N}_2:\text{He}$ laser mixtures, Davies¹⁹¹ also studied steady-state discharges in pure CO_2 for E/N between 76 and $99 \times 10^{-21} \text{ V m}^2$ emphasizing the region of $\lambda/N = 0$. The previously developed analysis technique of Davies²⁹ which gives accurate values of λ/N was applied to these measurements. The electron growth constant was reported with a maximum estimated uncertainty of $\pm 8\%$ at the lowest E/N , but with an estimated uncertainty of $\pm 3\%$ for higher E/N . Davies also reported η/N and α/N in this range of E/N and, at $E/N = 82.0 \times 10^{-21} \text{ V m}^2$ for which $\lambda = 0$, obtained α/N and η/N claimed to be accurate to $\pm 2\%$.

Davies also presents the swarm coefficients calculated

by Lowke and Kline using cross sections for pure CO_2 used earlier by Lowke and co-workers¹⁹² in calculations on laser mixtures.

Teich and co-workers¹⁹³ measured λ/N for E/N down to $40 \times 10^{-21} \text{ V m}^2$, and these data were taken from the Davies' paper.

In studies of air- CO_2 mixtures using standard spatial current growth techniques, Moruzzi and Price¹⁵⁶ reported η/N in pure CO_2 for a single value of E/N , i.e., $\eta/N = 0.3 \times 10^{-22} \text{ m}^2$ for $E/N = 106 \times 10^{-21} \text{ V m}^2$.

In connection with radial diffusion measurements discussed in the previous section, Lakshminarasimha, Lucas and Kontoleon¹⁸⁵ claimed to have obtained values of α/N in a higher E/N range, $135 < E/N < 1600 \times 10^{-21} \text{ V m}^2$. As their analysis did not consider attachment, it is assumed that λ/N was actually measured.

Risbud and Naidu⁹⁰ also used a modified Townsend method to measure α/P and η/P in CO_2 , but gave no description of the analysis used to obtain these coefficients.

Sakai and co-workers¹⁹⁴ extended previous Boltzmann equation calculations for CO_2 laser mixtures by including the effects of electron concentration gradients and of electron production and loss by ionization and attachment, as well as dissociation and dissociative ionization. They also calculated λ/N in pure CO_2 .

As a result of their Monte Carlo calculation, Kucukarpaci and Lucas¹⁸⁰ reported η/N and α/N over wide ranges of E/N , i.e., η/N for E/N between 30 and $3000 \times 10^{-21} \text{ V m}^2$ and α/N for E/N between 90 and $3000 \times 10^{-21} \text{ V m}^2$.

Figure 6.5 compares the recent data for the attachment coefficient with some of the earlier data, i.e., η/N measured by Alger and Rees,¹⁸⁸ Conti and Williams,¹⁸⁹ Davies,¹⁹¹ and Moruzzi and Price,¹⁵⁶ and calculated by Davies,¹⁹¹ Kucukarpaci and Lucas,¹⁸⁰ and Hake and Phelps.¹⁰³ The data of Risbud and Naidu,⁹⁰ which have been omitted for the sake of clarity, agree almost exactly with the earlier measurement of Bhalla and Craggs.¹⁸⁶ The early data Schlumbohm⁸⁵ and Conti and Williams¹⁹⁰ are lower, and similar to the recent

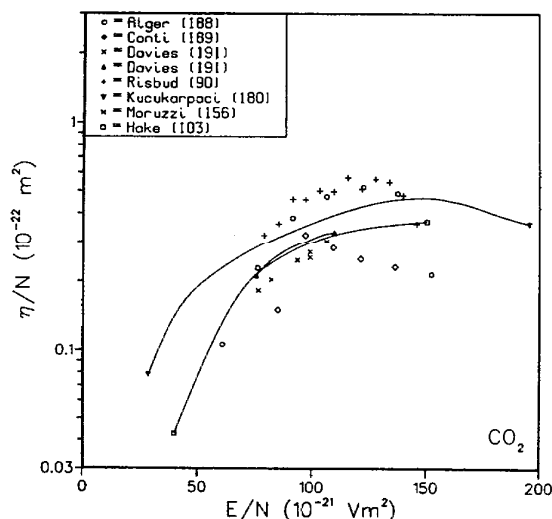


FIGURE 6.5. η/N in CO_2 as a function of E/N .

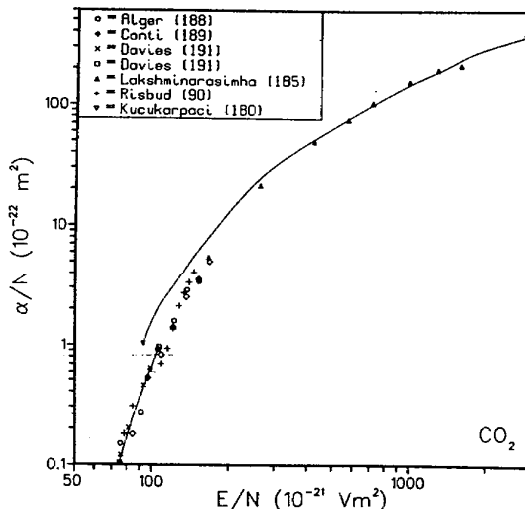


FIGURE 6.6. α/N in CO_2 as a function of E/N .

data of Conti and Williams. The data in the figure display as much dispersion as do the results of early work reported by Dutton¹ over the entire range of E/N . The decrease with increasing E/N (between 120 and $150 \times 10^{-21} \text{ V m}^2$) of the data of Alger and Rees and of Risbud and Naidu seems very unlikely in view of available theoretical predictions. The results of theory and other recent measurements suggest that these data are too high for E/N between 80 and $100 \times 10^{-21} \text{ V m}^2$. A good working set of data can thus be obtained by combining the experimental results of Davies with the theoretical curve of Hake and Phelps. More measurements are needed, however, to clarify attachment in CO_2 .

The values of α/N measured by Alger and Rees,¹⁸⁸ Conti and Williams,¹⁸⁹ Davies,¹⁹¹ Lakshminarasimha and co-workers,¹⁸⁵ and Risbud and Naidu⁹⁰ are compared in Fig. 6.6 with values calculated by Kucukarpaci and Lucas¹⁸⁰ and by Davies. The experimental data agrees to within about 15%, and those of Davies are recommended for E/N up to $100 \times 10^{-21} \text{ V m}^2$. Those of Conti and Williams and of Lakshminarasimha and co-workers are recommended for higher E/N .

As mentioned above, earlier measured and calculated values of λ/N are in good agreement. Figure 6.7 compares recent data with earlier work of Bhalla and Craggs,¹⁸⁶ Schlumbohm,⁸⁵ and Hake and Phelps.¹⁰³ Those of Risbud and Naidu⁹⁰ which lie below the other data for E/N below $130 \times 10^{-21} \text{ V m}^2$ and rise more sharply than the other data for higher E/N are not included. Most of the data shown are in good agreement over the entire range of E/N . Those calculated by Hake and Phelps are consistent with recently measured data for low E/N and represent a reasonable approximation to the measured data for E/N between 100 and $150 \times 10^{-21} \text{ V m}^2$. These data are, thus, recommended as giving a consistent set over a relatively broad range of E/N .

d. Excitation Coefficient, CO_2

Bulos and Phelps¹⁵ used a drift tube technique to measure the coefficient for excitation of $4.3 \mu\text{m}$ radiation in CO_2

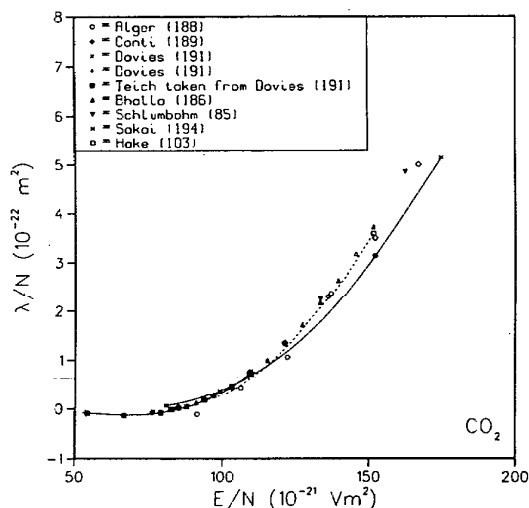


FIGURE 6.7. λ/N in CO_2 as a function of E/N . Values calculated by Hake (Ref. 103) are indicated by a dashed line.

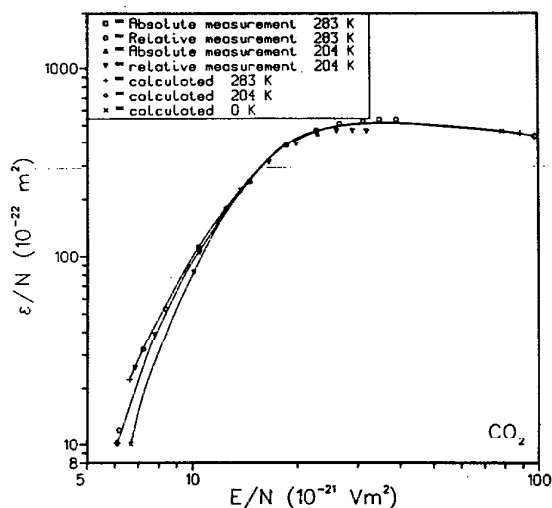


FIGURE 6.8. ϵ/N in CO_2 at different temperatures as functions of E/N . All data were taken from Bulos and Phelps (Ref. 15).

at 204 and 282 K and for E/N between 6 and $100 \times 10^{-21} \text{ V m}^{-2}$. This radiation is identified with $001 \rightarrow 000$ and $011 \rightarrow 010$ transitions. Using a set of recommended cross sections for excitation of the vibrational modes of CO_2 , these authors also calculated the excitation coefficients. The measured and calculated data are in excellent agreement, as shown in Fig. 6.8.

5.7. The Halogens and NF_3

Because the halogens and NF_3 are heavily used in laser systems, the properties of free electrons in these gases are currently a topic of much interest. Because these gases are highly reactive, little experimental work on their swarm properties has been carried out in the pure gases. The work that has been reported has been primarily with systems in which the halogen is buffered by a nonreactive, nonattaching gas. Usually the electronegative component of the mixture is so

small that an electron energy distribution (and drift velocity) equivalent to that of the pure buffer gas is assumed.

a. Drift Velocity, Halogens

The only data on electron drift velocities in the halogens are those reported by workers at the University of Sydney in the 1930's: for chlorine by V. A. Bailey and Healey¹⁹⁵; for bromine by J. E. Bailey and co-workers¹⁹⁶; and for iodine by Healey.¹⁹⁷ These data were obtained from an extrapolation of results obtained on mixtures; the analysis assumed the properties of components of the mixtures were unaffected by other components. The results obtained by this indirect method are of doubtful quality because of the stated experimental circumstances: the gas density of the pure gas diminished rapidly; in mixtures this gas density decrease was slowed; apparently the chlorine reacted with the silver sur-

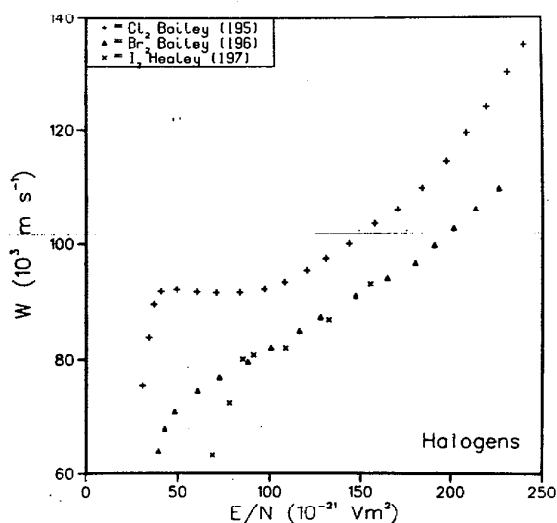


FIGURE 7.1. W for electrons in Cl_2 , Br_2 , and I_2 as functions of E/N .

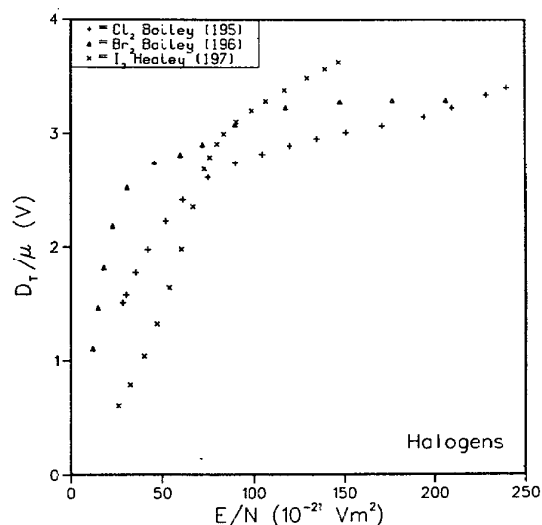


FIGURE 7.2. D_T/μ in Cl_2 , Br_2 , and I_2 as functions of E/N .

face from which electrons were produced by photoemission. In addition, interpretation of these measurements is approximate (see Gilardini, Ref. 4, Sec. 3.9.b).

These drift velocities for chlorine, bromine and iodine are shown in Fig. 7.1. The reader is cautioned that these, the only available data, should be considered as approximate.

b. (Diffusion Coefficient)/Mobility, Halogens

The only data reported for D/μ in the halogens are also from the Sydney group who used a combined electric- and magnetic-field technique. These authors reported k_T , the Townsend energy factor, which is defined in Sec. 2. As discussed in the previous section, problems were encountered concerning the handling of these reactive gases. In addition, the interpretation of data obtained by this technique is approximate (see, e.g., Huxley and Crompton, Ref. 2, Sec. 11.4.1, and Gilardini, Ref. 4, Sec. 3.9.B). Because no other data are available, however, values of D_T/μ obtained using k_T and $F=1$ (see Sec. 2 for discussion of F) for chlorine, bromine, and iodine reported in Refs. 195, 196, and 197, respectively, are given in Fig. 7.2. The user should keep in mind that these data represent, at best, an approximation.

c. Electron Gain and Loss Processes, Halogens and NF_3

Nygaard and co-workers²³ and Chantry²⁴ have both recently reviewed the attachment data for F_2 , Cl_2 , I_2 , and NF_3 .

F_2

Because fluorine is highly reactive, all observations of dissociative attachment have been made in mixtures of a small amount of fluorine in a nonreactive buffer gas. For fluorine concentrations of 0.3% and below, the electron energy distribution of the pure buffer gas was typically assumed to determine the mean electron energy.

Nygaard and co-workers¹⁹⁸ measured the two-body attachment coefficient for small amounts of fluorine (0.1 to 1.0%) in helium by observation of voltage transients in a

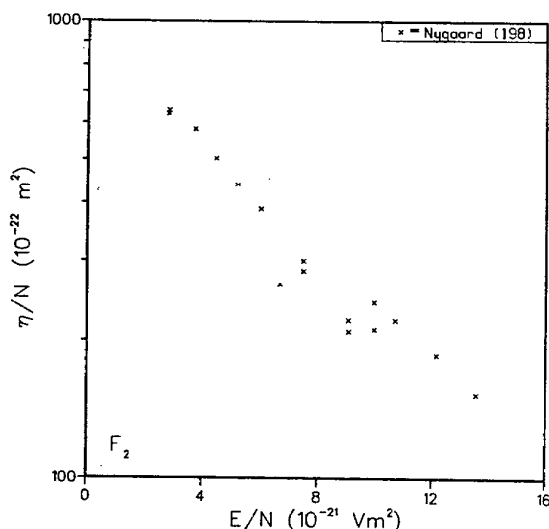


FIGURE 7.3. η/N' for 1% F_2 in He as a function of E/N . N' refers to the fluorine gas density, while E/N refers to the specific mixture.

spatial drift tube, and η/N' was measured, where N' is the fluorine density, as a function of E/N for the mixture. The data for 1% F_2 in helium, for which the authors claim an uncertainty of $\pm 12\%$, are shown in Fig. 7.3. In another paper,¹⁹⁹ Nygaard and co-workers report electron drift velocities measured in F_2 -He mixtures and determined that η increased with fluorine concentration. Nygaard, Brooks, and Hunter²³ used drift velocities for 1% F_2 in helium to convert η/N' to the attachment rate coefficient for that specific mixture which they represent as a function of the mean electron energy for pure helium.²³ An uncertainty of $\pm 20\%$ is stated for these data.

Nighan²⁰⁰ computed rate coefficients as a function of E/N for dissociative attachment to F_2 for a typical laser mixture of Ar-Kr- F_2 in proportions of 0.945:0.05:0.005 as a function of E/N for that specific mixture. Rate coefficients calculated for F_2 in the vibrational ground state ($v=0$) and in the first vibrational level ($v=1$) using the theoretical cross sections of Hall²⁰¹ are given in Fig. 7.4. The rate coefficient for dissociative attachment is greater for the vibrationally excited molecules than for the molecule in the vibrational ground state. The reader is cautioned that the E/N scale is expected to be different for a different mixture.

Chen and co-workers,²⁰² using a mixture of less than 0.25% fluorine in nitrogen in an electron-beam-sustained discharge, measured the discharge current density and, assuming an electron drift velocity equivalent to that of pure N_2 , obtained the rate coefficient for attachment to F_2 as a function of D/μ . Chantry²⁴ replotted these data as a function of the mean energy, based on the experimental values of E/N supplied by Chen, and this representation of Chen's data is reported below.

Sides and co-workers,²⁰³ using 0.065% fluorine in argon in a flowing afterglow system, measured the thermal rate for dissociative electron attachment in F_2 with two elec-

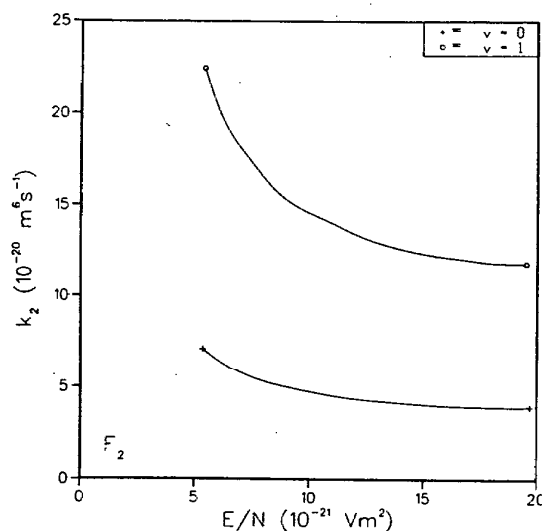


FIGURE 7.4. k_2 for a mixture of Ar-Kr- F_2 in proportions 0.945:0.05:0.005. The $v=0$ curve refers to attachment into the vibrational ground state; the $v=1$ curve, attachment into the first excited vibrational state. k_2 refers to attachment to F_2 , but E/N is appropriate to this specific mixture only. The data were taken from Nighan (Ref. 200).

tron sources, a microwave discharge for which the average electron temperature is estimated to be 600 K and a filament source for which the temperature is estimated to be 350 K.

Schneider and Brau²⁰⁴ obtained attachment rates by observing the rate of decay of the current carried in glow discharges of nitrogen and argon due to the addition of small quantities (0.01 to 0.03%) of fluorine. The corresponding electron mean energies were computed from the measured value of E/N using a Boltzmann code. These data represent averages over several runs in which proportions of fluorine and total gas density were varied by more than a factor of 2 and for which the scatter was typically 15%.

Using an electron-beam controlled discharge, Trainor and Jacob²⁰⁵ measured the attachment rate constant for 0.13% F_2 in N_2 at atmospheric pressure, normalizing against the attachment rate for Cl_2-N_2 mixtures measured by

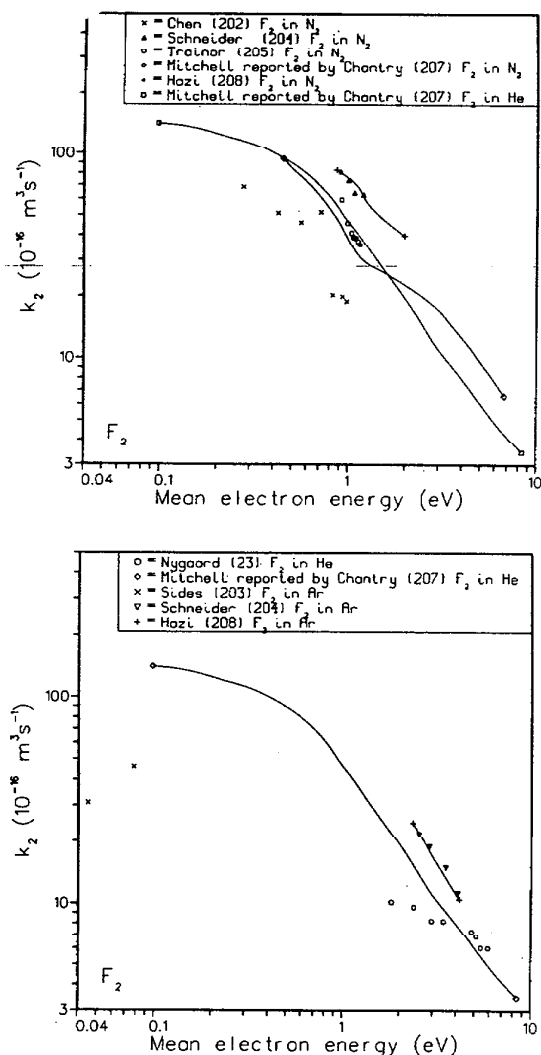


FIGURE 7.5. k_2 for F_2 as a function of mean electron energy. Measurements were made in the following mixtures: Nygaard (Ref. 23), 1% F_2 in He; Chen (Ref. 202), 0.25% F_2 in He; Sides (Ref. 203), 0.065% F_2 in Ar; Schneider (Ref. 204), 0.01 – 0.03% F_2 in Ar and 0.01 – 0.03% F_2 in N_2 ; Trainor (Ref. 205), 0.13% F_2 in N_2 . The calculations of Mitchell (Ref. 207) were for mixtures of F_2 in He and N_2 ; those of Hazi (Ref. 208) were for mixtures of F_2 in Ar and in N_2 .

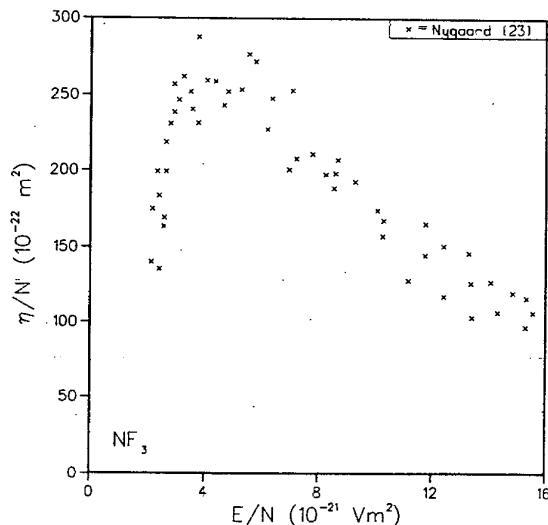


FIGURE 7.6. η/N' for 0.5% NF_3 in He as a function of mean electron energy. N' refers to the NF_3 gas density.

Rokni and co-workers²⁰⁶ using the same apparatus. The average electron energy corresponding to pure nitrogen was assumed. Measurements made at 300 and 500 K indicated an increase in the F_2 attachment rate with temperature.

Chantry²⁰⁷ measured dissociative attachment cross sections for F_2 using electron beam techniques. For these cross sections and a Maxwellian energy distribution, Chantry calculated the attachment coefficient as a function of mean electron energy. Chantry also reported unpublished rate coefficients calculated by Mitchell and Kline. These were obtained by numerical solution of the Boltzmann equation for electron energy distributions corresponding to small amounts of F_2 in N_2 and He, and are appropriate for comparison to the data measured by Chen and co-workers and by Nygaard and co-workers.

Recently, Hazi and co-workers²⁰⁸ reported ab initio calculations of the cross sections for dissociative attachment to F_2 and from these calculated attachment rate coefficients for mixtures of F_2 in N_2 and in Ar (although the exact percentages are not specified).

The rate coefficients for two-body dissociative attachment to F_2 as a function of mean electron energy obtained by the work discussed in the previous paragraphs are compared in Fig. 7.5. In view of the scatter in these data, no recommendation concerning a preferred set can be made.

NF_3

Prior to 1970, no reports were published on attachment rates and cross sections in NF_3 . For a mixture of 0.5% NF_3 in He for $N = 66 \times 10^{22} \text{ m}^{-3}$, Nygaard and co-workers²³ reported η/N' as a function of E/N (where N' is the NF_3 gas density), obtained from observation of voltage transients in a spatial drift tube. Prepassivated conditions assured no gas density decrease due to loss of NF_3 to the walls. These data are given in Fig. 7.6. The reader is cautioned that although the attachment coefficient refers to the nitrogen trifluoride gas density, the reduced field strength refers to the specific mixture in which the measurements were made. To make

comparisons to the other available data, these must be converted to rate coefficients. Nygaard has done this by assuming drift velocities and mean energies appropriate to pure helium.

Using the techniques described in the previous section, Trainor and Jacob²⁰⁵ measured the attachment rate coefficient for 0.13% NF_3 in N_2 at atmospheric pressure as a function of mean electron energy for pure N_2 . Measurements at 300 and 500 K indicated an increase in the attachment rate with temperature.

Chantry²⁰⁷ measured the attachment cross section for pure NF_3 using electron beam techniques, and calculated the rate coefficients as a function of mean electron energy assuming a Maxwellian distribution.

The other measurements of the attachment rate coefficients for NF_3 are for thermal electrons. The earliest data were reported in 1972 by Mothes and co-workers²⁰⁹ who used a flowing afterglow system to obtain a rate at 300 K. Sides and Tiernan²¹⁰ also used a flowing afterglow to measure the attachment rate for NF_3 buffered in argon at a density of $2.6 \times 10^{22} \text{ m}^{-3}$ at temperatures between 300 and 350 K. In connection with their study of processes in KrF lasers, Shaw and Jones²¹¹ observed the decrease in electron density when NF_3 was added to a helium or helium/argon flowing afterglow and determined an attachment rate for 300 K.

These data, compared in Fig. 7.7, show wide dispersion, and no recommendation concerning a preferred set can be made.

Cl_2

In chlorine, measurements in a pure gas are possible. Bozin and Goodyear²¹² obtained values of α/N , η/N , and λ/N using standard spatial current growth techniques for gas densities between 3.3 and $33 \times 10^{22} \text{ m}^{-3}$. No gas density dependence of these coefficients was observed.

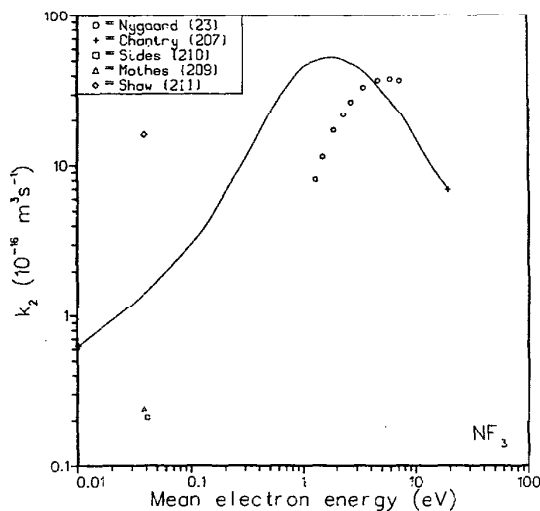


FIGURE 7.7. k_2 in NF_3 as a function of mean electron energy. The measurements were made in the following mixtures: Nygaard (Ref. 23), 0.5% NF_3 in He; Trainor (Ref. 205), 0.13% NF_3 in N_2 ; Sides (Ref. 210), Mothes (Ref. 209), and Shaw (Ref. 211), trace quantities of NF_3 in Ar, Ar, and He, respectively.

The values of η/N , α/N , and λ/N in chlorine measured by Bozin and Goodyear are given in Figs. 7.8, 7.9, and 7.10, respectively, and are recommended as a good estimate for pure chlorine.

Risbud and Naidu⁹⁰ fit the values of the data of Bozin and Goodyear to analytic expressions for α/N and η/N .

A third measurement of η/N , made by Bailey and Healey¹⁹⁵ shows a marked disagreement with the other two data sets. Bailey's data imply attachment in chlorine is negligible for E/N above $200 \times 10^{-21} \text{ V m}^2$. Bozin and Goodyear²¹² give convincing arguments that attachment is, in fact, appreciable for $E/N > 200 \times 10^{-21} \text{ V m}^2$. Bailey's data are not included here.

Rokni and co-workers²⁰⁶ measured the attachment rate for mixtures of Cl_2 and N_2 at 293 and 523 K using an electron-beam-controlled discharge and found an increase in k_2 with temperature. The authors also used Boltzman techni-

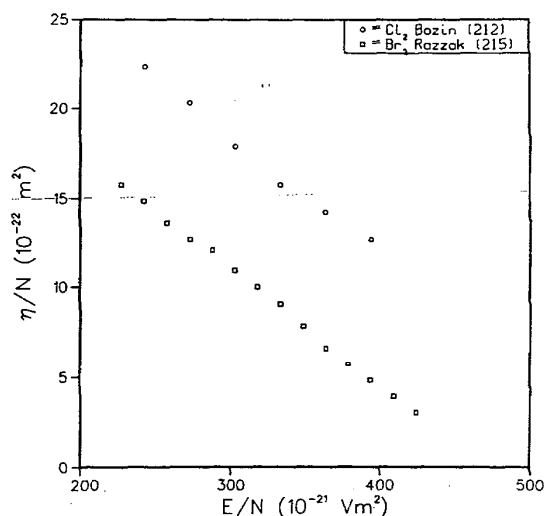


FIGURE 7.8. η/N in Cl_2 and Br_2 as functions of E/N .

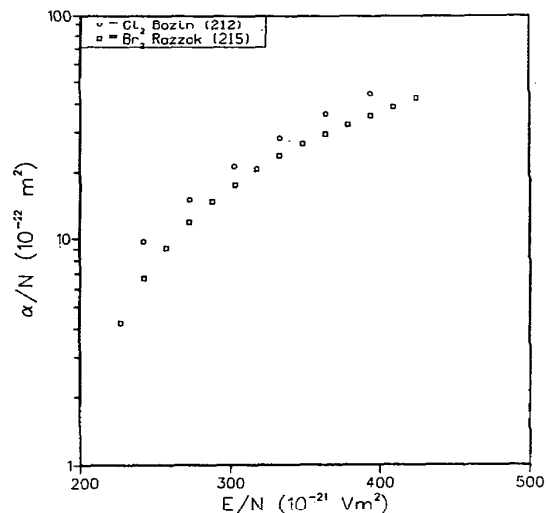


FIGURE 7.9. α/N in Cl_2 and Br_2 as functions of E/N .

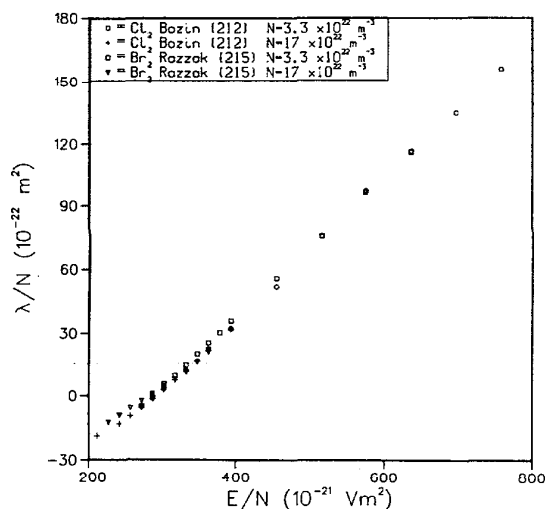


FIGURE 7.10. λ/N in Cl_2 and Br_2 as functions of E/N .

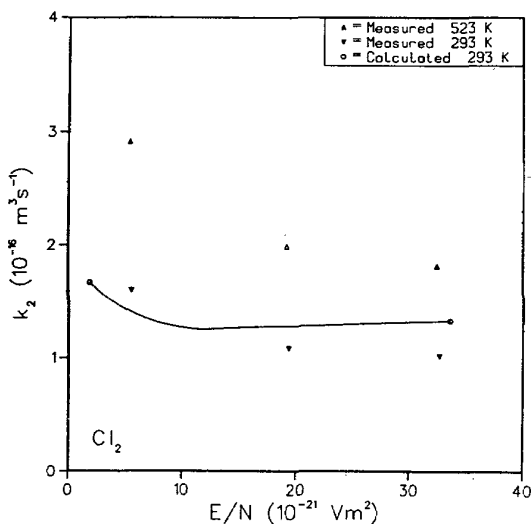


FIGURE 7.11. k_2 for Cl_2 in N_2 as functions of E/N . E/N refers to the mixture which is not specified. All data were taken from Rokni and co-workers (Ref. 206).

ques and attachment cross sections measured by Tam and Wong²¹³ to calculate the attachment rate. These data are given in Fig. 7.11. The mixture ratio for these data is not specified.

Br_2

In pure bromine, η/N , α/N , and λ/N have been measured by Razzak and Goodyear²¹⁵ using the Townsend current growth technique. No gas density dependence was observed for α/N , but a small increase in η/N and a decrease in λ/N with increasing N were observed. The authors suggest that three-body, nondissociative attachment occurring simultaneously with two-body dissociative attachment is the most likely explanation for these observations. These data are plotted with the corresponding coefficients for chlorine

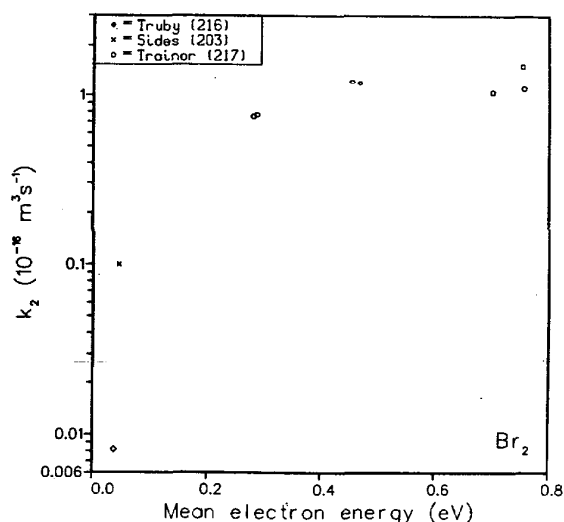


FIGURE 7.12. k_2 in Br_2 as a function of mean electron energy. Measurements were made in the following mixtures: Trainor (Ref. 217), 1% Br_2 in N_2 ; Truby (Ref. 216) and Sides (Ref. 203), trace quantities of F_2 in He and Ar, respectively.

in Figs. 7.8, 7.9, and 7.10, respectively, and are recommended as a good estimate for pure bromine.

Risbud and Naidu⁹⁰ fit the data of Razzak and Goodyear to an analytic expression for η/N .

Rate constants for dissociative attachment to molecular bromine in very low concentration in buffer gases were obtained by three different investigations: Truby²¹⁶ using microwave techniques for trace amounts of bromine in helium obtained a value of $0.0082 \times 10^{-16} \text{ m}^3 \text{ s}^{-1} \pm 10\%$ at 296 K. Sides and co-workers,²⁰³ using a small percentage of bromine in argon in a flowing afterglow system, measured the thermal rate for dissociative attachment in Br_2 to be $1.0 \pm 0.09 \times 10^{-16} \text{ m}^3 \text{ s}^{-1}$ at 350 K. Trainor and Boness,²¹⁷ using less than 1% bromine in nitrogen in an electron-beam-sustained discharge, measured the discharge current density. Using the discharge current density in pure nitrogen and assuming an electron drift velocity equal to that in pure nitrogen, they obtained the rate constant for dissociative attachment in bromine as a function of average electron energy. These rate coefficients, compared in Fig. 7.12, represent a reasonable approximation for a mean electron energy above 0.1 eV.

I_2

Brooks and co-workers²¹⁸ measured voltage transients in a temperature controlled drift tube containing 1% I_2 in N_2 at a gas density of $165 \times 10^{22} \text{ m}^{-3}$ to obtain η/N' as a function of E/N for E/N up to $40 \times 10^{-21} \text{ V m}^{-2}$ and at temperatures between 308 and 383 K. These data, shown in Fig. 7.13, display a large attachment coefficient which increases with gas temperature. The latter effect is attributed to thermal population of vibrationally excited states. The reader is cautioned that although the attachment coefficient refers to the iodine gas density, the reduced field strength refers to the specific mixture in which the measurements were made.

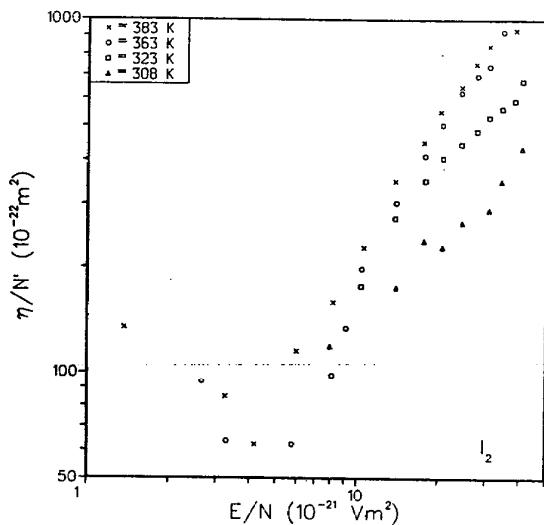


FIGURE 7.13. η/N' for 1% I_2 in N_2 at different temperatures as functions of E/N . N' refers to the I_2 gas density, while E/N is appropriate only to this mixture. All data were taken from Brooks and co-workers (Ref. 218).

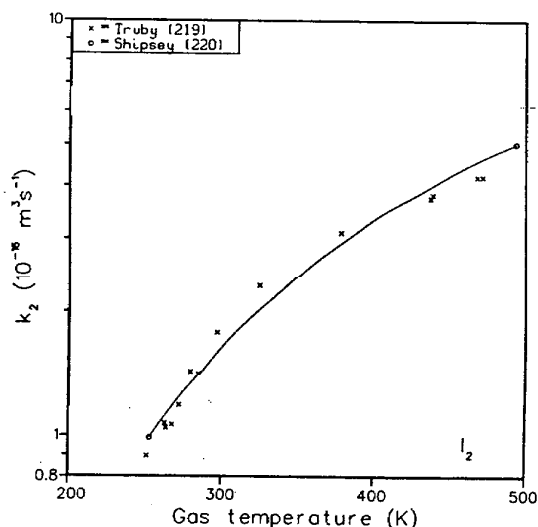


FIGURE 7.14. k_2 in I_2 as a function of temperature.

The early attachment data for I_2 reported by Healey,¹⁹⁷ obtained by the indirect method of mixtures, are in serious disagreement with the Brooks data and are not considered further here.

Truby²¹⁹ used microwave techniques to measure the attachment rate for thermal electrons as a function of gas temperature. Subsequently, Shipsey²²⁰ and Birtwistle and Modinos²²¹ made theoretical analyses of the Truby data to determine the I_2 potential curve. Truby's data and the best theoretical fit obtained by Shipsey for a specific set of descriptive parameters are given in Fig. 7.14.

5.8. Nitrogen Oxides

There are three electronegative nitrogen oxides: N_2O , nitrous oxide; NO , nitric oxide; and NO_2 , nitrogen dioxide.

As discussed by Parkes^{25,222} and by Dutton and co-workers,²²³ a complex ion-molecule reaction scheme occurs when free electrons are introduced into N_2O . Dissociative attachment to N_2O forms the negative oxygen ion O^- , which in turn reacts with N_2O to form NO and NO^- . Although negative ion identity and detachment effects are important at high E/N and high temperature in most gases, they are dominant whenever NO^- is formed at laboratory temperatures due to its low electron affinity. Thus, although the swarm coefficients and rate coefficients for the various nitrogen oxides are discussed separately, in reality these molecules and their ions often exist as a mixture. Another difficulty in the interpretation of observations in NO_2 is introduced by the formation of the N_2O_4 dimer.²²⁴

a. Drift Velocity, N_2 and NO

Using standard drift tube techniques, Pack, Voshall, and Phelps¹⁶⁴ measured the drift velocity for electrons in

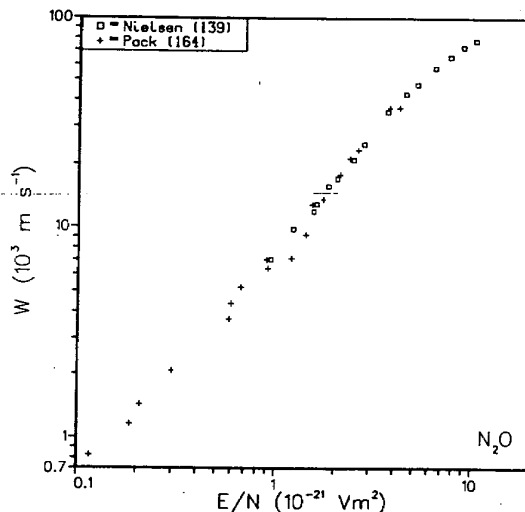


FIGURE 8.1. W for electrons in N_2O as a function of E/N .

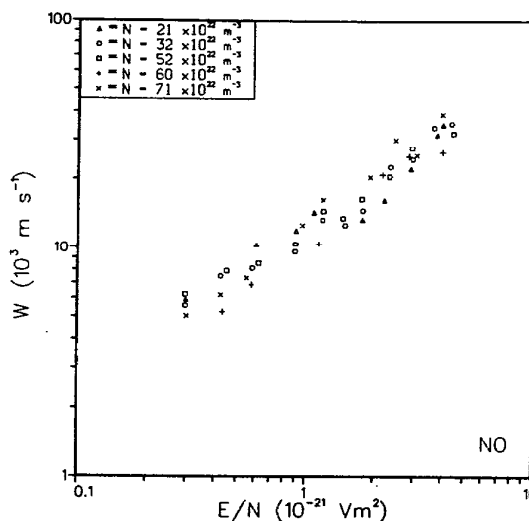


FIGURE 8.2. W for electrons in NO as a function of E/N . All data were taken from Parkes and Sugden (Ref. 225).

N_2O gas at 195 and 300 K and for $0.1 < E/N < 4.5 \times 10^{-21}$ V m^2 . The values obtained were the same for both temperatures. Nielsen and Bradbury¹³⁹ also applied sampling techniques to obtain drift velocities up to 10×10^{-21} V m^2 . The results of these two measurements, shown in Fig. 8.1, are in good agreement.

The drift velocity in NO was measured by Parkes and Sugden²²⁵ using a pulsed drift tube at gas densities between 21 and 71×10^{22} m^{-3} and at 294 and 459 K. No observable dependence on temperature or gas density was apparent. These data, given in Fig. 8.2, are recommended.

Early measurements of the drift velocity in N_2O by Bailey and Rudd,²²⁶ in NO by Bailey and Somerville,²²⁷ and in both gases by Skinker and White²²⁸ used the indirect method of crossed electric and magnetic fields which gives the "magnetic drift velocity" (see Dutton, Ref. 1, Sec. 3.1) and are not considered here.

No data have been published for drift velocities in NO_2 .

b. (Diffusion Coefficient)/Mobility, N_2O , NO

Two very early measurements of the ratio of diffusion to mobility in N_2O are the only ones available, those by Bailey²²⁶ and by Skinker and White.²²⁸ The presence of negative ions in the latter experiment seriously hindered the measurements, and the results will not be considered here. The Bailey measurements report k_T , the Townsend energy factor defined in Sec. 2. As discussed by Gilardini (Ref. 4, Sec. 3.9.b), the interpretation of these measurements is approximate. In view of the absence of other data on D_T/μ in N_2O , however, D_T/μ was determined from k_T using $F=1$ and is given in Fig. 8.3. The user should treat these data as approximate.

In NO, Bailey and Somerville²²⁷ and Skinker and White²²⁸ also reported early measurements of k_T . In this case, negative ions did not interfere as severely with Skinker and White's measurements as in N_2O , and their results agree fairly well with those of Bailey and Somerville. The same concerns, however, apply here as with regard to similar data

reported for the halogens and N_2O . Values of D_T/μ obtained from these data using $F=1$, displayed in Fig. 8.4, give a rough approximation in the region of low E/N where no other values are available.

Lakshminarasimha and Lucas¹⁵⁴ measured the radial distribution of the anode current for a steady-state swarm of electrons in NO and, by varying the gap separation and gas density and applying previously developed techniques of analysis, obtained values of D_T/μ for $300 \leq E/N \leq 1250 \times 10^{-21}$ V m^2 . No discussion of negative-ion effects was included in this publication. These data are also given in Fig. 8.4, and are recommended for high E/N .

There are no published data for D/μ for NO_2 .

c. Electron Gain and Loss Processes, Nitrogen Oxides

N_2O

As discussed by Parkes^{25,222} and Dutton and co-workers,²²³ a complex ion-molecular reaction scheme is associated with electron attachment to N_2O .

Bradbury and Tatel¹⁷¹ measured the attachment probability in nitrous oxide, but did not anticipate the complexity of the systems studied.

Phelps and Voshall²²⁹ extended drift tube measurements to low E/N (0.25×10^{-21} V m^2) and observed that below 2×10^{-21} V m^2 , η/N increased with gas density. This effect was interpreted as due to a three-body attachment process ($e + 2\text{N}_2\text{O} \rightarrow \text{N}_2\text{O}^- + \text{N}_2\text{O}$) similar to that observed in oxygen for low electron energies. Parkes²⁵ subsequently interpreted these observations using a complex ion-molecule reaction scheme in which dissociative attachment to N_2O forms O^- , which reacts with N_2O to form NO^- ; the NO^- detaches in collisions with N_2O . Expressing the entire reaction scheme analytically, Parkes obtains an effective attachment rate coefficient which is proportional to the square of the nitrous oxide density, i.e., an "apparent" three-body effect.

Above 2×10^{-21} V m^2 , Phelps and Voshall observed a more typical two-body behavior of the attachment coefficient.

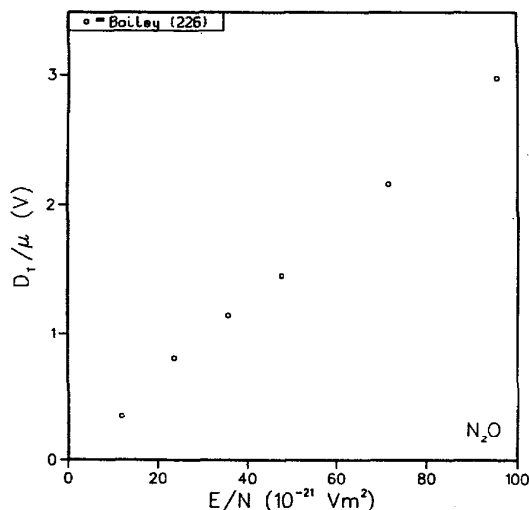


FIGURE 8.3. D_T/μ in N_2O as a function of E/N .

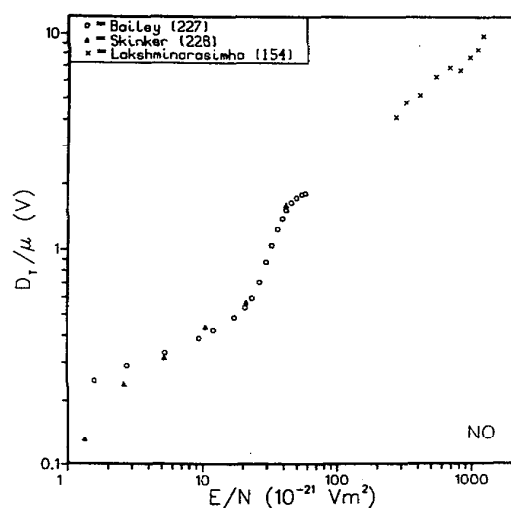


FIGURE 8.4. D_T/μ in NO as a function of E/N .

cient. The coefficients obtained were, however, much smaller than estimated from attachment cross sections measured by beam techniques (Rapp and Briglia²³⁰). Phelps and Vosshall suggest a detachment process as a possible explanation for this discrepancy.

For E/N above $3 \times 10^{-21} \text{ V m}^2$ Parkes²²² also calculated the two-body attachment coefficient for N_2O as a function of E/N using the measured cross sections of Rapp and Briglia.²³⁰ A Maxwellian distribution was assumed, and because the true distribution function is expected to be somewhat different, the calculated coefficients are probably in error. However, as shown in Fig. 8.5, these coefficients are a factor of 10 larger than those measured. Parkes attributes the difference to the rapid detachment from NO^- , a process which was not considered in the analysis of the measurements discussed above.

At even higher E/N ($150 < E/N < 182 \times 10^{-21} \text{ V m}^2$) Dutton, Harris, and Hughes²²³ measured prebreakdown current growth curves and applied at complete ion-molecular reaction scheme in their analysis including detachment from NO^- for which a rate of $1.0 \times 10^{-16} \text{ m}^3 \text{ s}^{-1}$ was assumed. A strong dependence of λ/N on N but a regular variation of λ/N with E/N at a given N was reported by Dutton and co-workers. These authors obtained values of α/N by two separate methods: (1) from spatial current growth curves and (2) from analyses of the variation of λ/N with N . These data, shown in Fig. 8.6, span a narrow range of E/N .

Measurements extending to low E/N are needed.

NO

The attachment of electrons to nitric oxide at low electron energies cannot be depicted as a simple two-body dissociative attachment. Three-body attachment has been found to be the dominant attachment process at low E/N . The electron affinity of NO is very low and detachment is a major complementary effect (McFarland and co-workers²³³). A complex set of gas density-dependent ion-molecule reactions also accompany these processes (Parkes²⁵). A temperature-dependent shift in the balance of reactions and, hence, con-

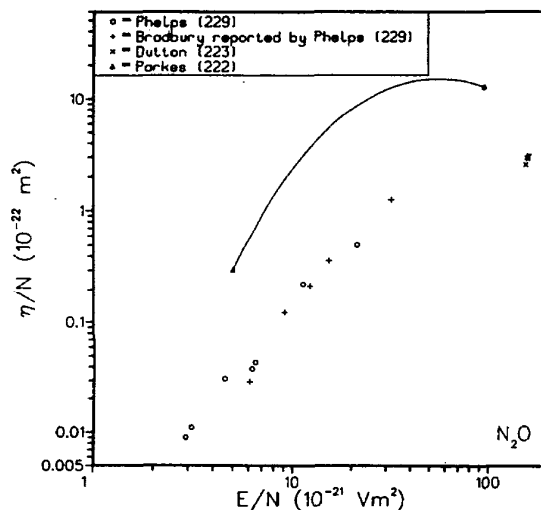


FIGURE 8.5. η/N in N_2O as a function of E/N .

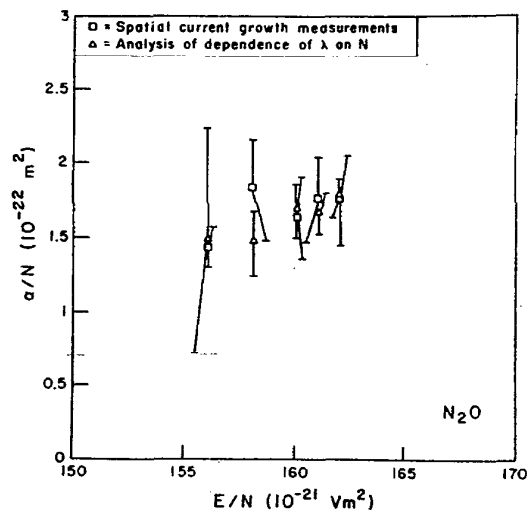


FIGURE 8.6. α/N in N_2O as a function of E/N obtained from two different methods by Dutton and co-workers (Ref. 223).

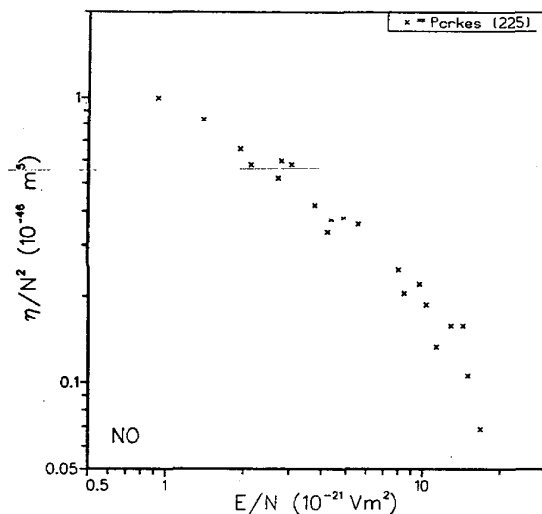


FIGURE 8.7. α/N in NO as a function of E/N .

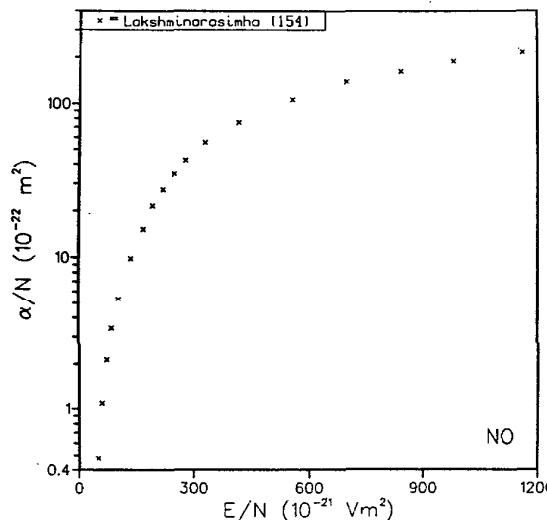


FIGURE 8.8. η/N^2 in NO as a function of E/N .

stituents in the system results in a modification of detachment.

The earliest observations of attachment in nitrogen oxide were those of Bradbury²³² who measured the attachment probability. Lakshminarasimha and Lucas,¹⁵⁴ using spatial current growth techniques, measured the electron growth constant in nitric oxide for $50 < E/N < 1200 \times 10^{-21} \text{ V m}^2$. The latter data are given in Fig. 8.7.

Parkes and Sugden²²⁵ used drift tube techniques to measure the three-body attachment coefficient in NO at 293, 341, and 493 K and at various gas densities. At 293 and 361 K, the ratio of attachment coefficient to gas density squared was independent of gas density and these data are shown in Fig. 8.8. However, at higher temperatures, a gas density dependence was observed, indicating the occurrence of detachment.

5.9. Miscellaneous Gases

a. Hydrogen Halides

In 1930, Bailey and Duncanson¹⁶² reported the drift velocity and attachment coefficient for HCl, which they determined using the magnetic and electric field technique. The interpretation of data obtained by this technique is approximate (see Gilardini, Ref. 4, Sec. 3.9.b). Bailey and Higgs²³⁴ reported k_T , the Townsend energy factor. As discussed above, similar data for other gases have been found to be unreliable. These data will not be considered further here, because recent, more credible data are now available.

Bradbury²³² reported the probability of electron attachment for HCl diluted in argon, but did not give the mixture ratio and stressed that these data are not appropriate for the pure gas.

Christophorou and co-workers²³⁵ measured attachment rates in dilute mixtures of the hydrogen halides (HCl, HBr, and HI) and their deuterated analogs in N_2 for E/N between 0.1 and $5 \times 10^{-21} \text{ V m}^2$. The explanation for the low energy behavior of these attachment rates (a minimum and an increase in k_2 as E/N approaches zero) is speculative (Refs. 235 and 3, pp. 460–461). The thermal attachment rate for small quantities of HCl in N_2 measured by Davis and co-workers²³⁶ is two orders of magnitude smaller than that predicted from the measurements of Christophorou and co-workers, a result which is consistent with the Bradbury measurements.²³² However, Sze and Greene²³⁷ reported an attachment coefficient measured for trace quantities of HCl in N_2 for mean electron energies between 0.7 and 1.2 eV of approximately $4.5 \times 10^{-16} \text{ m}^3 \text{ s}^{-1}$. This result, obtained from afterglow measurements, is consistent with that of Christophorou. For HBr, the thermal attachment rate reported by Mothes²⁰⁹ of $0.96 \times 10^{-16} \text{ m}^3 \text{ s}^{-1}$ is two orders of magnitude smaller than that predicted by the Christophorou measurements. The attachment rates reported by Christophorou and co-workers²³⁵ for HCl, HBr, and HI are shown in Fig. 9.1. In view of the controversy surrounding the data for E/N below $1 \times 10^{-21} \text{ V m}^2$, these are excluded.

Davies²³⁸ has reported measurements of swarm data in pure HCl in which a pulsed drift tube was used. An uncertainty of $\pm 5\%$ was estimated for E/N between 3 and $300 \times 10^{-21} \text{ V m}^2$. The data for W and η/N , subsequently published by Chantry,²⁴ are shown in Figs. 9.2 and 9.3.

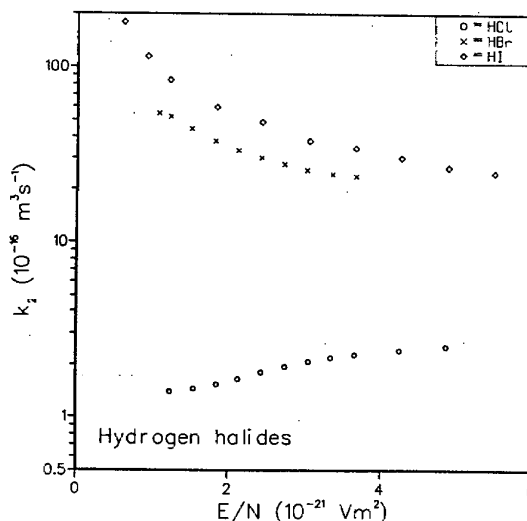


FIGURE 9.1. k_2 for the hydrogen halides as functions of E/N . All data were taken from Christophorou (Ref. 233).

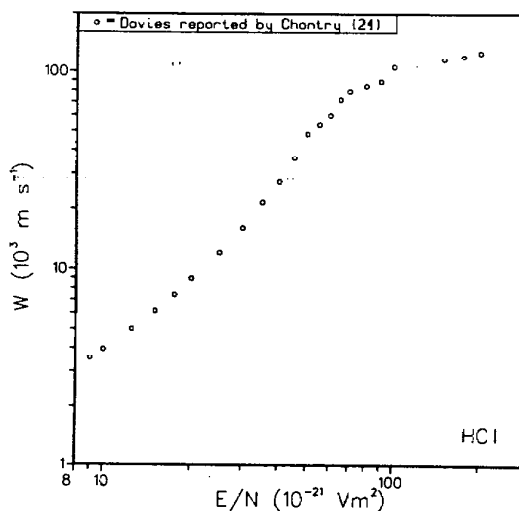


FIGURE 9.2. W for electrons in HCl as a function of E/N .

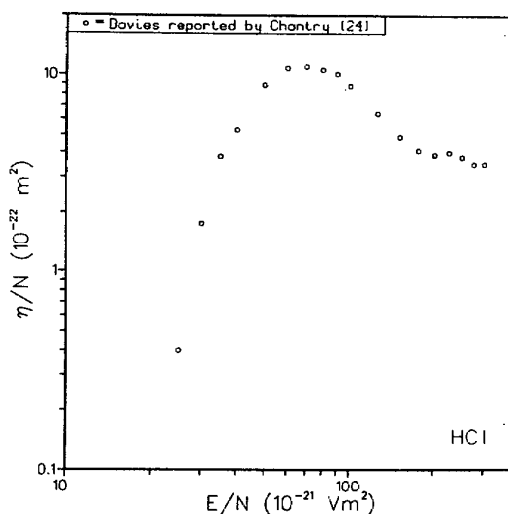


FIGURE 9.3. η/N for HCl as a function of E/N .

Trainor and Boness,²¹⁷ using an electron-beam-sustained discharge, measured the rate of dissociative attachment for less than 1% HBr in nitrogen. The electron drift velocity for pure nitrogen was assumed, and the attachment rate was reported as a function of the mean electron energy. Trainor and Boness also calculated the attachment rate constant for HBr assuming an energy distribution function for pure nitrogen and attachment cross sections for HBr measured by Ziesel and co-workers.²³⁹ The measured and calculated data are shown in Fig. 9.4.

b. Ammonia

A few measurements of the transport and swarm properties of NH_3 have been reported. As discussed in the pre-

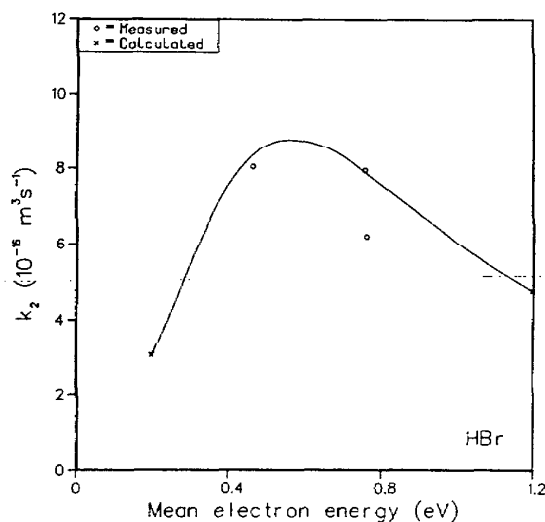


FIGURE 9.4. k_2 for HBr as a function of mean electron energy. The data were taken from Trainor and Jacob (Ref. 217).

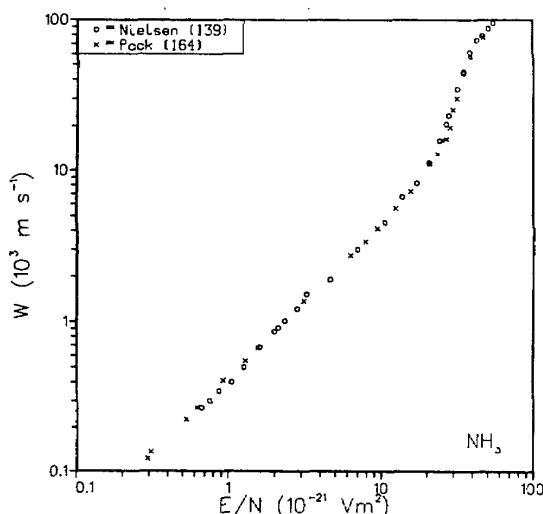


FIGURE 9.5. W for electrons in NH_3 as a function of E/N .

vious section, measurements by Bailey and co-workers^{162,240,234} are of doubtful quality and are not considered further here.

In 1937, Nielsen and Bradbury¹³⁹ reported measured drift velocities obtained with sampling techniques for E/N between 0 and $50 \times 10^{-21} \text{ V m}^2$. Subsequently, Pack, Voshall, and Phelps¹⁶⁴ used sampling techniques to measure the drift velocity at three temperatures (195, 300, and 381 K) for E/N between 0.03 and $60 \times 10^{-21} \text{ V m}^2$. Spontaneous dissociation of ammonia with time, which would influence the drift velocity, was avoided in these measurements. The measured drift velocity increased with temperature. The data of Bradbury and Nielsen and of Peak and co-workers for 300 K are in good agreement over their common range of E/N , as shown in Fig. 9.5.

In 1934, Bradbury²³² measured the probability of attachment for ammonia and interpreted his observations as due to a two-body dissociative process. Parr and Moruzzi¹⁷³ used a pulsed Townsend discharge to measure λ/N in ammonia for E/N between 0 and $90 \times 10^{-21} \text{ V m}^2$ and for gas densities between 8 and $67 \times 10^{22} \text{ m}^{-3}$. They observed a threshold for attachment at $E/N = 27 \times 10^{-21} \text{ V m}^2$.

Risbud and Naidu¹⁷⁵ used a pulsed discharge to measure α/N and λ/N in ammonia for E/N between 60 and $120 \times 10^{-21} \text{ V m}^2$. These values for α/N , shown in Fig. 9.6, are the only data available. Figure 9.7 shows data for λ/N measured by Parr and Moruzzi and by Risbud and Naidu, which are in serious disagreement. If the attachment probabilities measured by Bradbury are converted to swarm coefficients, their values are approximately a factor of 10 below the Parr and Moruzzi data (see Ref. 173).

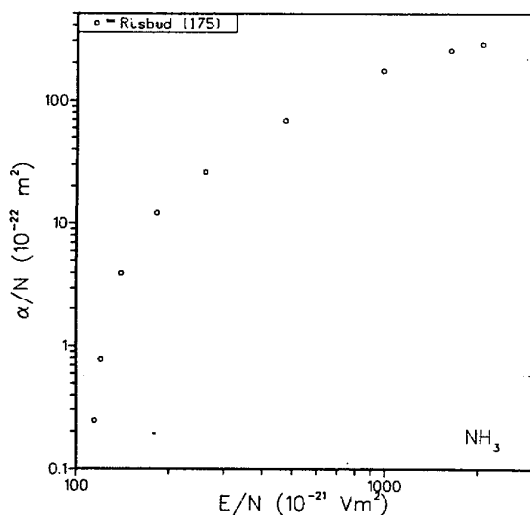
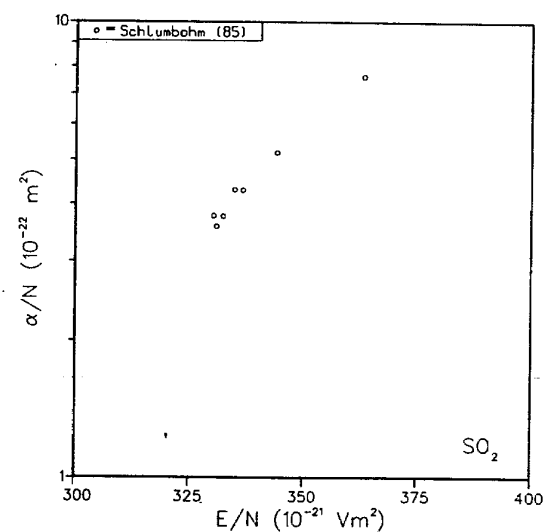
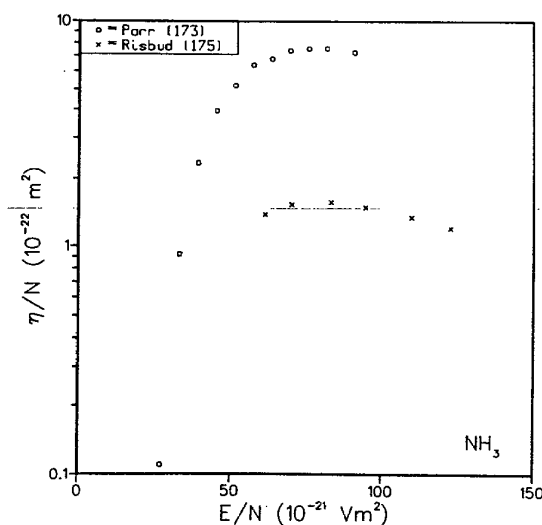
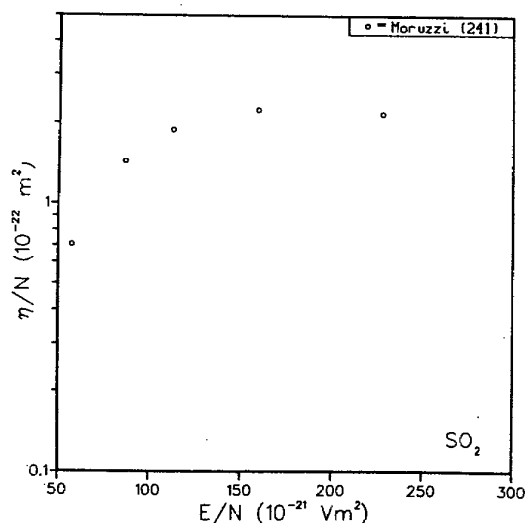
c. Sulphur Dioxide

No measurements of the drift velocity in SO_2 have been reported. In 1934, Bradbury and Tatel¹⁷¹ reported the first measurements of dissociative attachment. Significant attachment was observed for E/N above $18 \times 10^{-21} \text{ V m}^2$.

Moruzzi and Lakdawala²⁴¹ used pulsed Townsend techniques to measure the attachment coefficient for E/N between 3 and $240 \times 10^{-21} \text{ V m}^2$ and densities between 1.7 and $10 \times 10^{22} \text{ m}^{-3}$. They interpret their observations as due to three-body, pressure-dependent attachment for E/N below about $40 \times 10^{-21} \text{ V m}^2$ and to two-body dissociative attachment for higher E/N . The data for the two body region are shown in Fig. 9.8.

Schlumbohm⁸⁵ analyzed avalanche current growth curves to determine the ionization coefficient in SO_2 for high E/N (300 to $370 \times 10^{-21} \text{ V m}^2$), and these data are shown in Fig. 9.9. He also observed a density dependence in the attachment coefficient for N between 160 and $800 \times 10^{22} \text{ m}^{-3}$ which he interpreted as due to a three-body process.

Rademacher and co-workers²⁴² measured attachment rates for trace quantities of SO_2 in various nonattaching "buffer" gases using the techniques of the Oak Ridge group discussed in Sec. 5.2 above. These measurements were made at high buffer gas densities and over wide ranges of densities. The attachment rate displayed a strong dependence on buffer gas density.

FIGURE 9.6. α/N for NH_3 as a function of E/N .FIGURE 9.9. α/N in SO_2 as a function of E/N .FIGURE 9.7. η/N for NH_3 as a function of E/N .FIGURE 9.8. η/N in SO_2 as a function of E/N .

d. Other Gases

Stockdale and co-workers²⁴³ studied attachment processes in BF_3 and BCl_3 using both electron swarm and beam techniques. Davies²⁴⁴ measured α/N and λ/N in BF_3 .

6. Summary

In summary, this article presents data on the transport coefficients and swarm coefficients for the electronegative gases: SF_6 , the halogenated hydrocarbons, O_2 , air, H_2O , CO_2 , the halogens and NF_3 , the nitrogen oxides, the hydrogen halides, and NH_3 . The amount of effort which has been devoted to obtaining data, as well as the quality of these data, for these various gases is extremely uneven. In many cases, no more than one or two measurements have been reported and these, over a limited energy range. In other cases, many measurements have been made, often by different methods, but in spite of a large quantity of reported data, controversy exists concerning the reliability and interpretation of the various measurements and there is significant scatter in the results. Often, in these cases, the swarm coefficients are known only to within an order of magnitude.

The drift velocities are reasonably well established with the exceptions of SF_6 , the halogenated hydrocarbons, the halogens, and some of the miscellaneous gases. The ratio D_T/μ is known for some cases: O_2 for E/N above $100 \times 10^{-21} \text{ V m}^{-2}$, H_2O for E/N above $80 \times 10^{-21} \text{ V m}^{-2}$, air, and CO_2 . The only measurements for D_T/μ reported for these gases are for H_2O for E/N up to $80 \times 10^{-21} \text{ V m}^{-2}$ and for CO_2 for low E/N and high E/N .

For the description of electron gain and loss processes, data on the ionization coefficient are available and consistent for most of these gases; the exceptions are F_2 , NF_3 , I_2 , the nitrogen oxides, and HBr . The same is true of the electron growth constant. The data on the attachment coefficient are, however, subject to significant scatter in all cases where more than one measurement has been reported. In no case is this coefficient established to better than $\pm 20\%$.

The gases considered in this article are typically characterized by complex reaction schemes and, where possible, experimental work in these gases must be monitored by mass spectral analysis and a complete reaction scheme incorporated in the analysis of the data to obtain reliable results. In spite of much past effort, more work is clearly needed to obtain a complete set of reliable swarm data for many of these gases. Cases which are outstanding candidates are the following: in SF₆, η/N , α/N , λ/N for $E/N < 300$ and $> 600 \times 10^{-21} \text{ V m}^2$ and δ/N at all E/N ; in O₂, η/N and δ/N ; in CO₂, D_L/μ for E/N between 3 and $30 \times 10^{-21} \text{ V m}^2$ and, especially, η/N ; in H₂O, η/N and α/N , and D_T/μ for $E/N < 60 \times 10^{-21} \text{ V m}^2$.

7. Acknowledgments

The authors express deep appreciation to Dr. A. V. Phelps who patiently read and criticized the manuscript several times. Thanks are expressed to Dr. R. J. Van Brunt and Dr. J. A. Rees for helpful suggestions, to Lorraine Volsky, Leslie Haas, Gwendy Romey, and Patti Krog for expert editorial and typing assistance, and to Nancy Lewis for general assistance. This work was supported in part by DOE contract No. EA-77-01-6010/A053 EES.

8. References

- ¹J. Dutton, *J. Phys. Chem. Ref. Data* **4**, 577 (1975).
- ²L. G. H. Huxley and R. W. Crompton, *The Diffusion and Drift of Electrons in Gases* (Wiley, New York, 1974).
- ³L. G. Christophorou, *Atomic and Molecular Radiation Physics* (Wiley, London, 1971).
- ⁴A. Gilardini, *Low Energy Electron Collisions in Gases: Swarm and Plasma Methods Applied to Their Study* (Wiley, New York, 1972).
- ⁵H. S. W. Massey and E. H. S. Burhop, *Electronic and Ionic Impact Phenomena, Volume I: Collision of Electrons with Atoms*, 2nd ed. (Oxford University, London, 1969).
- ⁶E. W. McDaniel, *Collision Phenomena in Ionized Gases* (Wiley, New York, 1964).
- ⁷L. B. Loeb, *Basic Processes of Gaseous Electronics* (University of California, Berkeley, 1955).
- ⁸R. H. Healey and J. W. Reed, *The Behavior of Slow Electrons in Gases* (Amalgamated Wireless Ltd., Sydney, 1941).
- ⁹M. T. Elford, "Precision Measurements of Electron Transport Coefficients," in *Case Studies in Atomic Collision Physics II*, edited by E. W. McDaniel and M. R. C. McDowell (North-Holland, Amsterdam, 1972), pp. 91-158.
- ¹⁰A. N. Prasad and J. D. Craggs, "Attachment and Ionization Coefficients," in *Atomic and Molecular Processes*, edited by D. R. Bates (Academic, New York, 1962), pp. 206-244.
- ¹¹"Swarm Experiments in Atomic Collision Research," in *Proceedings of the International Seminar on Swarm Experiments in Atomic Collision Research, Rikkyo University, Tokyo, Japan, 6-7 September 1979*, edited by I. Ogawa (Rikkyo University, Tokyo, 1979).
- ¹²"Electron and Ion Swarms," in *Proceedings of the Second International Swarm Seminar, Oak Ridge, Tennessee, 22-23 July 1981*, edited by L. G. Christophorou (Pergamon, New York, 1981).
- ¹³L. C. Pitchford, S. V. O'Neil, and J. R. Rumble, Jr., *Phys. Rev. A* **23**, 294 (1981).
- ¹⁴S. L. Lin, R. E. Robson, and E. A. Mason, *J. Chem. Phys.* **71**, 3483 (1979).
- ¹⁵B. R. Bulos and A. V. Phelps, *Phys. Rev. A* **14**, 615 (1976).
- ¹⁶"Elementary Electron-Molecule Interactions and Negative Ion Resonances at Subexcitation Energies and Their Significance in Gaseous Dielectrics," in *Proceedings of the XIIIth International Conference on Phenomena in Ionized Gases 1977, Invited Lectures, Berlin, Germany, 12-17 September 1977*, edited by P. Bachmann and H. Kastelewick (Physical Society of the GDR, Berlin, 1977), pp. 51-71.
- ¹⁷"The Use of the Basic Physical Data in the Design of Multicomponent Gaseous Insulators," in *The Fifth International Conference on Gas Discharges, Liverpool, England, 11-14 September 1978*, edited by L. G. Christophorou (Institution of Electrical Engineers, London, 1978), pp. 1-8.
- ¹⁸"Gaseous Dielectrics," Proceedings of the International Symposium on Gaseous Dielectrics, Knoxville, Tennessee, 6-8 March 1978, Oak Ridge National Laboratory Report CONF-780301 (1978), edited by L. G. Christophorou.
- ¹⁹*Gaseous Dielectrics II*, edited by L. G. Christophorou (Pergamon, New York, 1980).
- ²⁰"The Role of Electron Swarm Studies in the Development of Gaseous Dielectrics," in *Electron and Ion Swarms, Proceedings of the Second International Swarm Seminar, Oak Ridge, Tennessee, 22-23 July 1981*, edited by L. G. Christophorou (Pergamon, New York, 1981), pp. 261-277.
- ²¹J. A. Rees, in *Electrical Breakdown of Gases*, edited by J. M. Meek and J. D. Craggs (Wiley, Chichester, 1978), pp. 1-128.
- ²²J. Dutton, in *Electrical Breakdown of Gases*, edited by J. M. Meek and J. D. Craggs (Wiley, Chichester, 1978), pp. 209-318.
- ²³K. J. Nygaard, H. L. Brooks, and S. R. Hunter, *IEEE J. Quantum Electron.* **15**, 1216 (1979).
- ²⁴P. J. Chantry, in *Applied Atomic Collision Physics, Volume 3*, edited by W. L. Nighan (Academic, New York, 1982), Chap. 2.
- ²⁵D. A. Parkes, *Vacuum* **24**, 561 (1974).
- ²⁶P. J. Chantry and R. E. Wooton, *J. Appl. Phys.* **52**, 2731 (1981).
- ²⁷E. C. Beaty, J. Dutton, and L. C. Pitchford, "A Bibliography of Electron Swarm Data," Joint Institute for Laboratory Astrophysics Information Center Report No. 20, University of Colorado, Boulder, Colorado, December 1979.
- ²⁸J. S. Townsend, *Nature (London)* **62**, 340 (1900).
- ²⁹D. K. Davies, *J. Appl. Phys.* **47**, 1916 (1976).
- ³⁰J. S. Townsend, *Electricity in Gases* (Oxford University, London, 1915).
- ³¹L. G. H. Huxley and F. W. Bennett, *Phil. Mag.* **30**, 396 (1940).
- ³²J. C. Bowe, *Phys. Rev.* **117**, 1411 (1960).
- ³³H. Raether, *Electron Avalanches and Breakdown in Gases* (Butterworths, London, 1964).
- ³⁴D. R. Nelson and F. J. Davis, *J. Chem. Phys.* **57**, 4079 (1972).
- ³⁵D. Edelson and K. B. McAfee, *Rev. Sci. Instrum.* **35**, 187 (1964).
- ³⁶W. P. Allis, "Motions of Ions and Electrons," in *Handbuch der Physik, Volume 21* edited by S. Flugge (Springer, Berlin, 1956), pp. 383-444.
- ³⁷K. Kumar, H. R. Skullerud, and R. E. Robson, *Aust. J. Phys.* **33**, 343 (1980).
- ³⁸T. Holstein, *Phys. Rev.* **70**, 367 (1946).
- ³⁹H. Parker, Jr. and J. J. Lowke, *Phys. Rev.* **181**, 290 (1969).
- ⁴⁰H. R. Skullerud, *J. Phys. B* **2**, 696 (1969).
- ⁴¹I. D. Reid, *Aust. J. Phys.* **32**, 231 (1979).
- ⁴²Y. Sakai, H. Tagashira, and S. Sakamoto, *J. Phys. D* **10**, 1035 (1977).
- ⁴³K. Kitamori, H. Tagashira, and Y. Sakai, *J. Phys. D* **11**, 283 (1978).
- ⁴⁴L. E. Kline, D. K. Davies, C. L. Chen, and P. J. Chantry, *J. Appl. Phys.* **50**, 6789 (1979).
- ⁴⁵B. Bederson and L. J. Kieffer, *Rev. Mod. Phys.* **43**, 601 (1971).
- ⁴⁶T. Yoshizawa, Y. Sakai, H. Tagashira, and S. Sakamoto, *J. Phys. D* **12**, 1839 (1979).
- ⁴⁷M. S. Naidu and A. N. Prasad, *J. Phys. D* **5**, 1090 (1972).
- ⁴⁸T. Teich and R. Sangi, "Discharge Parameters for Some Electronegative Gases and Emission of Radiation from Electron Avalanches," in *Proceedings of the Symposium on High Voltage Technology, Volume 1, Munich, Germany, 9-14 March 1972*, edited by F. Heilbronner (L. Plener, Munich, 1972), pp. 391-395.
- ⁴⁹F. M. Harris and G. J. Jones, *J. Phys. B* **4**, 1536 (1971).
- ⁵⁰J. Dutton, F. M. Harris, and G. J. Jones, "Drift Velocities of Electrons in Sulphur Hexafluoride," in *Proceedings of the Tenth International Conference on Phenomena in Ionized Gases, Volume 1, Oxford, 13-18 September 1971*, edited by R. N. Franklin (Donald Parsons, Oxford, 1971), p. 60.
- ⁵¹V. N. Maller and M. S. Naidu, *IEEE Trans. Plasma Sci.* **3**, 205 (1975).
- ⁵²A. Chutjian, *Phys. Rev. Lett.* **46**, 1511 (1981).
- ⁵³F. C. Fehsenfeld, *J. Chem. Phys.* **53**, 2000 (1970).
- ⁵⁴R. W. Crompton, A. G. Robertson, K. Nygaard, and R. Hegerberg, "Measurements of the Rate Coefficient for Attachment of Thermal Electrons to SF₆," in *The Thirty-Third Annual Gaseous Electronics Conference, Norman, Oklahoma, 7-10 October 1980* (University of Oklahoma, Norman, 1980), p. 84.
- ⁵⁵R. W. Odum, D. L. Smith, and J. H. Futrell, *Chem. Phys. Lett.* **24**, 227 (1974).

- ⁵⁶M. S. Foster and J. L. Beauchamp, *Chem. Phys. Lett.* **31**, 482 (1975).
- ⁵⁷B. M. Hochberg and E. J. Sandberg, *Zh. Tekh. Fiz.* **12**, 65 (1942).
- ⁵⁸B. M. Hochberg and E. J. Sandberg, *Compt. Rend. Acad. Sci. URSS* **53**, 511 (1946).
- ⁵⁹L. B. Loeb, *Basic Processes of Gaseous Electronics* (University of California, Berkeley and Los Angeles, 1955), Chap. 5, pp. 375-476.
- ⁶⁰M. S. Bhalla and J. D. Craggs, *Proc. Phys. Soc. London* **80**, 151 (1962).
- ⁶¹K. B. McAfee, *J. Chem. Phys.* **23**, 1435 (1955).
- ⁶²K. B. McAfee and D. Edelson, *Proc. Phys. Soc. London* **81**, 382 (1963).
- ⁶³H. A. Boyd and H. A. Crichton, *Proc. I.E.E.* **118**, 1872 (1971).
- ⁶⁴V. N. Maller and M. S. Naidu, *IEEE Trans. Plasma Sci.* **3**, 49 (1975).
- ⁶⁵V. N. Maller and M. S. Naidu, *Proc. I.E.E.* **123**, 107 (1976).
- ⁶⁶H. Itoh, M. Shimozuma, H. Tagashira, and S. Sakamoto, *J. Phys. D* **12**, 2167 (1979).
- ⁶⁷L. M. Bortnik and A. A. Panov, *Sov. Phys. Tech. Phys.* **16**, 571 (1971).
- ⁶⁸J. Dutton, F. M. Harris, and G. J. Jones, *Nature (London)* **227**, 702 (1970).
- ⁶⁹J. Dutton and F. M. Harris, "High Voltage Breakdown in Uniform Fields," in *First International Conference on Gas Discharges, London, 15-18 September 1970* (I.E.E., London, 1970), pp. 544-548.
- ⁷⁰T. H. Teich and D. W. Branstom, "Time Resolved Observation of Ionization and Electron Detachment in SF₆," in *Third International Conference on Gas Discharges, London, England, 9-12 September 1974* (I.E.E., London, 1974), pp. 109-113.
- ⁷¹M. J. Eccles, A. N. Prasad, and J. D. Craggs, *Electron. Lett.* **3**, 410 (1967).
- ⁷²B. C. O'Neill and J. D. Craggs, *J. Phys. B* **6**, 2634 (1973).
- ⁷³M. S. Naidu and A. N. Prasad, *J. Phys. D* **5**, 983 (1972).
- ⁷⁴A. N. Prasad and M. S. Naidu, "Drift Diffusion and Attachment of Electrons in Perfluoropropane," in *Proceedings of the First International Conference on Gas Discharges, London, 15-18 September 1970* (I.E.E., London, 1970), pp. 416-420.
- ⁷⁵L. G. Christophorou, D. L. McCorkle, D. V. Maxey, and J. G. Carter, *Nucl. Instrum. Methods* **163**, 141 (1979).
- ⁷⁶M. S. Naidu and A. N. Prasad, *J. Phys. D* **2**, 1431 (1969).
- ⁷⁷C. S. Lakshminarasimha, J. Lucas, and D. A. Price, *Proc. Inst. Electr. Eng.* **120**, 1044 (1973).
- ⁷⁸P. R. Howard, *Nature (London)* **181**, 645 (1958).
- ⁷⁹J. L. Moruzzi and J. D. Craggs, *Proc. Phys. Soc. London* **82**, 979 (1963).
- ⁸⁰J. C. Devins and R. J. Wolff, "Ionization and Attachment Coefficients in Perfluorocarbon Gases," in *Conference on Electrical Insulation*, Annual Report 1964 (National Academy of Sciences-National Research Council, Washington, DC, 1965), pp. 43-49.
- ⁸¹S. E. Bozin and C. C. Goodyear, *Brit. J. Appl. Phys.* **1**, 327 (1968).
- ⁸²S. A. A. Razzak and C. C. Goodyear, *Brit. J. Appl. Phys.* **1**, 1215 (1968).
- ⁸³C. S. Lakshminarasimha, J. Lucas, and R. A. Snelson, *Proc. Inst. Electr. Eng.* **122**, 1162 (1975).
- ⁸⁴M. A. Harrison and R. Geballe, *Phys. Rev.* **91**, 1 (1953).
- ⁸⁵H. Schlumbohm, *Z. Phys.* **166**, 192 (1962).
- ⁸⁶J. L. Moruzzi, *Brit. J. Appl. Phys.* **14**, 938 (1963).
- ⁸⁷H. A. Boyd, G. C. Crichton, and T. Munknielsen, "Determination of Ionization and Attachment Coefficients in CCl₂F₂," in *Proceedings of the First International Conference on Gas Discharges, Volume 1, London, 15-18 September 1970* (I.E.E., London, 1970), pp. 426-430.
- ⁸⁸C. Raja Rao and G. R. Govinda Raju, *Int. J. Electron. Phys.* **35**, 49 (1973).
- ⁸⁹V. N. Maller and M. S. Naidu, "Sparkign Potentials and Swarm Coefficients in Freon and Mixtures of Freon and Nitrogen," in *Proceedings of the Third I.E.E. International Conference on Gas Discharges, Volume 1, London, England, 9-12 September 1974* (Savoy Place, London, 1974), pp. 409-413.
- ⁹⁰A. V. Risbud and M. S. Naidu, *Indian J. Pure Appl. Phys.* **16**, 32 (1978).
- ⁹¹L. G. Christophorou, R. N. Compton, G. S. Hurst, and P. W. Reinhardt, *J. Chem. Phys.* **43**, 4273 (1965).
- ⁹²L. G. Christophorou, D. L. McCorkle, and J. G. Carter, *J. Chem. Phys.* **54**, 253 (1970). ERRATUM: *J. Chem. Phys.* **57**, 2228 (1972).
- ⁹³L. G. Christophorou, D. L. McCorkle, and V. E. Anderson, *J. Phys. B* **4**, 1163 (1971).
- ⁹⁴D. L. McCorkle, A. A. Christodoulides, L. G. Christophorou, and I. Szamrej, *J. Chem. Phys.* **72**, 4049 (1980). ERRATUM: *J. Chem. Phys.* **76**, 753 (1982).
- ⁹⁵D. L. McCorkle, L. G. Christophorou, and S. R. Hunter, "Electron Attachment Rate Constants and Cross Sections for Halocarbons," in *Electron and Ion Swarms, Proceedings of the Second International Swarm Seminar, Oak Ridge, Tennessee, 22-23 July 1981*, edited by L. G. Christophorou (Pergamon, New York, 1981), pp. 21-34.
- ⁹⁶A. A. Christodoulides and L. G. Christophorou, *J. Chem. Phys.* **54**, 4691 (1971).
- ⁹⁷K. S. Gant and L. G. Christophorou, *J. Chem. Phys.* **65**, 2977 (1976).
- ⁹⁸A. A. Christodoulides, L. G. Christophorou, R. Y. Pai, and C. M. Tung, *J. Chem. Phys.* **70**, 1156 (1979).
- ⁹⁹R. Y. Pai, L. G. Christophorou, and A. A. Christodoulides, *J. Chem. Phys.* **70**, 1169 (1979).
- ¹⁰⁰A. A. Christodoulides and L. G. Christophorou, *Chem. Phys. Lett.* **61**, 553 (1979).
- ¹⁰¹L. G. Christophorou, *Environ. Health Perspec.* **36**, 3 (1980).
- ¹⁰²R. W. Crompton and M. T. Elford, *Aust. J. Phys.* **26**, 771 (1973).
- ¹⁰³R. D. Hake and A. V. Phelps, *Phys. Rev.* **158**, 70 (1967).
- ¹⁰⁴I. D. Reid and R. W. Crompton, *Aust. J. Phys.* **33**, 215 (1980).
- ¹⁰⁵K. Masek, T. Ruzicka and L. Laska, *Czech. J. Phys. B* **27**, 888 (1977).
- ¹⁰⁶G. Fournier, J. Bonnet, and D. Pigache, *J. Phys. (Paris) Lett.* **41**, L173 (1980).
- ¹⁰⁷L. G. H. Huxley, R. W. Crompton, and C. H. Bagot, *Aust. J. Phys.* **12**, 303 (1959).
- ¹⁰⁸J. A. Rees, *Aust. J. Phys.* **18**, 41 (1965).
- ¹⁰⁹M. S. Naidu and A. N. Prasad, *J. Phys. D* **3**, 957 (1970).
- ¹¹⁰W. Roznerski and J. Mechliniska-Drewko, *J. Phys. (Paris) Colloq.* **C7** 40, 149 (1979).
- ¹¹¹T. Taniguchi, H. Tagashira, I. Okada, and Y. Sakai, *J. Phys. D* **11**, 2281 (1978).
- ¹¹²R. W. Crompton, R. Hegerberg, and H. R. Skullerud, *J. Phys. B* **13**, L455 (1980).
- ¹¹³R. E. Goans and L. G. Christophorou, *J. Chem. Phys.* **60**, 1036 (1974).
- ¹¹⁴C. G. J. Buursen, F. J. De Hoog, and L. H. Van Montfort, *Physica* **60**, 244 (1972).
- ¹¹⁵R. Grünberg, *Z. Naturforsch.* **24A**, 1039 (1969).
- ¹¹⁶P. A. Chatterton and J. D. Craggs, *J. Electron. Control* **11**, 425 (1961).
- ¹¹⁷M. J. Eccles and J. D. Craggs, *Electron Lett.* **3**, 146 (1967).
- ¹¹⁸M. J. Eccles, B. C. O'Neill, and J. D. Craggs, *J. Phys. B* **3**, 1724 (1970).
- ¹¹⁹M. K. Brabanec and A. W. Williams, "An Apparatus for the Study of Negative Ion Interactions Under Swarm Conditions," in *Proceedings of the Second International Conference on Gas Discharges, Volume 1* (I.E.E., London, 1972), pp. 332-334.
- ¹²⁰D. A. Price, J. Lucas, and J. L. Moruzzi, *J. Phys. D* **5**, 1249 (1972).
- ¹²¹D. A. Price and J. L. Moruzzi, *J. Phys. D* **6**, L17 (1973).
- ¹²²D. A. Price, J. Lucas, and J. L. Moruzzi, *J. Phys. D* **6**, 1514 (1973).
- ¹²³J. Lucas, D. A. Price, and J. L. Moruzzi, *J. Phys. D* **6**, 1503 (1973).
- ¹²⁴P. R. Kinsman and J. A. Rees, *Int. J. Mass Spectrom. Ion Phys.* **5**, 71 (1970).
- ¹²⁵S. A. Lawton and A. V. Phelps, *J. Chem. Phys.* **69**, 1055 (1978).
- ¹²⁶B. C. O'Neill and J. D. Craggs, *J. Phys. B* **6**, 2625 (1973).
- ¹²⁷L. Frommhold, *Fortschr. Phys.* **12**, 597 (1964).
- ¹²⁸D. W. Goodson, R. J. Corbin, and L. Frommhold, *Phys. Rev. A* **9**, 2049 (1974).
- ¹²⁹R. J. Corbin and L. Frommhold, *Phys. Rev. A* **10**, 2273 (1974).
- ¹³⁰F. Reberstrost, *Chem. Phys. Lett.* **21**, 368 (1973).
- ¹³¹D. T. A. Blair and H. W. Whittington, *J. Phys. D* **8**, 405 (1975).
- ¹³²K. Masek, L. Laska, and T. Ruzicka, *J. Phys. D* **10**, L25 (1977).
- ¹³³K. Masek, L. Laska, and T. Ruzicka, *Czech. J. Phys. B* **28**, 1321 (1978).
- ¹³⁴N. E. Bradbury, *Phys. Rev.* **44**, 883 (1933).
- ¹³⁵K. H. Wagner, *Z. Phys.* **241**, 258 (1971).
- ¹³⁶A. N. Prasad and J. D. Craggs, *Proc. Phys. Soc. London* **77**, 385 (1961).
- ¹³⁷N. Sukhum, A. N. Prasad, and J. D. Craggs, *Brit. J. Appl. Phys.* **18**, 785 (1967).
- ¹³⁸R. M. Snuggs, D. J. Volz, J. H. Schummers, D. W. Martin, and E. W. McDaniel, *Phys. Rev. A* **3**, 477 (1971).
- ¹³⁹R. A. Nielsen and N. E. Bradbury, *Phys. Rev.* **51**, 69 (1937).
- ¹⁴⁰H. Hessenauer, *Z. Phys.* **204**, 142 (1967).
- ¹⁴¹H. Ryzko, *Proc. Phys. Soc. London* **85**, 1283 (1965).
- ¹⁴²A. E. D. Heylen, *Proc. Phys. Soc. London* **79**, 284 (1962).
- ¹⁴³J. A. Rees, *Aust. J. Phys.* **26**, 427 (1973).
- ¹⁴⁴R. Hegerberg and I. D. Reid, *Aust. J. Phys.* **33**, 227 (1980).
- ¹⁴⁵H. B. Milloy, I. D. Reid, and R. W. Crompton, *Aust. J. Phys.* **28**, 231 (1975).
- ¹⁴⁶J. S. Townsend and H. T. Tizard, *Proc. R. Soc. London Ser. A* **88**, 336 (1913).
- ¹⁴⁷V. A. Bailey, *Phil. Mag.* **50**, 825 (1925).
- ¹⁴⁸L. G. H. Huxley and A. A. Zaazou, *Proc. R. Soc. London Ser. A* **196**, 402 (1949).
- ¹⁴⁹R. W. Crompton, L. G. H. Huxley, and D. J. Sutton, *Proc. R. Soc. London Ser. A* **218**, 507 (1953).
- ¹⁵⁰J. A. Rees and R. L. Jory, *Aust. J. Phys.* **17**, 307 (1964).
- ¹⁵¹C. Raja Rao and G. R. Govinda Raju, *J. Phys. D* **4**, 769 (1971).
- ¹⁵²V. N. Maller and M. S. Naidu, *Indian J. Pure Appl. Phys.* **14**, 733 (1976).

- ¹⁵³E. B. Wagner, F. J. Davis, and G. S. Hurst, *J. Chem. Phys.* **47**, 3138 (1967).
- ¹⁵⁴C. S. Lakshminarasimha and J. Lucas, *J. Phys. D* **10**, 313 (1977).
- ¹⁵⁵C. Raja Rao and G. R. Govinda Raju, *J. Phys. D* **4**, 494 (1971).
- ¹⁵⁶J. L. Moruzzi and D. A. Price, *J. Phys. D* **7**, 1434 (1974).
- ¹⁵⁷J. Comer and G. J. Schulz, *Phys. Rev. A* **10**, 2100 (1974).
- ¹⁵⁸F. C. Fehsenfeld, E. E. Ferguson, and A. L. Schmeltekopf, *J. Chem. Phys.* **45**, 1844 (1966).
- ¹⁵⁹E. Kuffel, *Proc. Phys. Soc. London* **74**, 297 (1959).
- ¹⁶⁰A. N. Prasad and J. D. Craggs, *Proc. Phys. Soc. London* **76**, 223 (1960).
- ¹⁶¹H. Schlumbohm, *Z. Phys.* **184**, 492 (1965).
- ¹⁶²V. A. Bailey and W. E. Duncanson, *Phil. Mag.* **10**, 145 (1930).
- ¹⁶³R. W. Crompton, J. A. Rees, and R. L. Jory, *Aust. J. Phys.* **18**, 541 (1965).
- ¹⁶⁴J. L. Pack, R. E. Voshall, and A. V. Phelps, *Phys. Rev.* **127**, 2084 (1962).
- ¹⁶⁵J. J. Lowke and J. A. Rees, *Aust. J. Phys.* **16**, 447 (1963).
- ¹⁶⁶J. F. Wilson, F. J. Davis, D. R. Nelson, R. N. Compton, and D. H. Crawford, *J. Chem. Phys.* **62**, 4204 (1975).
- ¹⁶⁷L. G. Christophorou and A. A. Christodoulides, *J. Phys. B* **2**, 71 (1969).
- ¹⁶⁸H. Ryzko, *Ark. Fys.* **32**, 1 (1966).
- ¹⁶⁹J. J. Lowke and J. H. Parker, *Phys. Rev.* **181**, 302 (1969).
- ¹⁷⁰R. W. Crompton, J. A. Rees, and R. L. Jory, "The Diffusion and Attachment of Electrons in Water Vapour," in *Proceedings of the Seventh International Conference on Phenomena in Ionized Gases, Volume 1, Belgrade, 22-27 August, 1965*, edited by B. Perovic and D. Tosic (Gradevinska, Knjiga Belgrade, 1966).
- ¹⁷¹N. E. Bradbury and H. E. Tatel, *J. Chem. Phys.* **2**, 835 (1934).
- ¹⁷²J. L. Moruzzi and A. V. Phelps, *J. Chem. Phys.* **45**, 4617 (1966).
- ¹⁷³J. E. Parr and J. L. Moruzzi, *J. Phys. D* **5**, 514 (1972).
- ¹⁷⁴J. L. Pack and A. V. Phelps, *J. Chem. Phys.* **45**, 4316 (1966).
- ¹⁷⁵A. V. Risbud and M. S. Naidu, *J. Phys. (Paris) Colloq.* **C7 40**, 77 (1979).
- ¹⁷⁶M. T. Elford, *Aust. J. Phys.* **19**, 629 (1966).
- ¹⁷⁷M. T. Elford and G. N. Haddad, *Aust. J. Phys.* **33**, 517 (1980).
- ¹⁷⁸H. T. Saelec, J. Lucas, and J. W. Limbeck, (*IEEE J.*) *Solid State Electron Devices* **1**, 111 (1977).
- ¹⁷⁹R. A. Sierra, H. L. Brooks, and K. J. Nygaard, *Appl. Phys. Lett.* **35**, 764 (1979).
- ¹⁸⁰H. N. Kucukarpaci and J. Lucas, *J. Phys. D* **12**, 2123 (1979).
- ¹⁸¹H. Schlumbohm, *Z. Phys.* **182**, 317 (1965).
- ¹⁸²J. A. Rees, *Aust. J. Phys.* **17**, 462 (1964).
- ¹⁸³R. W. Warren and J. H. Parker, *Phys. Rev.* **128**, 2661 (1962).
- ¹⁸⁴W. Roznerski and J. Mechliniska-Drewko, *Phys. Lett. A* **70**, 271 (1979).
- ¹⁸⁵C. S. Lakshminarasimha, J. Lucas, and N. Kontoleon, *J. Phys. D* **7**, 2545 (1974).
- ¹⁸⁶M. S. Bhalla and J. D. Craggs, *Proc. Phys. Soc. London* **76**, 369 (1960).
- ¹⁸⁷P. A. Chatterton and J. D. Craggs, *Proc. Phys. Soc. London* **85**, 355 (1965).
- ¹⁸⁸S. R. Alger and J. A. Rees, *J. Phys. D* **9**, 2359 (1976).
- ¹⁸⁹V. J. Conti and A. W. Williams, *J. Phys. D* **8**, 2198 (1975).
- ¹⁹⁰V. J. Conti and A. W. Williams, "Measurement of Ionization and Attachment Coefficients in Carbon Dioxide," in *Contributed Papers of the Eighth International Conference on Phenomena in Ionized Gases, Vienna, 27 August-2 September 1967* (Springer, Vienna, 1967), p. 23.
- ¹⁹¹D. K. Davies, *J. Appl. Phys.* **49**, 127 (1978).
- ¹⁹²J. J. Lowke, A. V. Phelps, and B. W. Irwin, *J. Appl. Phys.* **44**, 4664 (1973).
- ¹⁹³T. H. Teich, M. A. A. Jabbar, and D. W. Branston, in *Proceedings of the Second International High Voltage Symposium* (Swiss Federal Institute of Technology, Zurich, 1975), p. 390.
- ¹⁹⁴Y. Sakai, S. Kaneko, H. Tagashira, and S. Sakamoto, *J. Phys. D* **12**, 23 (1979).
- ¹⁹⁵V. A. Bailey and R. H. Healey, *Phil. Mag.* **19**, 725 (1935).
- ¹⁹⁶J. E. Bailey, R. E. B. Makinson, and J. M. Somerville, *Phil. Mag.* **24**, 177 (1937).
- ¹⁹⁷R. H. Healey, *Phil. Mag.* **26**, 940 (1938).
- ¹⁹⁸K. J. Nygaard, S. R. Hunter, J. Fletcher, and S. R. Foltyn, *Appl. Phys. Lett.* **32**, 351 (1978).
- ¹⁹⁹K. J. Nygaard, J. Fletcher, S. R. Hunter, and S. R. Foltyn, *Appl. Phys. Lett.* **32**, 612 (1978).
- ²⁰⁰W. L. Nighan, *IEEE J. Quantum Electron.* **14**, 714 (1978).
- ²⁰¹R. J. Hall, *J. Chem. Phys.* **68**, 1803 (1978).
- ²⁰²H.-L. Chen, R. E. Center, D. W. Trainor, and W. I. Fyfe, *J. Appl. Phys.* **48**, 2297 (1977).
- ²⁰³G. D. Sides, T. O. Tiernan, and R. J. Hanrahan, *J. Chem. Phys.* **65**, 1966 (1976).
- ²⁰⁴B. I. Schneider and C. A. Brau, *Appl. Phys. Lett.* **33**, 569 (1978).
- ²⁰⁵D. W. Trainor and J. H. Jacob, *Appl. Phys. Lett.* **35**, 920 (1979).
- ²⁰⁶M. Rokni, J. H. Jacob, and J. A. Mangano, *Appl. Phys. Lett.* **34**, 187 (1979).
- ²⁰⁷P. J. Chantry, "Attachment Measurements in Halogen Bearing Molecules," ARPA Technical Report No. 3342, Defense Advanced Research Projects Agency, Ballistic Missile Defense Advanced Technology Center, Huntsville, Alabama, Contract No. DASG60-77-C-0023, March 1978.
- ²⁰⁸A. U. Hazi, A. E. Orel, and T. N. Rescigno, *Phys. Rev. Lett.* **46**, 918 (1981).
- ²⁰⁹K. G. Mothes, E. Schultes, and R. N. Schindler, *J. Phys. Chem.* **76**, 3758 (1972).
- ²¹⁰G. D. Sides and T. O. Tiernan, *J. Chem. Phys.* **67**, 2382 (1977).
- ²¹¹M. J. Shaw and J. D. C. Jones, *Appl. Phys.* **14**, 393 (1977).
- ²¹²S. E. Bozin and C. C. Goodyear, *Brit. J. Appl. Phys.* **18**, 49 (1967).
- ²¹³W.-C. Tam and S. F. Wong, *J. Chem. Phys.* **68**, 5626 (1978).
- ²¹⁴A. A. Christodoulides, R. Schumacher, and R. N. Schindler, *J. Phys. Chem.* **79**, 1904 (1975).
- ²¹⁵S. A. A. Razzak and C. C. Goodyear, *J. Phys. D* **2**, 1577 (1969).
- ²¹⁶F. K. Truby, *Phys. Rev. A* **4**, 613 (1971).
- ²¹⁷D. W. Trainor and M. J. W. Boness, *Appl. Phys. Lett.* **32**, 604 (1978).
- ²¹⁸H. L. Brooks, S. R. Hunter, and K. J. Nygaard, *J. Chem. Phys.* **71**, 1870 (1979).
- ²¹⁹F. K. Truby, *Phys. Rev.* **188**, 508 (1969).
- ²²⁰E. J. Shipsey, *J. Chem. Phys.* **52**, 2274 (1970).
- ²²¹D. T. Birtwistle and A. Modinos, *J. Phys. B* **11**, 2949 (1978).
- ²²²D. A. Parkes, *J. Chem. Soc. Faraday Trans. 2* **68**, 2103 (1972).
- ²²³J. Dutton, F. M. Harris, and D. B. Hughes, *J. Phys. B* **8**, 313 (1975).
- ²²⁴J. B. Hasted and S. Beg, *Brit. J. Appl. Phys.* **16**, 1779 (1965).
- ²²⁵D. A. Parkes and F. M. Sugden, *J. Chem. Soc. Faraday Trans.* **68**, 600 (1972).
- ²²⁶V. A. Bailey and J. B. Rudd, *Phil. Mag.* **14**, 1033 (1932).
- ²²⁷V. A. Bailey and J. M. Somerville, *Phil. Mag.* **17**, 1169 (1934).
- ²²⁸M. F. Skinker and J. V. White, *Phil. Mag.* **46**, 630 (1923).
- ²²⁹A. V. Phelps and R. E. Voshall, *J. Chem. Phys.* **49**, 3246 (1968).
- ²³⁰D. Rapp and D. D. Briglia, *J. Chem. Phys.* **43**, 1480 (1965).
- ²³¹J. Dutton, F. M. Harris, and D. B. Hughes, "The Electrical Breakdown of Nitrous Oxide at High Voltages," in *Proceedings of the Second International Conference on Gas Discharges, London, England, 11-15 September 1972* (I.E.E., London, 1972), pp. 273-275.
- ²³²N. E. Bradbury, *J. Chem. Phys.* **2**, 827 (1934).
- ²³³M. McFarland, D. B. Dunkin, F. C. Fehsenfeld, A. L. Schmeltekopf, and E. E. Ferguson, *J. Chem. Phys.* **56**, 2358 (1972).
- ²³⁴V. A. Bailey and A. J. Higgs, *Phil. Mag.* **7**, 277 (1929).
- ²³⁵L. G. Christophorou, R. N. Compton, and H. W. Dickson, *J. Chem. Phys.* **48**, 1949 (1968).
- ²³⁶F. J. Davis, R. N. Compton, and D. R. Nelson, *J. Chem. Phys.* **59**, 2324 (1973).
- ²³⁷R. C. Sze and A. E. Greene, "Ground State Electronic Attachment Rates in HCl," in *The Thirty-Third Annual Gaseous Electronics Conference, Norman, Oklahoma, 7-10 October 1980* (University of Oklahoma, Norman, 1980), p. 85.
- ²³⁸D. K. Davies, "Measurements of Electron Transport, Attachment, and Ionization in HCl," in *The Thirty-Third Annual Gaseous Electronics Conference, Norman, Oklahoma, 7-10 October 1980* (University of Oklahoma, Norman, 1980), p. 85.
- ²³⁹J. P. Ziesel, I. Nenner, and G. J. Schulz, *J. Chem. Phys.* **63**, 1943 (1975).
- ²⁴⁰V. A. Bailey and J. D. McGee, *Phil. Mag.* **6**, 1073 (1928).
- ²⁴¹J. L. Moruzzi and V. K. Lakdawala, *J. Phys. (Paris) Colloq.* **C7 40**, 11 (1979).
- ²⁴²J. Rademacher, L. G. Christophorou, and R. P. Blaunstein, *J. Chem. Soc. Faraday Trans. 2* **71**, 1212 (1975).
- ²⁴³J. A. D. Stockdale, D. R. Nelson, F. J. Davis, and R. N. Compton, *J. Chem. Phys.* **56**, 3336 (1972).
- ²⁴⁴D. K. Davies, *J. Appl. Phys.* **47**, 1920 (1976).
- ²⁴⁵E. Schultes, A. A. Christodoulides, and R. N. Schindler, *Chem. Phys.* **8**, 354 (1975).